An Evidence-Based Approach to Understanding Blue Carbon Dynamics and Distribution on the Pacific Coast of Canada

by

Hasini Basnayake

B.Sc. (Environmental Science), Simon Fraser University, 2019

Thesis Submitted in Partial Fulfillment of the
Requirements for the Degree of
Master of Resource Management

in the
School of Resource and Environmental Management
Faculty of Environment

© Hasini Basnayake 2022
SIMON FRASER UNIVERSITY
Spring 2022

Copyright in this work is held by the author. Please ensure that any reproduction or re-use is done in accordance with the relevant national copyright legislation.

Declaration of Committee

Name:	**Hasini Basnayake**
Degree:	**Master of Resource Management**
Title:	**An Evidence-Based Approach to Understanding Blue Carbon Dynamics and Distribution on the Pacific Coast of Canada**
Committee:	**Chair**: **Chelsea Little** Assistant Professor, Resource and Environmental Management
	Karen Kohfeld Supervisor Professor, Resource and Environmental Management
	Marlow Pellatt Committee Member Adjunct Professor, Resource and Environmental Management
	Jessica Pilarczyk Examiner Assistant Professor, Earth Sciences

Abstract

Salt marshes are considered effective “blue carbon” sinks and potential NCSs. However, using blue carbon ecosystems in climate change mitigation requires reliable quantification of area and carbon dynamics. Here I examine sediment cores, vegetation, depth profiles, and porewater salinities to characterize carbon dynamics in the 222-ha Boundary Bay marsh, the largest salt marsh in British Columbia. The marsh exhibits substantial variability in carbon processes depending on marsh location, with marsh expansion and increased carbon storage in western Boundary Bay and marsh loss and erosion in the east. I also map and compare detailed areal estimates for three tidal salt marshes in southern British Columbia with regional and global datasets to test their reliability in estimating marsh extent for blue carbon calculations. My results indicate that existing salt marsh distribution datasets largely overestimate marsh distribution, leading to overestimations in blue carbon storage and accumulation.

Keywords: blue carbon; nature-based climate solutions; tidal salt marsh; Pacific Coast of Canada; spatial distribution; carbon dynamics

Dedication

To my parents, Senaka & Bhadra

For their selfless dedication to my growth and education.

Acknowledgements

My sincere thanks go out to my supervisor Karen Kohfeld for her insights, support, and guidance. You gave me the opportunity to join the COPE lab during the final year of my undergraduate and introduced me to the intriguing world of blue carbon. I will forever be grateful for that opportunity and your knowledge in blue carbon. I would like to thank my co-supervisor Marlow Pellatt for providing me with the resources and encouragement for the year-round fieldwork and lab work required to complete my research work.

In addition, I extend my thanks to Parks Canada for partially funding this project and providing me with fieldwork and lab equipment to process my samples, despite the restrictions of the COVID-19 pandemic. I thank Flett Research for conducting ^{210}Pb and ^{226}Ra analysis for my cores.

My gratitude goes out to Maija Gailis and Stephen Chastain for paving the way for blue carbon research at the Climate, Oceans, and Paleo-Environments Lab. The methodologies and manuscripts you developed enabled me to take blue carbon research in British Columbia one step further.

A huge thank you to my field and lab partner Alison Martin, who stuck by my side through thick and thin. I will forever remember your famous words “we did not choose the marsh; the marsh chose us.” You made my research experience feel lighter and more enjoyable out in the freezing marsh in January, and in our window-less lab burning up soil. My data collection would not have been possible without the unwavering support from my COPE lab mates Maggie Duncan, Jacqui Levi, John Morra and Ellie Simpson. Thank you for volunteering your time to come out to the field and sharing the REM experience with me. I extend my thanks to Srishti Kumar for your invaluable support collecting depth profiles.

My heart-felt gratitude goes to my partner, Dev, for patiently accompanying me to the marsh all summer, despite the marsh claiming your boots. Thank you for helping me stay on track and being my strength throughout this journey. Finally, I want to thank my sister for volunteering to help me out in the field numerous times, and my parents for supporting me from halfway across the world. I would not be where I am today if it were not for my family.

Table of Contents

List of Tables

List of Figures

List of Acronyms

ACA	Annual Carbon Accumulation
BB	Boundary Bay
BBE	Boundary Bay East
BBM	Boundary Bay Mid
BBW	Boundary Bay West
BC	British Columbia
C	Carbon
CAR	Carbon Accumulation Rate
CRF	Cypress River Flats
DBD	Dry Bulk Density
DoP	Depth of Peat Layer
DoR	Depth of Refusal
GBK	Grice Bay – Kennedy River
HM	High Marsh
LM	Low Marsh
MB	Mud Bay
Mg C	Megagrams Carbon
SCD	Soil Carbon Density
SP	Salt Panne

Chapter 1. Introduction

Tidal wetlands such as intertidal salt marshes are generally found in sheltered bays, estuaries, and river deltas in the Pacific Northwest region of North America. These ecosystems occupy the upper portion of the intertidal zone along tidal reaches of coastal bays, with elevation ranging from 1.5 – 2.0 m above sea level (Brophy 2014; Marcoe and Pilson 2017; Janousek et al. 2021). Blue Carbon refers to organic carbon that is captured and stored by the oceans and coastal ecosystems, particularly by vegetated coastal ecosystems such as seagrass meadows, salt marshes, and mangrove forests (Macreadie et al. 2019). Salt marshes sequester blue carbon through *in-situ* primary production and organic matter produced elsewhere and transported to site through tidal action (Chmura et al. 2003; Macreadie et al. 2019; Janousek et al. 2021). Wetland plants fix inorganic carbon dioxide (CO_2) absorbed from the atmosphere through photosynthesis during the daytime and produce organic C that is stored in the plant biomass and soil over long periods of time. However, up to 50% of the C is released back into the atmosphere through plant respiration, while a fraction of the organic C produced is re-mineralized through decomposition by microbial activity in the soil, exported elsewhere through tidal action, or consumed in food webs at the terrestrial-ocean interface (Janousek et al. 2021; Rosentreter et al. 2018). The proportion of C stored in soil over the long term is dependent on the rate of decomposition in the wetland environment, based on several factors including soil microbial communities, porewater salinity, air and soil temperature, vegetation, and rates of photosynthesis and plant respiration (Poffenbarger et al. 2011; Huntingford et al 2017). These factors influence how much C is lost to the atmosphere as well, which affects our quantification of C storage and accumulation rates.

Ecosystem services provided by tidal marshes make them potentially important contributors to natural climate solutions (NCSs). NCSs are defined as actions that use natural systems to enhance climate mitigation and adaptation while providing co-benefits such as enhanced biodiversity, improved ecosystem resilience, and carbon capture and storage (Temmerman et al. 2013; ECCC 2021). They are a suite of protection, improved management, and restoration actions (“pathways”) in wetlands that provide additional climate mitigation beyond business as usual (Drever et al. 2021). For example, tidal wetlands can reduce flooding in coastal areas through tide, wave, and storm attenuation

(Temmerman et al. 2013). The dense plant communities and the gradual intertidal elevation slope help slow storm surge waves and resultant coastline damage during high-tide flooding events. With anticipated impacts of climate change, this role of tidal wetlands as a protective buffer is expected to become increasingly important for coastal communities impacted by rising sea levels and stronger and more frequent storm surge events (Janousek et al. 2021).

Integration of salt marsh ecosystem services into NCSs for climate change mitigation requires accurate quantification of marsh areal extents and carbon dynamics. In British Columbia (BC), current understanding of salt marsh blue carbon lacks comprehensive research, posing challenges to its integration in regional and national climate change conservation policy. In this thesis, I map salt marsh areal extents, quantify carbon sequestration rates and storage for previously unexamined marsh areas, and document new environmental factors such as porewater salinity as a contributing factor of greenhouse gas emissions. The thesis is divided into two chapters based on the extent of their focus for ease of navigation.

In chapter 2, I document the marsh area, carbon stocks, accumulation rates, and porewater salinities on the eastern portion of the Boundary Bay salt marsh. Boundary Bay is home to the largest salt marsh in southern BC with documented levels of stored blue carbon in the western section, and the planned construction of a living dike - a type of flood protection structure that uses a naturally existing salt marsh to enhance its protection against storm surges and flooding - will likely modify its carbon dynamics in the foreseeable future. While initial work focused on the western portion of Boundary Bay (Gailis et al. 2021), a complete understanding of the carbon dynamics requires integrated knowledge of carbon storage and accumulation in the eastern portion of the Bay along with an understanding of greenhouse gas (GHG) emissions. I combine new results from this chapter with previous blue carbon work at western Boundary Bay marsh to provide a holistic representation of blue carbon dynamics at Boundary Bay prior to the implementation of a living dike structure. In addition, I compare our values with regional and global estimates to provide a well-rounded case study to facilitate the integration of the blue carbon dynamics of Boundary Bay into regional coastal planning of nature-based solutions for climate change mitigation.

In chapter 3, I expand our area of focus to include Boundary Bay and two

additional salt marshes in southern British Columbia – Cypress River Flats and Grice Bay – Kennedy River salt marshes in Clayoquot Sound region. Here I investigate how the use of different spatial datasets of salt marsh extent might impact regional estimates of blue carbon storage and accumulation rates within the province of British Columbia, Canada. In this chapter, I map areal extents for all salt marshes, and compare our estimates with regional and global salt marsh distribution datasets. I then analyze the impact of changes in areal estimations on carbon storage and annual carbon accumulations for each of the three salt marshes. Our work emphasizes the importance of accurate mapping efforts in facilitating more precise integration of blue carbon ecosystems into regional and global coastal planning of NCSs.

This research makes a valuable contribution to the work being undertaken at the School of Resource and Environmental Management (REM) at Simon Fraser University and Parks Canada through integration of biophysical quantification of salt marsh areas, C storage and accumulation rates and placing those findings in a policy context. Our salt marsh case studies create an understanding of the complexity of blue carbon dynamics, while identifying uncertainties and knowledge gaps which need to be addressed for nature-based solutions to contribute meaningfully towards climate change mitigation. This research resonates with REM's idea that environmental problems cannot be solved based only on narrow research conducted in single disciplines, but through interactions among both the social and natural sciences.

Chapter 2. Blue Carbon at Boundary Bay

2.1. Abstract

Boundary Bay is home to the 222-ha salt marsh in southern British Columbia with documented levels of stored carbon, while the planned construction of a living dike will likely modify its carbon dynamics. This study collected 18 sediment cores and vegetation surveys, year-round porewater salinities at 22 coring locations and 128 additional depth profiles to quantify C stocks, storage, and accumulation rates (CARs) from the middle (BBM), eastern (BBE) and far east Mud Bay (MB) sites within Boundary Bay. C stocks (±SD) in Boundary Bay averaged 69.7 ± 35.7 (high marsh) and 40.7 ± 36.4 Mg C ha^{-1} (low marsh) down to the depth of peat layer, with C stocks in western Boundary Bay (BBW, BBM) significantly higher than the east (BBE, MB). C storage at Boundary Bay ranged between (mean ± SD) 16,000 ± 4,300 - 18,000 ± 5,000 Mg C (depending on the methodology used), with western study sites (BBW, BBM) comprising 87% of that total, while eastern study sites (BBE, MB) only made up 13% of that total. Average CARs in BBE (37 ± 27 g C m^{-2} yr^{-1}) are significantly lower than regional averages, while overall Boundary Bay marsh CAR average (103 ± 37 g C $m^{-2}yr^{-1}$) is comparable to regional averages on the Pacific coast of North America. Annual average porewater salinities in Boundary Bay's western portion (21.1 ± 4.26) were significantly higher compared to the east (12.5 ± 2.75). High marsh sites at BBE measured salinities below 18 ppt 80% of the time, with groundwater within 20 cm of the surface at all times of year. These results suggest potentially high CH_4 emissions at BBE high marsh, which could be prioritized for future GHG monitoring, especially during the warm summer months. Low marsh areas in eastern Boundary Bay (BBE, MB) made up 62% of the eastern marsh area, and 37-42% of the total carbon stock. The planned expansion of low marsh area in BBE and MB through living dike construction has implications for a long-term increase in low-marsh C stocks. This study suggests that the eastern portion of the marsh (BBE, MB) has decreased by ~35% since 1930, which might be partially attributed to the construction of Highway 99 in 1942.

Keywords: blue carbon; salt marsh; Boundary Bay; carbon stock; porewater salinities; coastal management

2.2. Introduction

Tidal salt marshes are recognized for their important role in blue carbon (C) sequestration and long-term storage capacity while occupying a relatively small percentage of land area (Drexler et al. 2019, McLeod et al. 2011; Duarte et al. 2013; Crooks et al. 2014; Chmura et al. 2003; Bridgham et al. 2006; Kauffman et al. 2020, Peck et al. 2020). In recent years, restoration and conservation of tidal salt marshes have received increased attention as a natural method for blue carbon ecosystems to compensate for anthropogenic global C emissions (Janousek et al. 2021; Irving et al. 2011). Ecosystem services provided by tidal marshes make them potentially important contributors to natural climate solutions (NCSs). NCSs are defined as a suite of protection, improved management, and restoration actions or pathways in wetlands to conserve, manage and restore ecosystems and provide additional climate mitigation beyond business as usual (Drever et al. 2021; ECCC 2021). However, NCSs require further investigation to ensure their sustainability due to limited available information on blue carbon dynamics of salt marshes in British Columbia. For example, our site in eastern Boundary Bay currently lacks specific knowledge about marsh area, C stocks, C accumulation rates, associated GHG emissions, and historic processes of marsh expansion or erosion, all of which could influence its ability to serve as a long-term C sink.

Boundary Bay salt marsh is an excellent example of coastal tidal marsh ecosystem that is being considered for application of an NCS. Boundary Bay is the largest salt marsh in southwestern British Columbia, spanning more than 200 ha. It provides critical habitat for many aquatic organisms and is considered a potentially important blue carbon ecosystem (Gailis et al. 2021; Dashtgard 2011). Environment and Climate Change Canada has committed to help fund a living dike pilot project in Delta and Surrey (City of Surrey 2021; Readshaw, Wilson, and Robinson 2018). A living dike is a type of flood protection structure that uses a naturally existing salt marsh to enhance its protection against storm surges and flooding. It is a nature-based alternative to fortifying or building new grey infrastructure such as the existing man-made dike. In addition, this green infrastructure (i.e., natural vegetative system that provides ecosystem services) has the potential to play a role in climate change mitigation through C storage while helping protect neighboring farmlands and regional infrastructure (Gailis

et al. 2021). This project involves collaboration between the two municipalities and the Semiahmoo First Nation to manage and enhance portions of the Boundary Bay marsh as a natural sea level rise defense mechanism (Readshaw, Wilson, and Robinson 2018).

The C sequestration potential of Boundary Bay salt marsh may be further enhanced due to implementation of the living dike project. However, while previous work has quantified the areal extent, C stocks, and CARs in the far western portion of Boundary Bay (Gailis et al. 2021), data on C dynamics are lacking for the eastern portion of Boundary Bay marsh, where the proposed experimental sites for the living dike are located (Readshaw, Wilson, and Robinson 2018). Filling in this missing piece of the puzzle is an important next step to obtain a more holistic understanding of the areal extent of its ecosystems and the different processes operating in high and low marsh zones. In addition, we lack the context of how the marsh is changing in response to local environmental conditions (river inputs and storm events) and human modifications such as its man-made dike and the influx of logs from forestry and nutrients from agricultural lands adjacent to the marsh.

Even less is known about the potential contributions of greenhouse gas emissions to the total C budget of Boundary Bay salt marsh. While wetland ecosystems can act as a C sink, they can also act as C sources that emit greenhouse gases such as methane (CH_4) and nitrous oxide (N_2O) to the atmosphere (Poffenbarger et al. 2011; Wollenberg et al. 2018). Among these indicators, porewater salinity has been identified as an important driver of methanogenesis, which is the production of methane by microbes known as methanogens. Poffenbarger et al. 2011 suggests that polyhaline tidal marsh ecosystems with porewater salinities greater than 18 are suspected to have significantly lower CH_4 emissions compared to other freshwater marshes with lower salinities. However, recent research suggest that methane emissions are influenced by multiple environmental factors, including groundwater table between 10-20 cm of the soil surface, low porewater salinity, warm air temperature, near-neutral pH, and microbial communities (Janousek et al. 2021). Therefore, initial measurements of these environmental indicators that provide information on the overall GHG balance of the Boundary Bay salt marsh is critical for developing effective wetland conservation and climate mitigation policies.

In this chapter, I map the total areal extent, volume, C stocks, and accumulation rates (CARs) at the eastern portion of Boundary Bay, including Mud Bay. I measure dry bulk density (DBD), percent carbon (%C), estimated C stocks and storage for all Boundary Bay marsh based on 40 sediment cores collected from the high and low marsh areas. I used ^{210}Pb radiometric dating on three cores to estimate marsh age and CARs for eastern Boundary Bay site (BBE). I also present new, year-round porewater salinity measurements as a first step towards examining the relationship between marsh C storage and greenhouse gas (GHG) emissions, which is currently not well understood in the Boundary Bay salt marsh. I combine these new results with the previously published data on the western portion of the marsh (Gailis et al. 2021) to provide a more holistic quantification of area and carbon dynamics in Boundary Bay for use in climate change mitigation efforts. In addition, I compare our values with regional and global estimates to provide a well-rounded case study to facilitate the integration of the blue carbon dynamics of Boundary Bay into regional coastal planning of nature-based solutions for climate change mitigation.

2.3. Methods

2.3.1. Study Area

Boundary Bay is a shallow, sheltered bay situated on the Canada-United States border in southwestern British Columbia (BC), adjacent to the municipalities of Delta to its west and Surrey to its east, and is the traditional territory of the Semiahmoo Nation. Prior to the late 1950s, the shoreline of Boundary Bay was one of the most productive shellfish harvesting locations in the Pacific coast, mainly used for oyster farming. In early 1960's, operation licences were suspended due to sewage pollution from the Serpentine and Nicomekl rivers (Readshaw, Wilson, and Robinson 2018). One of Semiahmoo Nation's traditional use of the Bay included the use of oyster shells as a natural marsh barrier.

To its north, the entire length of the urban marsh is bounded by a 26 km man-made dike built in 1895 and renovated in 1948 following the Fraser Valley Flood (Shepperd 1981). The dike is adjacent to agricultural and residential land, greenhouses, a golf course, a domestic airport, and a highway. The Boundary Bay salt marsh spans 19 km from Mud Bay to western Boundary Bay and extends approximately 0.5 km at its

widest points, measured perpendicular to the dike in its western and eastern portions. For the purposes of this study, I divide the Bay into four study areas: Mud Bay, eastern, mid, and western Boundary Bay, located within cities of Surrey and Delta, BC (Figure 1).

Boundary Bay receives its freshwater and sediment inflows through the Serpentine and Nicomekl Rivers located in the northeast by Mud Bay. These small rivers originate a ~35 kilometers inland and discharge a minor amount of sediment into the bay (Swinbanks and Murray 1981). To the north, the Fraser River discharges a large amount of freshwater and sediment into the Strait of Georgia. However, freshwater and sediment input from the Fraser River into Boundary Bay is limited by Point Roberts peninsula extending down on the west side of the bay. Sediment breaking off the Pleistocene cliffs at Point Roberts is a present-day source of surface sediment to the Bay, which include gravel, sand, silty sand, mud, peat, and driftwood/shell accumulations (Shepperd 1981; Swinbanks and Murray 1981). The circulation in the bay is impacted by dominant large-wave-generating winds approaching Boundary Bay from the south-east, while tidal currents flow in from the south-west (Dashtgard 2011). The bedrock beneath the bay is known to be Pliocene/Miocene formations (Shepperd 1981).

The rates of sedimentation at Boundary Bay are low (0.42 mm yr^{-1}) with relatively clear, saline (24-29 ppt) waters (Swinbanks and Murray 1981). The western portion of the marsh is expanding (Kellerhals and Murray (1969); Gailis et al. 2021), whereas most of the mid and eastern portions are thought to be receding due to the water current and wind dynamics in the Bay (Swinbanks and Murray 1981). The tides in the Bay are a mixed semidiurnal type, with two high and two low tides every day (Shepperd 1981). The mean tidal range is 2.7 m, with a maximum spring tide of 4.1 m and minimum neap tide of 1.5 m (Swinbanks and Murray 1981).

Boundary Bay is protected from westerly and southwesterly winds by the Point Roberts peninsula. The prevailing winds come from the east and southeast. The area experiences a west coast maritime climate with mild, wet winter and warm, dry summers (Shepperd 1981). Historical meteorological records from 2000-2010 recorded at Delta Ladner South station, located 5 km northwest of western Boundary Bay study site record an annual average rainfall of 976.5 mm and annual snowfall of 31.6 mm. Highest precipitation is recorded in November, and the least in August. Average annual

temperature is 9.6°C, with the highest recorded in July and August at 16.9°C and lowest in January at 2.8°C (Government of Canada 2021).

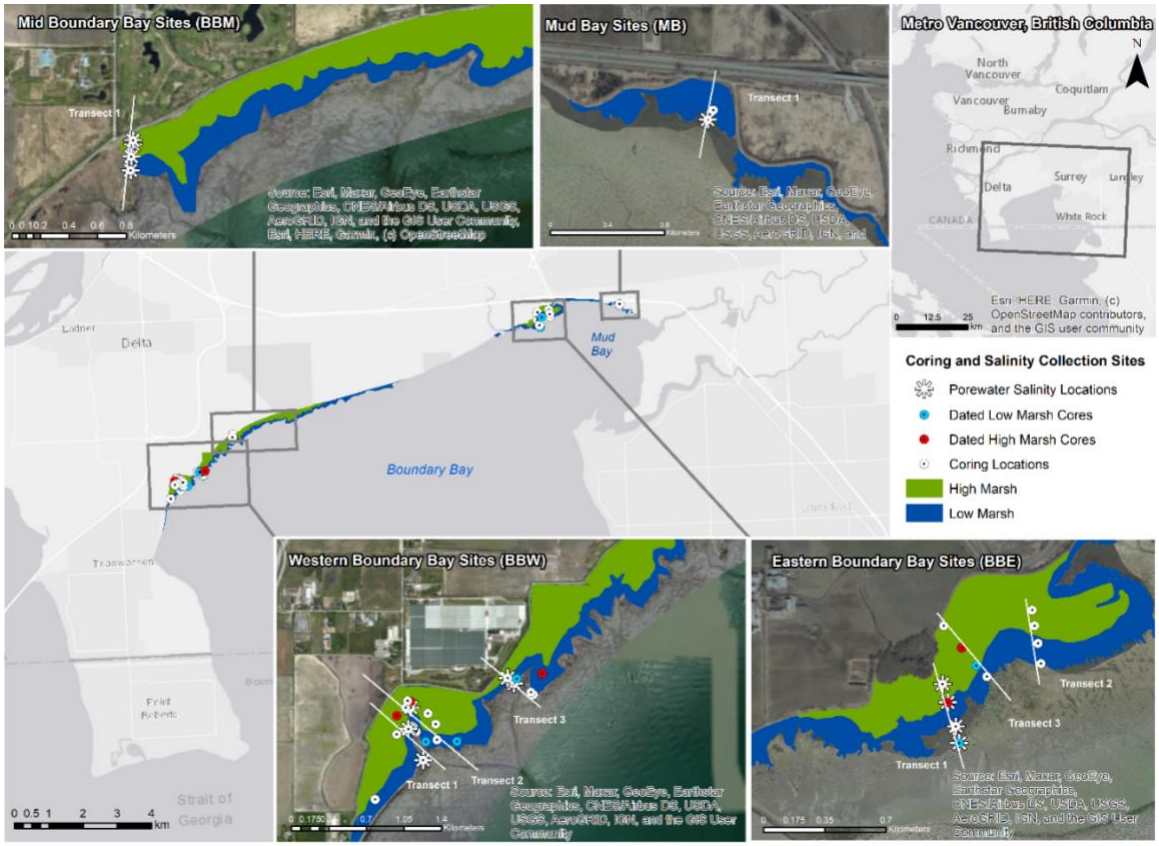

Figure 2.1. Map of the location of Boundary Bay marsh in the municipalities of Delta and Surrey, British Columbia.
The map inserts show the locations of four study sites within the western, mid, eastern and Mud Bay portions of Boundary Bay. The red dots indicate the high marsh cores that were dated; the blue dots indicate the low marsh cores that were dated; the white dots indicate all other cores. The fourteen locations where year-round pore water salinities were collected are marked using a white asterisk beneath the coring markers. Base map source: ArcGIS 2021.

2.3.2. Field Sampling

At western Boundary Bay, 22 sediment cores (13 high marsh, 9 low marsh) were collected by Gailis et al. (2021) between 2014-2018. To build upon this work, I collected an additional 18 cores (8 high marsh, 10 low marsh) at three new study areas along Boundary Bay: mid (BBM), eastern (BBE) and Mud Bay (MB). These cores were collected between October 2020 - January 2021 using an AMS sediment corer pushed into the ground to the depth of refusal (Table 1). All cores were collected into PVC tubes of 4.7 cm diameter at the field site and stored in Parks Canada laboratory and

refrigerated at 4˚C. Sampling included vegetation surveys at all coring sites using a 50 x 50 cm quadrat. Since it was the largest study site, additional sample collection in BBE involved collection of marsh depth measurements and ^{210}Pb dating of four selected cores (2 high marsh, 2 low marsh).

Finally, to understand how seasonal changes in porewater salinity might influence greenhouse gas emissions, monthly porewater salinities were collected at 22 sampling sites within the four study areas from biweekly from June to August 2020, and monthly from November 2020 to May 2021 (Figure 1). One low marsh porewater collection site was located at MB; two high marsh and two low marsh sites each were located at BBE, BBM, and BBW, with one additional salt panne site at BBW. Porewater salinities were collected at 8 additional sites at the time of sediment core collection at eastern Boundary Bay along transects BBE2 (n=4) and BBE3 (n=4) (Table 5). Porewater was collected using a porewater sipper and a syringe to suction water from the soil at a depth of 25 cm. Approximately 60 mL of soil porewater were extracted, and the salinity was tested using hand-held YSI 556 and YSI ProQuatro conductivity meters (± 0.1 ppt) calibrated for salinity and conductivity.

Western Boundary Bay (BBW)

This study area is in the northwestern tip of Boundary Bay, to the east of 64th St, Delta, B.C (Figure 1) that was previously sampled in 2014-2018 (Gailis, 2020; Gailis et al. 2021). The salt marsh at this study site is 6 km long at its leading edge, 0.5 km wide at its widest point measured perpendicular to the dike. Gailis et al. (2021) measured vegetation composition, marsh volume and area, C stocks and C accumulation rates. To these estimates I have added year-round monthly porewater salinity measurements at two high marsh, two low marsh, and one salt panne site.

Mid Boundary Bay (BBM)

This study area is located to the south of 72nd St, Delta, BC (Figure 1), just to the east of BBW. The salt marsh at this study site is 6.0 km long at its leading edge, 0.4 km wide at its widest point measured perpendicular to the dike. To the east, there is no marsh present for 3.2 km in the center portion of the bay due to water currents and wind patterns (Dashtgard 2011). To the west, the marsh expands and reaches one of its widest portions. For sediment coring, one transect was chosen perpendicular to the dike,

and I collected four sediment cores in total, with two each from high and low marsh zones (Table 1).

Eastern Boundary Bay (BBE)

This region represents the second largest study area and is located south of the Highway 99 loop to the east of 112 St, Delta, BC, on the eastern side of the bay, built in 1942 (Figure 1). The salt marsh at this study site is 5 km long at its leading edge, 0.5 km wide at its widest point measured perpendicular to the dike. Sampling occurred at the widest portion of the marsh.

For sediment coring, three transects were chosen perpendicular to the dike to best represent the marsh variability from high to low marsh. To evenly distribute the cores between high and low marsh zones, I collected 12 sediment cores in total, with four cores along each transect, with each transect having two cores from high and two cores from the low marsh zones (Table 1).

To estimate the total volume of the marsh, marsh depths were also measured with their associated GPS coordinates at 128 additional sampling sites throughout the eastern portion of Boundary Bay (Appendix A, Table A2). Twenty transects separated every 50 m were selected; the seven sampling sites along each transect were approximately 20 m apart. The depth measurements were collected by inserting a 6ft plasticized metal garden stick down the marsh until it hit the depth of refusal. Depth of refusal is a reasonable estimate of organic soil thickness because it assumes that organic soil is easier to penetrate than underlying sands and/or bedrock (Howard et al. 2014). For the purposes of this study at Boundary Bay, I assume that the underlying sand layer was formed prior to marsh initiation (Howard et al. 2014). These depth profiles were used to calculate marsh thickness to derive more robust estimates of C stocks.

Mud Bay (MB)

This study area is in farthest east portion of Boundary Bay in Mud Bay Park, to the east of 127a St, Surrey, B.C (Figure 1). The salt marsh at this study area is 2.0 km long at its leading edge, 0.1 km wide at its widest point measured perpendicular to the dike. It is located at the northeast corner of Boundary Bay, close to the freshwater influx from Serpentine and Nicomekl Rivers to its east. The marsh in this area is

underdeveloped due to the low sediment input from the rivers and receding marsh due to eroding water currents (Dashtgard 2011). A high marsh area was not present due to the small size of the marsh. For sediment coring, one transect was chosen perpendicular to the dike, and I collected two sediment cores in total, one from mid marsh and one from low marsh areas (Table 1). Previous measurements were conducted by Ducks Unlimited at this MB study site to monitor surface elevations using rod surface elevation tables and marker horizons, groundwater levels, water salinities, and water temperature (Christensen and Vadeboncoeur 2019).

Table 2.1. Sediment core sampling information collected in mid, eastern and Mud Bay portions of Boundary Bay, Delta/Surrey, B.C. Location coordinated collected using a handheld Garmin GPS device.

Site	Core ID	Latitude	Longitude	Date Collected	Soil Type at Bottom of Core	Compression Factor
Mid Boundary Bay	BBM1H2	49.059523	-123.023055	Dec 2020	Peat	1.50
	BBM1H1	49.059350	-123.023039	Dec 2020	Silt	1.43
Eastern Boundary Bay	BBE1H2	49.086211	-122.899688	Oct 2020	Silt	1.15
	BBE1H1	49.085586	-122.899418	Oct 2020	Clay/Peat	1.67
	BBE2H2	49.088689	-122.895083	Nov 2020	Peat	2.00
	BBE2H1	49.088160	-122.894959	Nov 2020	Clay/Peat	1.74
	BBE3H2	49.088167	-122.899620	Jan 2021	Sand	1.04
	BBE3H1	49.087424	-122.898694	Jan 2021	Sand	1.11
Mid Boundary Bay	BBM1M	49.058850	-123.023169	Dec 2020	Sand	1.15
	BBM1L	49.058290	-123.023210	Dec 2020	Sand	1.16
Eastern Boundary Bay	BBE1M	49.084792	-122.899006	Oct 2020	Sand	1.04
	BBE1L	49.084225	-122.898820	Oct 2020	Sand	1.14
	BBE2M	49.087579	-122.894784	Nov 2020	Silt	1.69
	BBE2L	49.086900	-122.894637	Nov 2020	Silt	1.48
	BBE3M	49.086833	-122.897938	Jan 2021	Sand	1.78
	BBE3L	49.086460	-122.897408	Jan 2021	Sand	1.17
Mud Bay	MB1M	49.089408	-122.866763	Dec 2020	Sand	1.07
	MB1L	49.089140	-122.867000	Dec 2020	Silt	1.63

2.3.3. Marsh Area and Volume

Marsh Area

To estimate the area of high and low marsh zones, Google Earth Pro 2021 tools were used with a Google satellite base map compiled from images taken on June 12, 2019. High and low marsh zones were delineated by eye using differences in vegetation color on Google Satellite base map imagery (Figure 5 and Figure C1). Low-marsh plant assemblages were a lighter shade of green compared to the darker green of the high marsh plant assemblages (Chastain et al. 2021; Gailis et al. 2021). This delineation was further verified by vegetation surveys at 18 sediment coring and salinity sampling sites. Gailis et al. (2021) determined that using vegetation surveys aligned perfectly with the visual delineations made using satellite color. Therefore, all areas not containing sediment cores were delineated only by eye using 2019 Google Satellite base map vegetation coloration.

High and low marsh area calculations for BBW, BBM, BBE and MB were done separately and summed up to derive the total Boundary Bay marsh area. The 140-ha study area determined as “western marsh” by Gailis et al. was split into BBW (80 ha) and BBM (84 ha) sites for the purposes of this study. A 24-ha low marsh area adjacent to the eastern edge of Gailis et al. marsh was added on to our BBM study site for more accurate total marsh area reporting (Figure C1).

Marsh Volume

The volume of all marsh area of BBE study site, located south of the Highway 99 loop to the east of 112 St. was calculated using ArcMap 10.3 tools (Figure C1). The volume was calculated using the 140 depth profiles to interpolate a surface elevation using the Kriging geostatistical method, which uses surface elevation to calculate an estimate of the volume. In the process, the highest surface elevations are made lower than the deepest points recorded (0.98 m) and the lowest surface elevations are then higher than the shallowest points recorded (0.07 m). Moreover, due to the shallow depths recorded (0.07m – 0.98 m) in relation to the distance between measurements (25 – 75 m) and the variable topography of the marsh, the estimated volume can result in high uncertainty (Amante 2018; Gailis et al. 2021). Thus, a second, simplified method was used to verify the interpolated volume through kriging by multiplying the area of the

same bounded area used for the kriging method and multiplying it by the average of the un-compacted core lengths.

Change in Marsh Area

Google Earth Pro tools were used with 50 by 50 m resolution Google Satellite base map and an air photo taken on July 28, 1930 (provided by NRCan, National Earth Observation Data) to estimate marsh expansion in Eastern Boundary Bay and Mud Bay. The 1930 air photo was overlain on the Google Satellite base map to measure how much the marsh has changed (Figure 6). This study acknowledges that significant changes to marsh area were likely made during Highway 99 construction in South Surrey between 1940's and 1960's.

2.3.4. Laboratory Work

Sediment cores (n=18) were sectioned into 1-cm increments in the Parks Canada laboratory. Each 1-cm section represented a 17.35-cm^3 volumes of sediment for the entire length of each core on average (PVC pipe diameter = 4.7 cm). Some materials were found across both high and low marsh cores. First, thin layers of white-colored clay mixed in with peat or silt were found between 15 – 62 cm below surface across four high marsh cores and three low marsh cores in BBM and BBE. Previous work suggested that 15% of the sediment load in the lower Fraser River is clay, which could be one source of this material (Dashtgard and La Croix 2015). Other sources could be sediment input into the Bay from local rivers such as Nicomekl and Serpentine, and sediment breaking off from Point Roberts bluffs (Shepperd 1981; Swinbanks and Murray 1981). Second, wood debris was common in all four cores at BBM, and in two high marsh cores and four low marsh cores in BBE. Wood chunks were found more in low marsh cores (n=6) than high marsh cores (n=4). As wood chunks are obvious sources of allochthonous carbon, all wood chunks were removed at this step before weighing and %LOI measurements.

The samples were weighed for wet weight using a laboratory analytical balance (± 0.01 mg) and then oven-dried at 60˚C for 72 hours. The dry weight was then used to determine dry bulk density (DBD, g/cm^3) of each sample (Howard et al. 2014):

$$DBD\ (\frac{g}{cm^3}) = \frac{DW_i\ (g)}{V_w\ (cm^3)} \quad (1)$$

Where DW_i is the dry weight and V_w is the wet volume of the sample (17.35 cm^3).

After any wood chunks and roots were removed, these samples were then ground individually using a 500 ml porcelain lab mortar and pestle to avoid carbon contamination. Ground soil samples were combusted in a muffle furnace (4 hrs at 550 ˚C) to burn off all the organic compounds (Howard et al. 2014). These samples were then weighed to calculate loss-on ignition (%LOI) to quantify the fraction of organic carbon (%C) lost in each sample:

$$\%\, LOI_{550} = \left(\frac{DW_i - DW_f}{DW_i}\right) \times\ 100 \quad (2)$$

Where DW_i is the initial dry weight and DW_f is the dry weight after burning.

To quantify the fraction of organic C more accurately, a subset of samples (n = 39) was burnt a second time in the muffle furnace for 2 hours at 1000ºC to determine inorganic carbon (IC) (Heiri et al. 2001):

$$\%LOI_{1000} = \left(\frac{DW_{550} - DW_{1000}}{DW_i}\right) \times\ 100 \quad (3)$$

Where DW_i is the initial dry weight, DW_{550} is the dry weight after the 500ºC burn and DW_{1000} is the dry weight after the 1000ºC burn.

Percent inorganic carbon (IC) was assumed to be negligible in all samples based on coulometric measurements conducted previously in western Boundary Bay showing that IC values were less than 0.01% (Gailis et al. 2021). Due to inaccessibility of laboratories during the COVID-19 pandemic, an elemental analysis could not be completed to determine a regression relationship to calculate %C from %LOI for this study. This assumption was confirmed based on the 1000ºC burn conducted in this study. Therefore, based on geographical proximity of our sites, I used the regression relationship determined by Gailis et al. (2021) for western Boundary Bay to calculate %C from %LOI for all mid, eastern and Mud Bay sites, where r^2 = 0.97.

$$\%C = 0.44(\%LOI) - 1.33 \quad (4)$$

2.3.5. Carbon Stocks

Soil carbon densities and carbon stocks

Carbon stocks were quantified by measuring the soil carbon density (SCD) for each 1-cm sample down to the basal peat layer (n = 18, n = 8 for high marsh, n = 10 for low marsh). I measure C stocks down to the base of peat layer due to the shallow depth and young age of BC salt marshes (Chastain et al. 2021). In Clayoquot Sound, C stocks accumulated in the past 30 years accounted for 81% of C calculated down to the base of the peat layer. Similarly, at western Boundary Bay, CARs averaged 20 ± 17% higher during the last 30 years than for the entire core due to higher carbon concentrations in the upper layers of the marsh (Gailis et al. 2021).

Soil carbon density (SCD, $\frac{g}{cm^3}$) is derived from the measured dry bulk density (DBD) and percent carbon for each centimeter interval sampled (Gailis et al. 2021; Howard et al. 2014).

$$SCD\left(\frac{gC}{cm^3}\right) = \left(\frac{\%C}{100}\right) \times DBD\left(\frac{g}{cm^3}\right) \quad (5)$$

The C stock for each core (g C cm^{-2}) was calculated by summing all SCDs at 1-cm intervals down to the base of peat layer in each core (Chastain et al. 2021).

$$Cstock_{core}\left(\frac{gC}{cm^2}\right) = \sum_{i=0}^{n} SCD_i \times 1\,cm \quad (6)$$

where n is the depth within the core (cm) and SCD_i is the SCD of each 1-cm interval of soil (g C cm^{-3}).

Compression factors

As the cores experienced various levels of compression during field sampling, a compression factor was used to compensate for the error. To calculate the compression factor (Table 1), the length of core penetration was divided by the length of core sample recovered:

$$Compression\ Factor = \frac{length\ of\ core\ penetration\ (cm)}{length\ of\ core\ (cm)} \quad (7)$$

$$Uncompressed\ Depth\ (cm) = Compression\ Factor\ x\ Compressed\ Length\ of\ Core\ \ (cm) \quad (8)$$

To calculate the uncompressed SCD, the compressed SCD for each 1 cm soil section was divided by the compression factor for that specific core (Howard et al. 2014):

$$Uncompressed\ SCD\ estimation\ (\frac{g\ C}{cm^3}) = \frac{Compressed\ SCD\ (\frac{g\ C}{cm^3})}{Compression\ Factor} \quad (9)$$

The compression factor is used for the entire length of the core, which assumes that all sections of the core are compacted equally. However, I note that soil type, moisture content, dry bulk density, and therefore also the ability to compact are likely to vary throughout the core. As a result, assuming a constant compression factor may be an oversimplification (Howard et al. 2014; Morton and White 1997).

High marsh, Low marsh, and Total Marsh Carbon Storage

I calculate C storage (Mg C) for high and low marsh zones separately to avoid generalizations between high and low marsh C stocks, SCDs, and depth of peat layers (DoPs). I add the C storage for high and low marsh zones together to obtain the total marsh C storage down to the base of the peat layer. Then, I calculate C storages at each of the four study sites separately and add them together to derive the total C storage of Boundary Bay marsh. Although previous C storage was calculated for BBW by Gailis et al. (2021), I re-calculate C stocks to the basal peat layer for each BBW core for consistency with BBE sites. Based on this re-calculation, I also revise BBW C storage since our areal estimates for the BBW marsh are also larger than reported in Gailis et al. 2021.

Three methods are used to calculate C storages. The traditional method estimates total C storage by calculating core C stocks (Mg C ha^{-1}) to the base of the peat layer in each core, using compressed SCDs and multiplying it by the area (ha) of the marsh (Gailis et al. 2021). I use compressed SCDs in this calculation because the amount of carbon down to the base of peat layer of each core remains the same regardless of whether the core is compressed.

$$Cstorage_{Marsh}\ (Mg\ C\ ) = A \times C\ stock_{core} \quad (10)$$

Where $C\ stock_{core}$ is the average core C stock to the base of the peat layer calculated using compressed SCDs, and A is the area of the marsh.

The other two methods, kriging volume and simplified volume methods, use volume of the marsh (m^3) to calculate the total C stock.

The simplified volumetric approach multiplies the marsh area by mean uncompressed core length (averaged from 12 cores for BBW, 4 cores for BBM, 12 cores for BBE, 2 cores for MB, total n = 30) down to the peat layer to derive the simplified volume (m^3), which is then multiplied by the uncompressed SCD. This calculation is done for each of the four study sites separately and then added together to derive the Boundary Bay marsh total.

$$Cstorage_{Marsh}\,(Mg\ C) = A \times Z_{core} \times Average\ Uncompressed\ SCD \quad (11)$$

Where A is the area of the marsh and Z_{core} is the average uncompressed core length down to the peat layer.

For the third approach, the kriging volume (m^3) is calculated using the kriging geostatistical tool on ArcMap 10.3 derived from depth profiles. This method was only completed for our two sites with extensive depth profiling: BBW (n=176) and BBE (n=140). Although this measurement does not estimate C storage for the entire Boundary Bay marsh, it is a useful reference for comparing C storage to other estimation methods for two of our most extensively cored study sites. The kriging volume for the BBW and BBE is then multiplied by the average of uncompressed SCDs for each site to derive the marsh C stock (Gailis et al. 2021).

$$Cstorage_{Marsh}\,(Mg\ C) = V_{kriging} \times Average\ Uncompressed\ SCD \quad (12)$$

Where $V_{kriging}$ is the geostatistical kriging-derived marsh volume (m^3)

2.3.6. Carbon Accumulation Rates

To determine carbon accumulation rate (CARs), wet subsamples from four BBE cores (BBE1H1 and BBE3H1 for high marsh, BBE1L and BBE3M for low marsh) were sent to Flett Research Ltd (Winnipeg, MB) for ^{210}Pb radiometric dating analysis. Cores were selected to best represent the spatial variability and typical sediment layers in the marsh. All cores were corrected for depth compression using the compression factors

calculated above to ensure accurate sedimentation rates (Morton and White 1997; Gailis et al. 2021).

All samples sent for radiometric dating were freeze dried for four days, and the dry sample material was ball milled before being sent for radioisotope analyses. Between seven to 13 dried subsamples per core were analyzed for ^{210}Pb measurements. Activities of ^{210}Pb were determined by α-spectrometry through its granddaughter ^{210}Po, assumed in secular equilibrium. The atmospheric, unsupported, or excess ^{210}Pb ($^{210}Pb_{exs}$) fraction used to derive the age-depth model was determined as the difference between the total ^{210}Pb activity and its parent nuclide ^{226}Ra activity (Table A3) (Eakins and Morrison 1978; Mathieu et al. 1988; USDE 1997). One to three ^{226}Ra measurements per core were measured and assumed to equal the supported ^{210}Pb ($^{210}Pb_{sup}$) measurements (Arias-Ortiz et al. 2018; Callaway et al. 2012; Appleby and Oldfield 1978; Ritchie and McHenry 1990). ^{226}Ra activities were determined by α-spectrometry at Flett Research using calibrated geometries in a glass vessel, Spectech UCS 30 Alpha Scintillation Spectrometer purged with helium, and sealed for at least 11 days. Samples were sealed and stored for two hours before counting to ensure secular equilibrium of ^{226}Ra daughters. ^{226}Ra was determined through counting ^{222}Rn activity for 60,000 seconds (Minimum Detectable Activity (MDA) = 0.0167 Bq kg^{-1}) (Durham and Joshi 1980; Pennington et al. 1973; Anderson and Hesslein 1987; Snidvongs and Smith 1992).

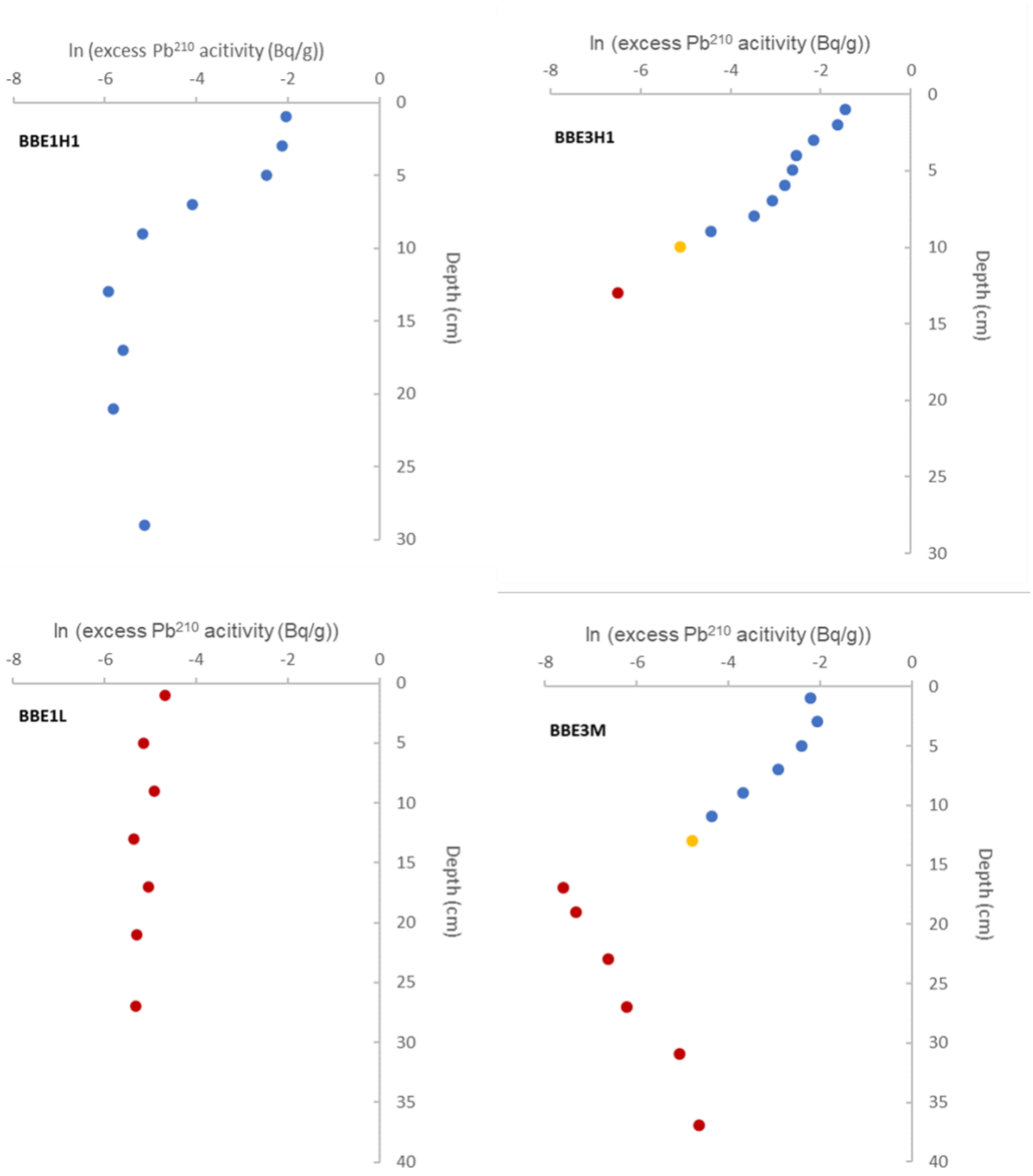

Figure 2.2 Downcore distribution of $^{210}Pb_{exs}$ in ln from the high marsh (top panels) and low marsh (bottom panels) in the eastern portion of Boundary Bay (BBE). Blue dots represent peat, orange dots represent silt, and red dots represent sand.

The 210Pb activity profile for BBE3M shows an exponential decrease of 210Pbexs with depth until 17.5 cm, and an unusual increase below that depth that is significantly higher than its 226Ra activity, indicating that the background level of 210Pb has not been achieved at the bottom in this core. It is suspected that the atmospheric sourced 210Pb was diluted by heavy sediments. For the purposes of the CRS analysis in this study, the deeper portion of the BBE3M core below 9.5 cm is discarded due to the increasing uncertainty of the sedimentation process.

The Constant Rate of Supply (CRS) model was used to develop the ^{210}Pb depth-age model (Appleby and Oldfield 1978; Appleby 2001; Arias-Ortiz et al. 2018). The CRS model assumes the supply of $^{210}Pb_{exs}$ to the sediment surface remains constant through time. In addition, any deviation from a constant concentration of $^{210}Pb_{exs}$ in the sediment is assumed to be due to changes in sedimentation rate. This model does not require that the rate of sediment accumulation be constant over time (Appleby and Oldfield 1978; O'Keefe Suttles et al. 2021; van Ardenne et al. 2021).

The CRS model uses the integration of the total inventory of $^{210}Pb_{exs}$ in a core, the length of the uncompressed sediment core, and the inventory of $^{210}Pb_{exs}$ in each interval in a core. Here, the interval (i) represents the sediment layer (or thickness) between each $^{210}Pb_{exs}$ measurement (cm). Flett Research Ltd. derived ages at each depth interval from the CRS model (t_{CRS}, yr) using the following method:

$$t_{CRS}\ (yr) = ln\left(\frac{total\ inventory\ of\ ^{210}Pb_{exs}}{i\ I_i\ DBD_i}\right) * 1/\ \lambda \qquad (13)$$

where *the total inventory of* $^{210}Pb_{exs}$ is the sum of the $^{210}Pb_{exs}$ in the sediment column, i is the interval thickness (cm) between each $^{210}Pb_{exs}$ measurement, I_i is the activity of $^{210}Pb_{exs}$ for interval (i), DBD_i is the dry bulk density (g cm^{-3}) for interval (i), and λ (0.03114) is the decay constant of ^{210}Pb.

Sedimentation Accumulation Rate (SAR, $\frac{cm}{yr}$) was calculated as:

$$SAR\left(\frac{cm}{yr}\right) = \frac{i}{t_x - t_0} \qquad (14)$$

Where i is the uncompressed depth interval (cm) between points A_x and A_0 within the core, t_x is the age estimated at the base of a given sediment core interval (A_x), and t_0 is the age at the top of the sediment interval (A_0).

The mass accretion rate (MAR, g cm^{-2}yr^{-1}) for each depth interval (i) in each core was calculated as:

$$MAR_i\ \left(\frac{g}{cm^2 yr}\right) = DBD_i\ \times\ SAR\ \left(\frac{cm}{yr}\right) \qquad (15)$$

where DBD_i is the measured uncompressed DBD for the depth interval between t_x and t_o.

For all cores sent for ^{210}Pb dating, carbon accumulation rates (CARs) were calculated from uncompressed core depths down to the depth at which percent carbon became negligible and $^{210}Pb_{exs}$ activity was still detectable. CARs are calculated in two steps. First, the fraction of carbon (C_i) was estimated as the total mass of carbon divided by the total mass of the bulk sediment in each core. This fraction was estimated by summing the soil carbon densities and dry bulk densities for each depth interval:

$$C_i = \frac{\sum_0^n SCD\left(\frac{g\,C}{cm^3}\right)}{\sum_0^n DBD\left(\frac{g}{cm^3}\right)} \quad (16)$$

Second, the carbon accumulation rate (CAR, $(\frac{g\,C}{m^2 yr})$) is calculated as the product of the mass accretion rate and the carbon fraction for each depth interval:

$$CAR\ \left(\frac{g\,C}{m^2 yr}\right) = C_i \times MAR\ \left(\frac{g}{m^2 yr}\right) \quad (17)$$

The average SAR, MAR, and CAR ± SD was then calculated for each core by averaging the values for all depth intervals where ^{210}Pb was measured.

2.3.7. Statistical Analysis

All data were tested for normality using the Shapiro-Wilk test for normality. T-tests were conducted for DBDs, SCDs, %C, C stocks, C storages, SARs, MARs, and CARs to test for any significant differences between high and low marsh sites, and between the four study areas (BBW, BBM, BBE, MB). The significance level of all the tests was set at α = 0.05. All statistical analyses were performed in R (RStudio 2015).

All raw data for BBW was derived from a previous study by Gailis et al. 2021. DBDs, SCDs, %C, C stocks and C storages were recalculated in this study down to the base of peat layer for consistency between all sites. I conducted new T-tests for recalculated DBDs, SCDs, %C, C stocks and C storages values in BBW to test for any significant differences between high and low marsh sites.

2.4. Results

2.4.1. Sediment Properties

Uncompressed depths of cores ranged from 27 to 66 cm (Table 1). Compression occurred in all cores during field sampling and was similar in both high and low marsh. Compression factors ranged between 1.04 and 2.00 in high marsh cores (n=8, average ± SD = 1.45 ± 0.34) and 1.04 to 1.78 in low marsh cores (n=10, average ± SD = 1.33 ± 0.28) (Table 1).

Soil horizons in high and low marsh cores differed in their composition (Figure 3), in terms of their organic peat layer thickness and materials found in their basal layers. High marsh cores (n=8) generally had a thick top organic peat layer composed of dark brown organic material (uncompressed average ± SD = 31 ± 24 cm), followed by layers with a mix of peat and silt or silty sand (Table 2). Cores BBE2H2 and BBE2H1 had the thickest organic peat layers at 66 and 63 cm, respectively. The bottom of two high marsh cores consisted of sand, two consisted of clay/peat mixture, two ended in silt, and two in peat. In contrast, low marsh sediment cores (n=10) had thinner top organic layers compared to high marsh cores (uncompressed average ± SD = 19 ± 15 cm). The bottoms of seven low marsh cores ended in a sand layer, and three in silt.

In all cores, percent weight carbon (%C) was highest in top peat layers, with the maximum being 30 %C in BBM1L for low marsh cores and 29 %C in BBE3H2 for high marsh cores. %C declined with depth (Figure B1, Appendix B). Bottom sand layers contained the lowest %C, reaching 0% C in both high and low marsh cores.

Across all Boundary Bay marsh cores, high marsh %C ± SD (14.5 ± 5.2 %) (n= 16) down to the base of peat layer was significantly greater than low marsh %C ± SD (6.6 ± 3.1 %) (n=14)) ($p<0.001$) (Figure 4e). A similar trend was observed in BBE (high marsh ± SD = 13.6 ± 3.2 % (n=6), low marsh ± SD = 5.8 ± 2.8 % (n=6)) ($p<0.01$) and BBW (high marsh ± SD = 16.2 ± 5.4 % (n=8), low marsh ± SD = 8.4 ± 3.8 % (n=4)) ($p<0.05$). No significant difference was observed between high and low marsh %C in BBM ($p>0.05$). No significant difference in %C was observed in cores with and without wood debris ($p=0.829$).

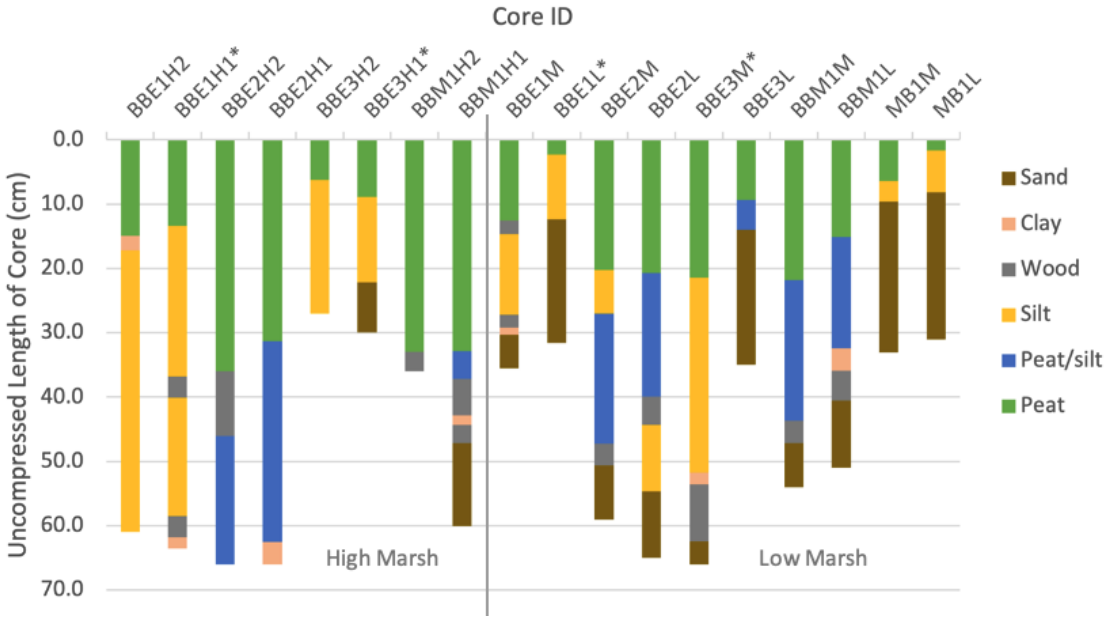

Figure 2.3 Soil horizons for all cores sampled in eastern (BBE), mid Boundary Bay (BBM) and Mud Bay (MB) in relationship to length of core (cm) (n=18).

Brown represents sand, light peach represents clay, grey represents wood, yellow represents silt, blue represents peat and silt mix, and green represents the top peat layer. All cores are shown with uncompressed depths. Wood chunks were removed for %C analyses. Dates cores are marked in asterisks*.

Overall, average %C down to the base of peat layer across both high and low marsh zones in western study sites (BBW, BBM, n=16) was significantly higher than %C in eastern study sites (BBE, MB, n=14) at Boundary Bay ($p<0.05$) (Figure 4f). Among all Boundary Bay sites, %C down to the base of peat layer was highest at BBW for high marsh zones (16.2 ± 5.4 %) (n=8) and BBM for low marsh zones (12.5 ± 5.5 %) (n=2) (Table 2, Figure 4a). MB had the lowest marsh %C values at 2.9 ± 1.3 % (n=2) (Figure 4c).

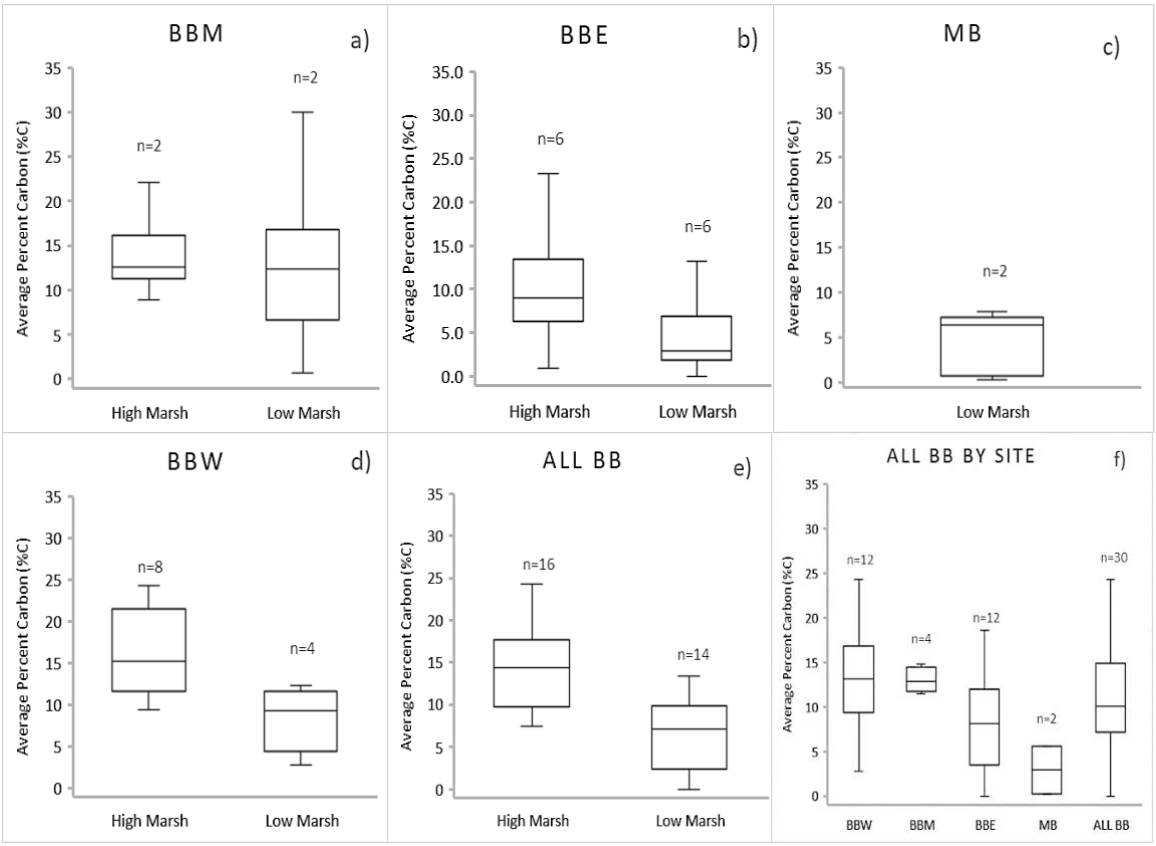

Figure 2.4 Average percent carbon (%C) down to the base of peat layer comparing high marsh cores to low marsh cores.

a) BBM) (t-value=0.739, p-value=0.537, p>0.05), b) BBE) (t-value=3.257, p-value=0.009, p<0.05), c) MB), and d) BBW (t-value=2.555, p-value=0.0286, p<0.05). e) all parts of Boundary Bay (ALL BB) (t-value=4.571, p-value=0.0001, p<0.001). f) Comparison of %C for all parts of Boundary Bay by site. ALL BB is a compilation of all cores in Boundary Bay (n=30). The middle line is the median and the top and bottom of the box are quantiles (Q1 and Q3), and the error bar is the largest and smallest value.

Across all Boundary Bay marsh cores, average uncompressed DBDs down to the base of peat layer in high marsh cores was significantly lower than in low marsh cores, where high marsh = 0.26 ± 0.11 g cm^{-3} (n=16), and low marsh = 0.46 ± 0.13 g cm^{-3} (n=14) (p<0.01) (Figure B4, Appendix B). A similar significance is observed in BBE (high marsh = 0.25 ± 0.14 g cm^{-3} (n=6), low marsh = 0.48 ± 0.13 g cm^{-3} (n=6)) (p<0.05) (Table 3). No significant difference in average DBD was found between high and low marsh cores in BBM and BBW (p>0.05).

When comparing all sites, MB had the highest average uncompressed DBD across all low marsh sites at 0.65 ± 0.15 g cm^{-3}, while BBM had the lowest DBD values for both high (0.23 ± 0.06 g cm^{-3}) (n=2) and low marsh cores (0.36 ± 0.21 g cm^{-3}) (n=2) (Figure B4, Appendix B). No significant difference in uncompressed DBD was observed

between the western (BBW, BBM) and eastern study sites (BBE, MB) at Boundary Bay ($p>0.05$).

Across all study sites at Boundary Bay, uncompressed high marsh SCD down to the base of peat layer (0.031 ± 0.007 g C cm^{-3}) (n=16) was significantly higher than uncompressed low marsh SCD (0.018 ± 0.007 g C cm^{-3}) (n=14) ($p<0.05$) (Figure 5e). At BBE, a similar significance was observed, where high marsh SCD = 0.025 ± 0.007 g C cm^{-3} (n=6) was significantly higher than low marsh SCD = 0.015 ± 0.006 g C cm^{-3}) (n=6) ($p<0.05$) (Table 3, Figure 5b). No significant difference in SCDs was observed between high and low marsh cores in BBM and BBW ($p>0.05$).

Uncompressed SCDs in the western portion of the marsh (BBW, BBM, n=16) were significantly higher than that of eastern study sites (BBE, MB, n =14) at Boundary Bay ($p<0.05$) (Figure 5f). Average low marsh SCD was significantly higher in BBM (0.031 ± 0.012 g C cm^{-3}) (n=2) compared to all other sites (BBW, BBE, MB) (n=12) ($p<0.05$).

Across all cores, the uncompressed DoP was recorded to estimate the base of the marsh (Table 3, Figure 6). Across Boundary Bay, no significant difference was observed in DoP between low (19 ± 13 cm) and high (29 ± 20 cm) marsh areas ($p>0.05$) (Table 2). The maximum uncompressed DoP was recorded in core BBE2H2 at 66 cm, and the minimum was recorded in cores BBE1L and MB1L at 2 cm each. No significant difference was observed between cores from the western portion and eastern portions of Boundary Bay ($p>0.05$).

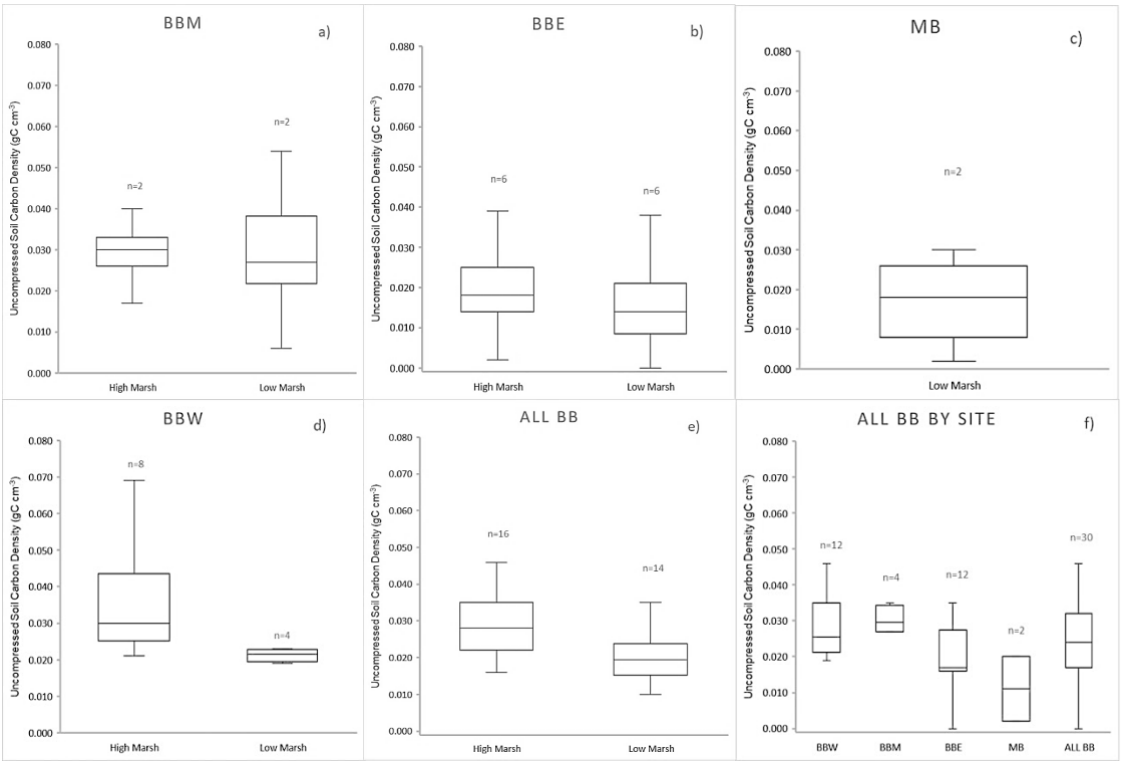

Figure 2.5 Average uncompressed soil carbon density (SCD, g C cm^{-3}) down to the base of peat layer comparing high marsh cores to low marsh cores.

a) BBM (t-value=0.3180, p-value=0.781, p>0.05), b) BBE (t-value=3.782, p-value=0.013, p<0.05), c) MB and d) BBW (t-value=2.009, p-value=0.1382, p>0.05). e) all parts of Boundary Bay (ALL BB) (t-value=3.4553, p-value=0.0043, p<0.05). f) Comparison of SCD for all parts of Boundary Bay by site. ALL BB is a compilation of all cores in Boundary Bay (n=30). The middle line is the median and the top and bottom of the box are quantiles (Q1 and Q3), and the error bar is the largest and smallest value.

Table 2.2 **Summary of compressed core sediment data (± SD): depth of core, depth of peat layer, dry bulk density (DBD), average percent carbon (%C), average soil carbon density (SCD), and core C stock down to the base of peat layer for all cores in Boundary Bay, Delta/Surrey, B.C. The compressed C stocks are used in C storage calculations.**

Site	Core ID	Compressed Depth of Core (cm)	Compressed Depth of Peat Layer (cm)	Average Compressed DBD (gcm^{-3})	Average %C	Average Compressed SCD ($g\ C\ cm^{-3}$)	Compressed Core Carbon stock down to peat layer ($Mg\ C\ ha^{-1}$)
High Marsh							
Mid Boundary Bay	BBM1H2	24	24	0.41 ± 0.10	12.4 ± 3.2	0.048 ± 0.007	115.8
	BBM1H1	42	26	0.27 ± 0.06	14.8 ± 3.1	0.039 ± 0.010	100.2
	Average ± SD	33 ± 13	25 ± 1	0.34 ± 0.08	13.6 ± 3.2	0.044 ± 0.009	108.0 ± 11.1
Eastern Boundary Bay	BBE1H2	53	13	0.21 ± 0.15	18.6 ± 6.4	0.032 ± 0.008	41.7
	BBE1H1	38	8	0.40 ± 0.26	8.7 ± 4.3	0.026 ± 0.005	20.8
	BBE2H2	33	33	0.40 ± 0.15	9.3 ± 3.9	0.034 ± 0.012	112.3
	BBE2H1	38	36	0.42 ± 0.15	7.4 ± 3.8	0.028 ± 0.011	100.9
	BBE3H2	26	6	0.33 ± 0.30	17.8 ± 9.7	0.037 ± 0.007	22.0
	BBE3H1	27	8	0.36 ± 0.16	12.9 ± 6.4	0.039 ± 0.013	30.9
	Average ± SD	36 ± 10	17 ± 14	0.35 ± 0.19	12.5 ± 5.8	0.033 ± 0.009	54.8 ± 41.0
High Marsh Average ± SD		**35 ± 10**	**19 ± 12**	**0.35 ± 0.17**	**12.8 ± 5.1**	**0.035 ± 0.009**	**68.1 ± 42.7**
Boundary Bay Average* ± SD		**27 ± 10**	**18 ± 11**	**0.38 ± 0.15**	**14.5 ± 5.2**	**0.044 ± 0.009**	**69.7 ± 35.7**
Low Marsh							
Mid Boundary Bay	BBM1M	47	38	0.35 ± 0.21	11.5 ± 4.0	0.031 ± 0.010	118.1
	BBM1L	44	28	0.46 ± 0.26	13.4 ± 6.9	0.040 ± 0.018	112.0
	Average ± SD	46 ± 2	33 ± 7	0.41 ± 0.23	12.5 ± 5.5	0.036 ± 0.014	115.0 ± 4.3
Eastern Boundary Bay	BBE1M	34	12	0.75 ± 0.15	2.5 ± 0.9	0.018 ± 0.004	21.8
	BBE1L	28	2	0.78 ± 0.22	0.0 ± 0.0	0.000 ± 0.000	0
	BBE2M	35	12	0.43 ± 0.19	7.7 ± 2.9	0.029 ± 0.007	34.8
	BBE2L	44	27	0.74 ± 0.16	2.2 ± 1.6	0.015 ± 0.010	40.2
	BBE3M	37	12	0.52 ± 0.25	8.5 ± 6.3	0.032 ± 0.017	33.0
	BBE3L	30	12	0.49 ± 0.09	6.5 ± 3.0	0.031 ± 0.015	32.5
	Average ± SD	35 ± 6	13 ± 8	0.62 ± 0.17	4.6 ± 2.5	0.021 ± 0.009	27.1 ± 14.6
Mud Bay	MB1M	31	6	0.49 ± 0.31	5.6 ± 2.6	0.021 ± 0.008	12.7
	MB1L	19	1	1.36 ± 0.00	0.25 ± 0.0	0.003 ±0.000	0.3

	Average ± SD	25 ± 8	4 ± 4	0.92 ± 0.16	2.9 ± 1.3	0.012 ± 0.004	6.52 ± 8.74
Low Marsh Average ± SD		**35 ± 9**	**15 ± 12**	**0.64 ± 0.18**	**5.8 ± 2.8**	**0.022 ± 0.009**	**40.6 ± 41.7**
Boundary Bay Average* ± SD		**29 ± 10**	**14 ± 10**	**0.60 ± 0.16**	**6.6 ± 3.1**	**0.024 ± 0.009**	**40.7 ± 36.4**

*Boundary Bay Average ± SD value is calculated using data collected in this study in mid, east Boundary Bay and Mud Bay, combined with data collected by Gailis et al. 2021 (Table 2) in western Boundary Bay down to the base of peat layer. Compressed Core Carbon stock down to peat layer (Mg C ha^{-1}) is calculated by summing all SCDs at 1-cm intervals down to the base of peat layer in each core.

Table 2.3 Summary of uncompressed core sediment data (± SD) for compression factor, depth of core, depth of peat layer, dry bulk density (DBD), average soil carbon density (SCD) down to the base of peat layer for all cores in Boundary Bay, Delta/Surrey, B.C.

Site	Core ID	Compression Factor	Uncompressed Depth of Core (cm)	Uncompressed Depth of Peat Layer (cm)	Average Uncompressed DBD (gcm^{-3})	Average Uncompressed SCD ($g\ C\ cm^{-3}$)
High Marsh						
Mid Boundary Bay	BBM1H2	1.50	36	36	0.27 ± 0.07	0.032 ± 0.004
	BBM1H1	1.43	60	37	0.19 ± 0.05	0.027 ± 0.007
	Average ± SD	1.46 ± 0.05	48 ± 17	37 ± 1	0.23 ± 0.06	0.030 ± 0.006
Eastern Boundary Bay	BBE1H2	1.15	61	15	0.18 ± 0.13	0.028 ± 0.007
	BBE1H1	1.67	63	13	0.24 ± 0.15	0.016 ± 0.003
	BBE2H2	2.00	66	66	0.20 ± 0.07	0.017 ± 0.006
	BBE2H1	1.74	66	63	0.24 ± 0.09	0.016 ± 0.006
	BBE3H2	1.04	27	6	0.32 ± 0.29	0.035 ± 0.007
	BBE3H1	1.11	30	9	0.32 ± 0.14	0.035 ± 0.011
	Average ± SD	1.45 ± 0.40	52 ± 19	29 ± 28	0.25 ± 0.14	0.025 ± 0.007
High Marsh Average ± SD		1.45 ± 0.34	51 ± 17	31 ± 24	0.25 ± 0.12	0.026 ± 0.006
Boundary Bay Average* ± SD		1.53 ± 0.51	45 ± 19	29 ± 20	0.26 ± 0.11	0.031 ± 0.007
Low Marsh						
Mid Boundary Bay	BBM1M	1.15	54	44	0.31 ± 0.19	0.027 ± 0.009
	BBM1L	1.16	51	32	0.40 ± 0.22	0.035 ± 0.015
	Average ± SD	1.15 ± 0.01	52 ± 2	38 ± 8	0.36 ± 0.21	0.031 ± 0.012
Eastern Boundary Bay	BBE1M	1.04	35	13	0.72 ± 0.14	0.017 ± 0.004
	BBE1L	1.14	32	2	0.68 ± 0.19	0.000 ± 0.000
	BBE2M	1.69	59	20	0.26 ± 0.11	0.017 ± 0.004
	BBE2L	1.48	65	40	0.50 ± 0.11	0.010 ± 0.006
	BBE3M	1.78	66	21	0.29 ± 0.14	0.018 ± 0.009
	BBE3L	1.17	35	14	0.42 ± 0.08	0.026 ± 0.013
	Average ± SD	1.38 ± 0.31	49 ± 16	18 ± 13	0.48 ± 0.13	0.015 ± 0.006
Mud Bay	MB1M	1.07	33	6	0.46 ± 0.29	0.020 ± 0.008
	MB1L	1.63	31	2	0.83 ± 0.00	0.002 ±0.000
	Average ± SD	1.35 ± 0.40	32 ± 1	4 ± 3	0.65 ± 0.15	0.011 ± 0.004
Low Marsh Average ± SD		1.33 ± 0.28	46 ± 14	19 ± 15	0.49 ± 0.15	0.017 ± 0.007
Boundary Bay Average* ± SD		1.33 ± 0.26	43 ± 13	19 ± 13	0.46 ± 0.13	0.018 ± 0.007

Boundary Bay Average ± SD value is calculated using data collected in this study in mid, east Boundary Bay and Mud Bay, combined with data collected by Gailis et al. 2021 (Table 2) in western Boundary Bay down to the base of peat layer.

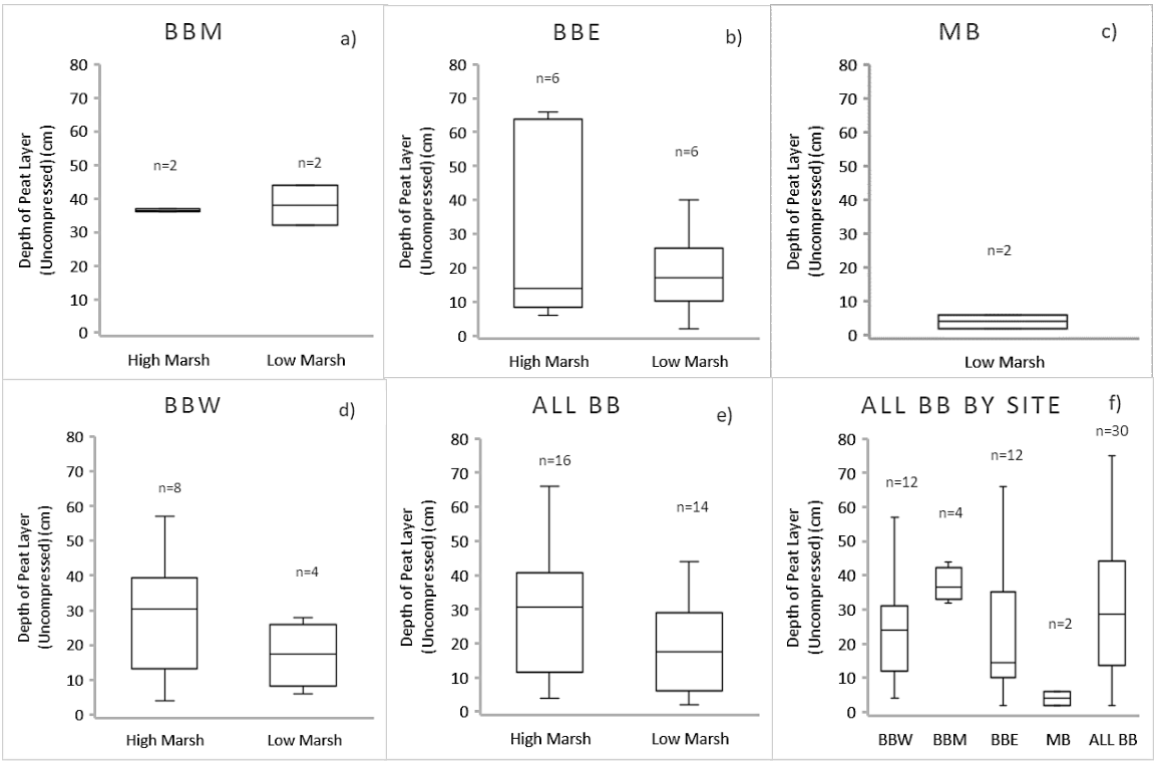

Figure 2.6 Uncompressed depth of peat layer (cm) comparing high marsh cores to low marsh cores.

a) BBM (t-value = 0.249, p-value = 0.827, p>0.05), b) BBE (t-value =0.826, p-value = 0.428, p>0.05), c) MB and d) BBW (t-value =0.8819, p-value =0.4428, p>0.05) e) all parts of Boundary Bay (t-value =1.767, p-value =0.088, p>0.05). f) all cores in Boundary Bay by site. ALL BB is a compilation of all cores in Boundary Bay (n=30). The middle line is the median and the top and bottom of the box are quantiles (Q1 and Q3), and the error bar is the largest and smallest value.

2.4.2. Marsh Area, Carbon Stocks, Carbon Storage, and Accumulation Rates

The total area of the Boundary Bay salt marsh is 222 ha, with high and low marsh each accounting for 50% of the total marsh area. In the western portion of the Boundary Bay marsh, BBW covers a total area of 80 ha, with high marsh accounting for 62.5% (50 ha), and low marsh accounting for 37.5% (30 ha) of the total marsh area. BBM contains the highest marsh area among all sites at 84 ha, with high marsh accounting for 46% (39 ha), and low marsh accounting for 54% (45 ha) of the total marsh area (Figure 7a). A marsh area comparison with a 1930 aerial photo of BBW and a portion of BBM conducted by Gailis et al. (2021) indicates that the western portion of the Boundary Bay marsh has expanded by about 26 ha (~20%) in the past 88 years (1930 - 2018) (Gailis et al. 2021).

In the eastern portion of the Boundary Bay marsh, BBE spans 52 ha, with high marsh accounting for 42% (22 ha), and low marsh accounting for 58% (30 ha) of the total marsh area. MB marsh spans an area of 6 ha, with low marsh accounting for 100% of the total marsh area (Figure 7b). The black arrow in Figure 8a indicates a channel in the 1930s imagery that is larger than present-day channel, which inundated a larger portion of BBE high marsh area. Additionally, the construction of Highway-99 appears to have cleared and filled some areas of the low marsh located between BBE and MB sites, indicated by red circles in Figure 8a. Dike renovations appear to have impacted the shape and size of the MB marsh, primarily near the coring sites. The MB marsh area on which cores were extracted appear to have developed after 1930 (Figure 8b). Overall, the eastern portion of the Boundary Bay marsh (BBE, MB) has reduced in area by about 18 ha (~35%) in the past 91 years (1930 - 2021) (Figure 8b). We are aware of changes to marsh area made through Highway 99 construction in South Surrey in 1942. Comparison with 1930s satellite photos shows that the marsh is smaller likely due to highway construction.

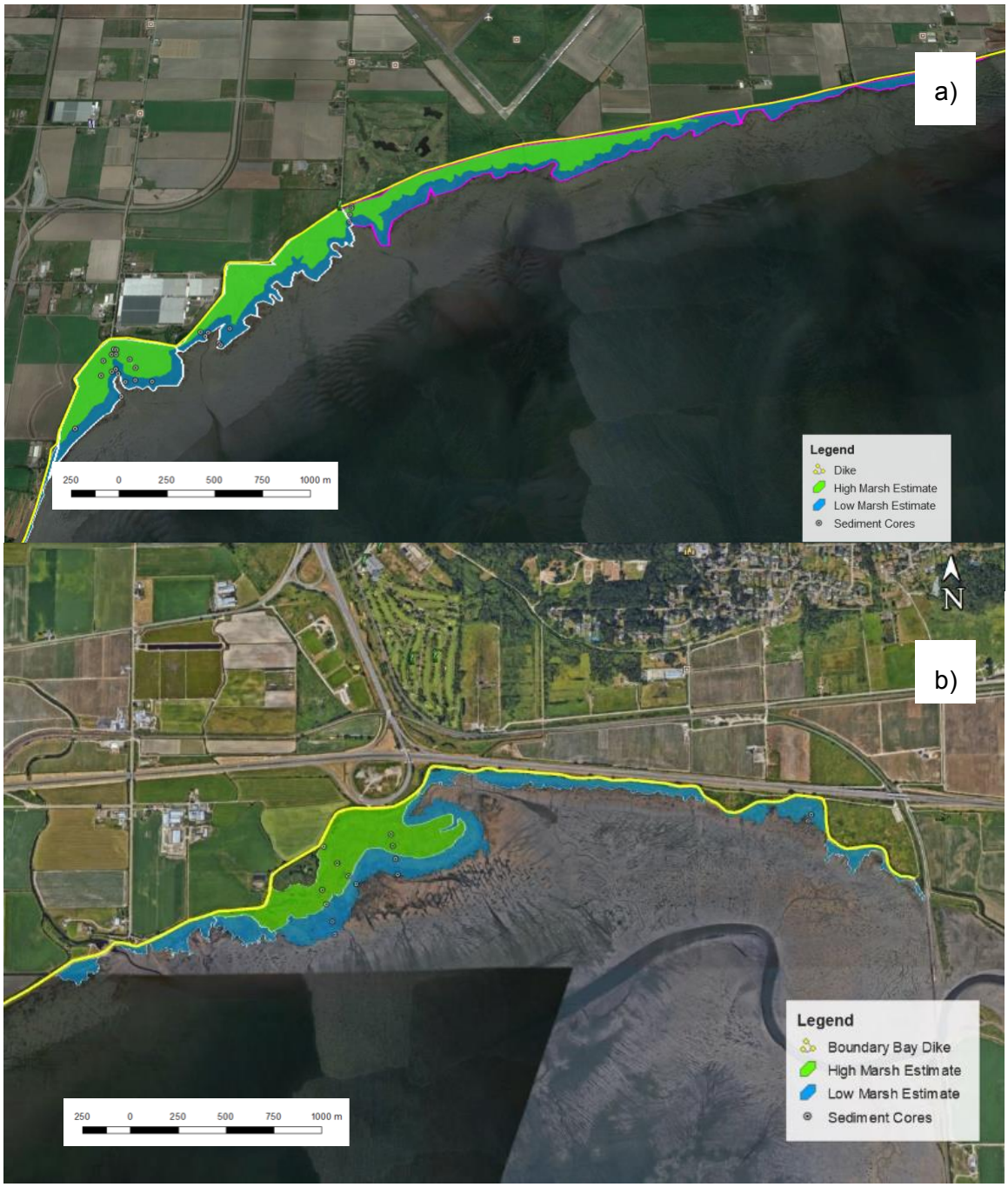

Figure 2.7 (a) High and low marsh areas in western Boundary Bay: BBW (white outline) and BBM (purple outline) in Delta, B.C. (b) High marsh and low marsh areas in eastern Boundary Bay: BBE and MB in Delta/Surrey, B.C.

High marsh is represented by green and low marsh by blue solid fill. High and low marsh areas in BBW and BBE were determined through vegetation surveys at 176 and140 sample points, respectively. All other areas were determined by variations in vegetation color using Google satellite base map imagery and field notes. Base Map: Google Earth Pro 2021.

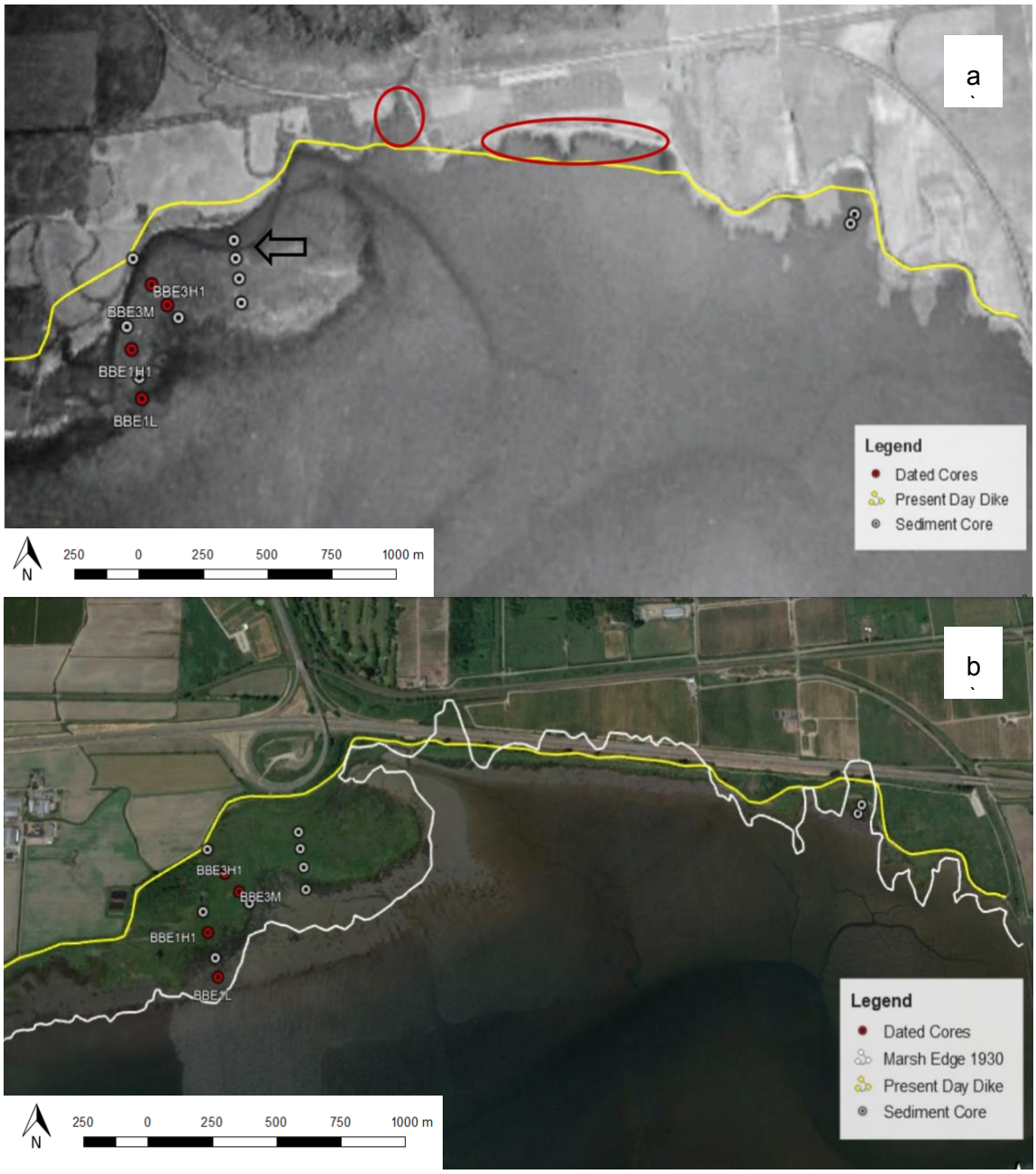

Figure 2.8 (a) Historical imagery of BBE and MB from 1930. Air photo from 1930 was superimposed onto Google Earth 2021 base map allowing for marsh area comparison.

The yellow line represents the present-day dike along the marsh. The red dots represent the four dated cores from eastern Boundary Bay. The white dots represent all other sediment cores. The black arrow indicates a larger than present-day channel in BBE high marsh area. The red circles indicate marsh areas cleared out and filled in during Highway 99 and dike construction post-1930s. Base Map Source: NRCan, National Earth Observation Data.

(b) Map of present-day BBE and MB relative to the leading edge of marsh in 1930.

The white line represents the marsh edge in 1930. The yellow line represents the present-day dike along the marsh. The red dots represent the four dated cores from eastern Boundary Bay. The white dots represent all other cores. The 1930 air photo used to delineate the leading edge of the marsh in 1930 was obtained from NRCan, National Earth Observation Data. Base Map Source: Google Earth Pro 2021.

In BBE, average compressed C stocks ranged from 20.8 to 112.3 Mg C ha^{-1} (n=6, mean= 54.8 ± 41.0 Mg C ha^{-1}) in high marsh and 0 to 40.2 Mg C ha^{-1} (n=6, mean = 27.1 ± 14.6 Mg C ha^{-1}) in low marsh (Figure 9b, Table 2). The average of 27.1 ± 14.6 Mg C ha^{-1} for low marsh cores is skewed by the negligible C stock of core BBE1L (0 Mg C ha^{-1}). When BBE1L is not considered, the average low marsh C stock is significantly higher at 32.5 ± 6.71 Mg C ha^{-1}.

No significant difference between C stocks for high and low marsh was observed at all sites in Boundary Bay ($p>0.05$) (Figure 9a, 9b, 9d). MB reported the lowest average C stock for low marsh cores at 6.52 ± 8.74 Mg C ha^{-1} (n=2) (Figure 9c). Among all sites, BBM (n=4) reported significantly higher C stocks compared to all other sites at Boundary Bay (n=28) (Figure 9f) ($p<0.01$). Overall, high marsh C stocks at Boundary Bay (69.7 ± 35.7 Mg C ha^{-1}) were significantly higher than low marsh C stocks (40.7 ± 36.4 Mg C ha^{-1}) (Figure 8e) ($p<0.05$). In addition, C stocks in the western sites (BBW, BBM, n=18) were significantly higher than in the eastern sites (BBE, MB, n=14) ($p<0.01$) (Figure 9f).

According to calculations conducted in this study down to the base of peat layer of the marsh, BBW had a total carbon storage (C storage) of 4,800 ± 2,300 Mg C (traditional method), with 3,600 ± 1,600 Mg C in the high marsh and 1,200 ± 680 Mg C in the low marsh (Table 4). Total C storage using the simplified volume-based method was 6,100 ± 1,300 Mg C (high marsh = 5,000 ± 1,000 Mg C, low marsh = 1,100 ± 300 Mg C). The simplified volumetric method yielded similar low marsh C storage as the traditional method, but higher C storage for high marsh. Lastly, Kriging Volume yielded the highest C storage estimate out of all three methods at 6,400 ± 1,300 Mg C.

BBM had a total C storage of 9,400 ± 630 Mg C (traditional method), with 4,200 ± 430 Mg C in the high marsh and 5,200 ± 200 Mg C in the low marsh. Based on average core lengths down to the peat layer (n=4), the estimated C storage for BBM was estimated at 9,600 ± 3,000 Mg C using the simplified volume-based method (high marsh

= 4,200 ± 850 Mg C, low marsh = 5,400 ± 2,100 Mg C). Detailed depths were not collected at this site for kriging volumetric carbon stock estimates.

BBE had a total C storage of 2,000 ± 1,300 Mg C (traditional method), with 1,200 ± 890 Mg C in the high marsh and 820 ± 440 Mg C in the low marsh. C storage for BBE was estimated at 2,300 ± 780 Mg C using the simplified volume-based method (high marsh = 1,500 ± 440 Mg C, low marsh = 820 ± 340 Mg C). Kriging volume method (2,400 ± 800 Mg C) yielded a similar total C storage estimate to the simplified volumetric method at BBE.

At MB, the marsh had a total C storage of 38 ± 51 Mg C (traditional method) in the low marsh. Based on average core lengths down to the peat layer (n=2), the simplified volume estimate was lower at 5.4 ± 9.4 Mg C. Detailed depths were not collected at this site for kriging volumetric estimates.

The Boundary Bay marsh had a total C storage of 16,300 ± 4300 Mg C (traditional method), with 9000 ± 2900 Mg C in the high marsh and 7300 ± 1400 Mg C in the low marsh. The simplified volumetric C storage estimate for Boundary Bay was 18,000 ± 5,000 Mg C (high marsh = 10,700 ± 2,300 Mg C, low marsh = 7,300 ± 2,700 Mg C). The kriging volumetric C storage total for BBW and BBE was 8,800 ± 2,100 Mg C, which is comparable to its simplified volumetric total (8,400 ± 2,100 Mg C). The traditional total for BBW and BBE was 6,800 ± 3,600 Mg C.

Based on the traditional and simplified volumetric approaches, BBM reported significantly higher C storages compared to all other sites ($p<0.01$). On the other hand, C storage at MB was two to three orders of magnitude lower than other sites (Table 4). The simplified volumetric C storage estimate was consistently higher than the traditional estimate for all sites except MB. Out of all C storage estimate approaches, the kriging volumetric approach yielded the highest C storage for sites with detailed depth profiling. Using both the traditional and simplified methods, the combined C storage in western study sites (BBW, BBM) is one of magnitude higher compared to that of eastern study sites (BBE, MB). Western boundary bay (BBW and BBM) holds nearly 90% of the total C storage at Boundary Bay marsh using both the traditional and simplified methods.

Table 2.4 Comparison of carbon storage estimates (Mg C) for all sites at Boundary Bay, derived from three different methods.

The traditional method was calculated using the total high and low marsh area (m^2) multiplied by the average compressed core carbon stock down to peat base (Mg C ha^{-1}) (Equation 10). The two volumetric methods multiply volume (m^3) by the average uncompressed soil carbon density (g C m^{-3}) down to peat base. Volumes are estimated using a simplified approach of multiplying average uncompressed core lengths (m) down to peat base by area (m^2) (Equation 11), and a kriging geostatistical method (Equation 12) using ArcMap 10.3 tools.

Marsh Zonation	Area (m^2)	Simplified Volume (m^3)	Kriging Volume (m^3)	Average Uncompressed SCD down to peat base (g C cm^{-3}) ± SD	Carbon Storage (Mg C) ± SD		
					Traditional Method	Simplified Volume	Kriging Volume
BBW							
High	500,000	140,000	150,000	0.035 ± 0.007	3,600 ± 1,600	5,000 ± 1,000	5,300 ± 1,100
Low	300,000	51,000	60,000	0.021 ± 0.006	1,200 ± 680	1,100 ± 300	1,200 ± 360
Total	800,000	190,000	210,000	0.031 ± 0.006	4,800 ± 2,800	6,100 ± 1,300	6,400 ± 1,300
BBM							
High	390,000	140,000	-	0.030 ± 0.006	4,200 ± 430	4,200 ± 850	-
Low	450,000	170,000	-	0.031 ± 0.012	5,200 ± 200	5,400 ± 2,100	-
Total	840,000	310,000	-	0.030 ± 0.009	9,400 ± 630	9,600 ± 3,000	-
BBE							
High	220,000	63,000	64,000	0.025 ± 0.007	1,200 ± 890	1,500 ± 440	1,600 ± 450
Low	310,000	56,000	58,000	0.015 ± 0.006	820 ± 440	820 ± 340	860 ± 350
Total	530,000	120,000	120,000	0.020 ± 0.007	2,000 ± 1,300	2,300 ± 780	2,400 ± 800
MB							
Low	59,000	2,400	-	0.002 ± 0.004	38 ± 51	5.4 ± 9.4	-
All Boundary Bay							
High	1,100,000	340,000	-	0.031 ± 0.007	9,000 ± 2,900	11,000 ± 2,300	-
Low	1,100,000	280,000	-	0.018 ± 0.007	7,300 ± 1,400	7,300 ± 2,700	-
Total	2,200,000	620,000	-	0.025 ± 0.007	16,000 ± 4,300	18,000 ± 5,000	-

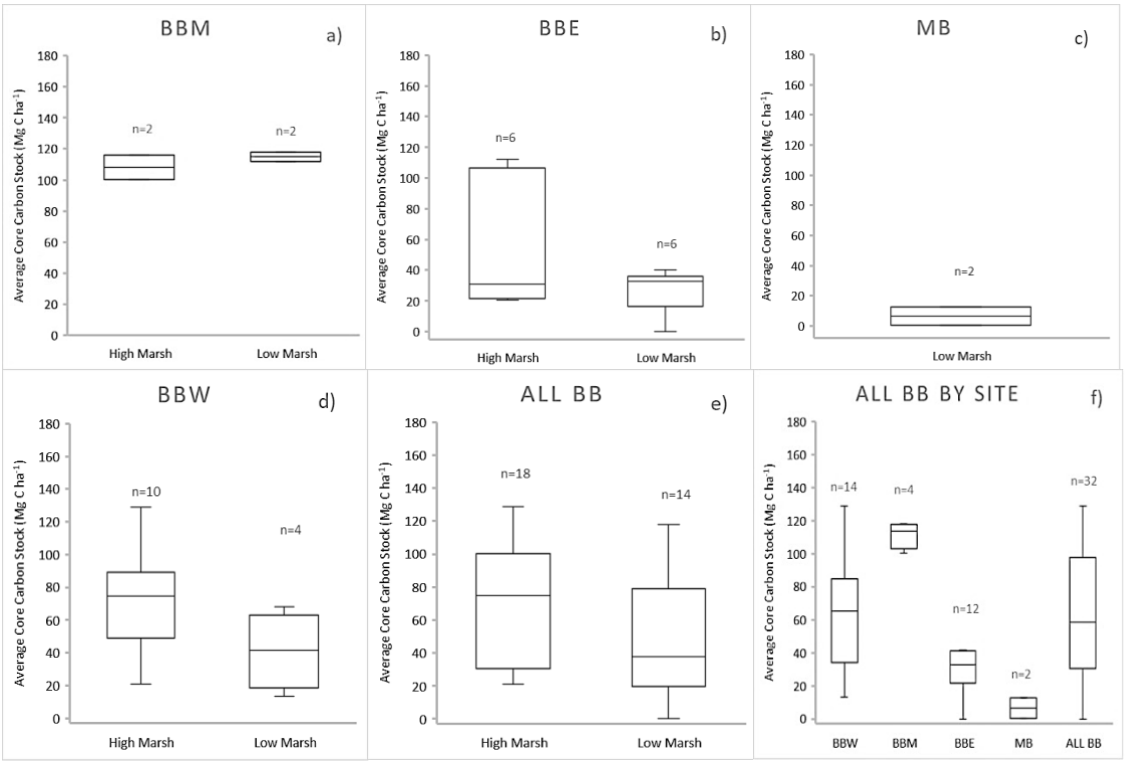

Figure 2.9 Average compressed core C stocks (Mg C ha^{-1}) down to the base of peat layer calculated using compressed SCDs comparing high and low marsh cores.

a) BBM (t-value =0.842, p-value =0.489, p>0.05). b) BBE (t-value =1.561, p-value =0.150, p>0.05) c) MB d) BBW (t-value =1.314, p-value =0.280, p>0.05) e) all parts of Boundary Bay (t-value =2.959, p-value =0.0111, p<0.05). f) Average core C stocks (Mg C ha^{-1}) for all cores at each site. ALL BB is a compilation of all cores in Boundary Bay (n=32). The middle line is the median and the top and bottom of the box are quantiles (Q1 and Q3), and the error bar is the largest and smallest value.

In BBE, high marsh SARs ranged from 0.13 ± 0.051 to 0.25 ± 0.078 cm yr^{-1} and low marsh SAR was 0.15 ± 0.10 cm yr^{-1} (Table 5). High marsh MARs ranged from 426 ± 92 to 982 ± 762 g m^{-2}y^{-1} and low marsh MAR was 309 ± 138 g m^{-2} y^{-1}. High marsh CARs ranged from 24 ± 13 to 46 ± 26 g C m^{-2} yr^{-1} (average = 35 ± 20 g C m^{-2} y^{-1}). Low marsh CAR was 40 ± 41 g C m^{-2} yr^{-1}. No significant differences were found between the high and low marsh SARs, MARs, and CARs for BBE (p>0.05). The basal ages of the sediment cores (depth of sand layer) ranged from 50 to 88 years, with no statistically significant difference between high and low marsh settings sampled (p>0.05).

CARs averaged 103 ± 37 g C m^{-2} yr^{-1} for all sites at Boundary Bay, with higher rates near the surface and declining with depth. MARs averaged 1130 ± 399 g m^{-2}y^{-1} for all sites, with lower rates near the surface and increasing with depth (Figure 10a, 10d, and 10g), displaying an inverse relationship to CARs. SARs averaged 0.29 ± 0.18 cm yr

f)

$^{-1}$ for all sites at Boundary Bay (Figure 10b, 10e, and 10h). The average basal age for all dated cores was 78 ± 29 years, with no statistically significant difference between BBW and BBE sites (p = 0.627). No significant differences were observed between average SARs, MARs, and CARs between BBW and BBE (p=0.460) (Table 4, Figure 11).

The CRS model could not be applied to the low marsh core BBE1L since it did not meet the following assumptions: constant input of ^{210}Pb, core that is long enough to include all measurable atmospheric source ^{210}Pb, constant sediment accumulation rate. In addition, the ^{210}Pb activity at the top of the core is significantly higher than the ^{226}Ra activity measured, indicating that the background level of ^{210}Pb has not been achieved in this core. The irregular shape of BBE1L ^{210}Pb profile indicates intense mixing, erosion, and highly variable sediment accumulation rates at this sampling site. The maximum age estimated for the base of this core is 45 years. Since the CRS model could not be applied to this core, SARs, MARs, and CARs could not be calculated for BBE1L.

Table 2.5 Geochronological analyses (^{210}Pb dating) and carbon content were used to estimate individual core, high and low marsh means ±SD, eastern marsh means ±SD, and all marsh means ±SD, sedimentation rates (SAR), mass accumulation rates (MAR), and carbon accumulation rates (CAR) using the CRS model.

Depth of uncompressed core represents the maximum depth at which carbon was recorded for samples that were sent for ^{210}Pb dating and the depth that was used to calculate SAR, MAR, and CAR. See Appendix Table A3 for raw data.

Core ID	Uncompressed core depth (cm)	Average uncompressed DBD ± SD (g cm^{-3})	SAR ± SD (cm yr^{-1})	MAR ± SD (g m^{-2} yr^{-1})	CAR ± SD (g C m^{-2}yr^{-1})	Basal Age (yr)
High Marsh						
BBE1H1	28	0.36 ± 0.22	0.25 ± 0.078	982 ± 762	24 ± 13	50
BBE3H1	10	0.39 ± 0.24	0.13 ± 0.051	426 ± 92	46 ± 26	88
Average ± SD	19 ± 13	-	0.19 ± 0.065	704 ± 427	35 ± 20	69 ± 27
Low Marsh						
BBE3M	16	0.22 ± 0.05	0.15 ± 0.100	309 ± 138	40 ± 41	75
All Marsh						
Eastern Avg ± SD	18 ± 9	-	0.18 ± 0.076	572 ± 331	37 ± 27	71 ± 19
Boundary Bay Avg* ± SD	20 ± 6	-	0.29 ± 0.18	1130 ± 399	103 ± 37	78 ± 29

*Boundary Bay Avg ± SD values are calculated using data collected in this study in BBE, combined with CIC CARs calculated by Gailis et al. 2021 in BBW (Table 3). Average DBD ± SD is calculated down to the depth to which SAR, MAR, and CAR were calculated.

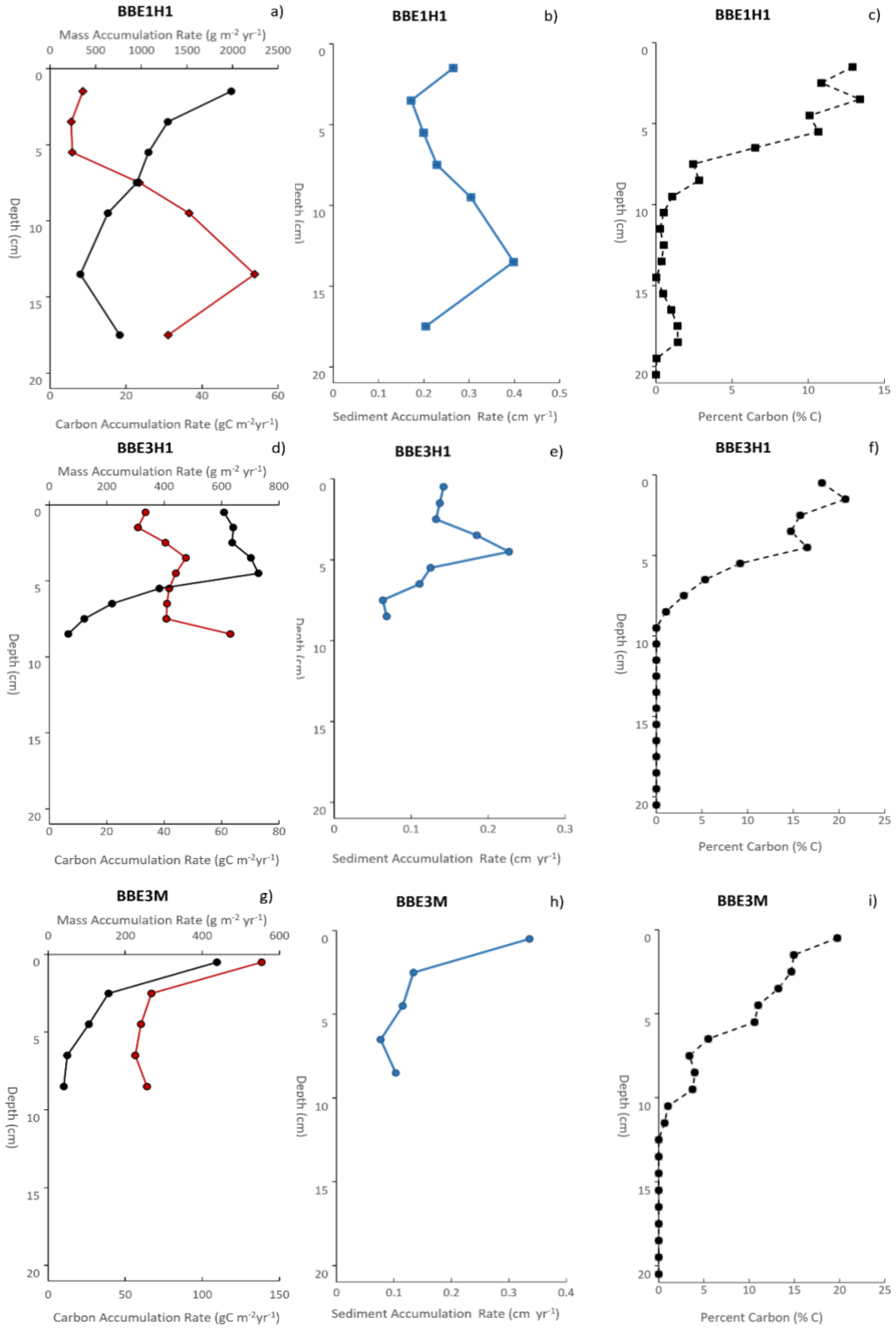
BBE1H1
a)
Mass Accumulation Rate (g m-2 yr-1)
0 500 1000 1500 2000 2500
Depth (cm)
0 5 10 15 20
0 20 40 60
Carbon Accumulation Rate (gC m-2yr-1)
BBE1H1
b)
Depth (cm)
0 5 10 15 20
0 0.1 0.2 0.3 0.4 0.5
Sediment Accumulation Rate (cm yr-1)
BBE1H1
c)
Depth (cm)
0 5 10 15 20
0 5 10 15
Percent Carbon (% C)
BBE3H1
d)
Mass Accumulation Rate (g m-2 yr-1)
0 200 400 600 800
Depth (cm)
0 5 10 15 20
0 20 40 60 80
Carbon Accumulation Rate (gC m-2yr-1)
BBE3H1
e)
Depth (cm)
0 5 10 15 20
0 0.1 0.2 0.3
Sediment Accumulation Rate (cm yr-1)
BBE3H1
f)
Depth (cm)
0 5 10 15 20
0 5 10 15 20 25
Percent Carbon (% C)
BBE3M
g)
Mass Accumulation Rate (g m-2 yr-1)
0 200 400 600
Depth (cm)
0 5 10 15 20
0 50 100 150
Carbon Accumulation Rate (gC m-2yr-1)
BBE3M
h)
Depth (cm)
0 5 10 15 20
0 0.1 0.2 0.3 0.4
Sediment Accumulation Rate (cm yr-1)
BBE3M
i)
Depth (cm)
0 5 10 15 20
0 5 10 15 20 25
Percent Carbon (% C)

Figure 2.10 Downcore distribution of a, d, g) CARs (g C m^{-2} yr^{-1}) and MARs (g m^{-2} yr^{-1}) b, e, h) SARs (cm yr^{-1}) and c, f, i) percent carbon (%C) with depth (cm) for high marsh cores BBE1H1 (a-c), BBE3H1 (d-f), and low marsh core BBE3M (g-i) in eastern Boundary Bay (BBE), Delta, B.C.

Solid black lines represent CARs, solid red lines represent MARs, solid blue lines represent SARs, and dotted black lines represent %C. All values displayed are down to the peat layers of the cores.

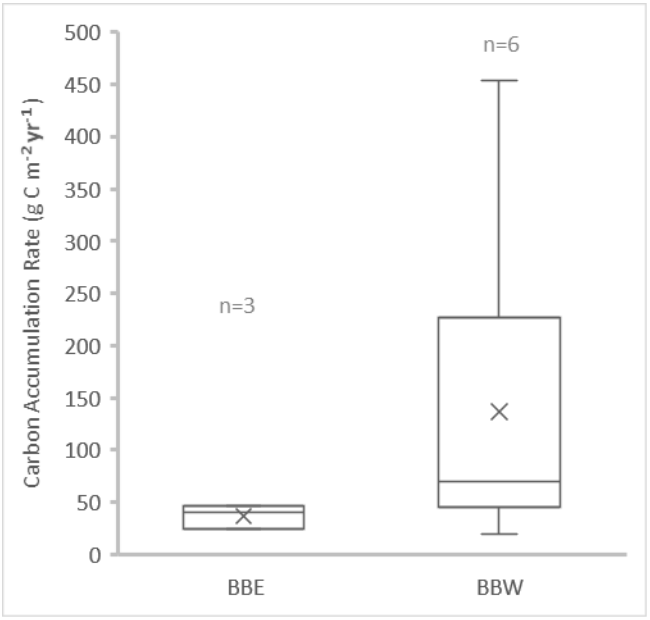

Figure 2.11 Comparison of CARs (g C m^{-2} yr^{-1}) for all dated sites for cores in eastern Boundary Bay (BBE) (n=3) and western Boundary Bay (BBW) (n=6) (t-value = 1.037, p-value = 0.334, p>0.05).

The middle line is the median, the top and bottom of the box are quantiles (Q1 and Q3), the error bar is the largest and smallest value, and the x is the mean.

2.4.3. Year-Round Porewater Salinities

Porewater salinity at Boundary Bay ranged from 3.9 – 32.9 (Table 5), with the lowest at BBE (high marsh) in May, and the highest at BBM (low marsh) in early August. Average summer porewater salinity was significantly higher than average winter porewater salinity across both high marsh (summer =19.2 ± 5.43, winter = 13.5 ± 4.48) (p-value=0.016, p<0.05), and low marsh areas (summer = 22.6 ± 4.60, winter = 15.2 ± 3.47 (p-value=0.0006, p<0.001). However, no significant difference was observed between annual high marsh (n=11) (14.6 ± 5.16) and low marsh salinity averages (n=11) (17.4 ± 4.50) (p=0.165).

The highest average salinities were recorded in August for both high marsh (26.7 ± 5.20) and low marsh areas (25.4 ± 6.88) (Figure 12), when precipitation levels are low (52 mm), while soil and air temperatures are high (16.9 °C and 18.5 °C, respectively) (ECCC, 2021). On the other hand, the lowest average salinities were recorded in January for both high marsh (12.9 ± 4.60) and low marsh (15.2 ± 4.72) areas. Precipitation levels in January are high (225 mm), whereas soil and air temperatures are low (8.2 °C and 3.4 °C, respectively) (ECCC, 2021). In general, average soil temperature was 1-2.5 °C lower than average air temperature in the summer months (April – June), and 0.7-6 °C higher in the winter months (November – March).

Average annual and summer porewater salinities at 25 cm depth at western Boundary Bay (BBW, BBM) (annual = 21.1 ± 4.26, summer = 23.4 ± 3.63) were significantly higher than the east (BBE, MB) (annual = 12.5 ± 2.75, summer = 16.5 ± 5.08) ($p<0.001$, $p<0.05$). However, no significant trend was observed in the winter months, although the average western Boundary Bay salinity (17.9 ± 1.54) was higher that of eastern Boundary Bay (12.2 ± 1.95).

Manual porewater salinity measurement was dependent on several marsh and weather conditions. At some sites, conditions during the summer months were too dry to measure porewater salinity at 25 cm depth. During winter months, some sites were inaccessible for porewater measurement due to marsh inundation. Throughout the year, some low marsh sites were inaccessible due to high tides during field days. Site inaccessibility due to marsh geography (channels, pits, mud) was an additional factor.

At the BBW high marsh site T3-2, conditions during mid-late August were too dry to obtain porewater and the site was inundated by a local freshwater channel between November 2020 to May 2021. Similarly, salt panne site C1 was inundated in January and low marsh site BB1-1 was inaccessible due to high tides in winter between November 2020 - January 2021 during time of field visit. At BBM, both high marsh locations (BBM1H2, BBM1H1) lacked soil moisture to obtain porewater in the summer months (May-August) and were inundated in November. At BBE, all low marsh sites were inundated by high tides in March during the time of visit. Low marsh site BBE1L was inundated by high tides in June, July, and November. All measurements along BBE 2 (n=4) and BBE3 (n=4) were only obtained during the time of sediment coring between November 2020 - January 2021 since site access was limited by a large channel that

runs perpendicular to the marsh. At MB, high tides inundated the site in December and February.

Ten complete year-round porewater salinity measurements were obtained at three high marsh (BB2-5 in BBW, BBE1H2 and BBE1H1 in BBE) and three low marsh sites (BB2-4 in BBW, BBM1L and BBM1M in BBM) across Boundary Bay. At BBW, both high (BB2-5) and low marsh (BB2-4) sites consistently measured salinities above 18 ppt in both summer and winter months 100% of the time. Moving eastward to BBM, low marsh sites BBM1M and BBM1L measured salinities above 18 ppt 80% and 60% of the time, respectively. Further east, high marsh sites BBE1H2 and BBE1H1 measured salinities above 18 ppt only 20% of the time.

Table 2.6 Year-round porewater salinity readings (ppt) sampled from June – August 2020 and November 2020 – May 2021 at 22 coring locations at Boundary Bay.

Average summer salinity (± SD) indicates the average porewater salinity recorded over five months from April – August and winter salinity over five months from November – March. Annual salinity averages winter and summer records. No porewater collections were made in September and October 2020 due to technical errors with the YSI meter.

Location ID	Marsh Zonation	Jun	Jul	Aug	Nov	Dec	Jan	Feb	Mar	Apr	May	Avg. Summer Salinity (ppt)	Avg. Winter Salinity (ppt)	Avg. Annual Salinity (ppt)
Tidal Range (m)		2.2 - 3.9	0.4 - 4.3	0.6 - 4.1	1.0 - 4.1	0.4 - 4.4	0.4 - 4.4	2.0 - 3.8	1.5 - 3.7	1.2 - 3.7	1.5 - 3.9	-		
Air Temperature (°C)		19	18	22	8	7	8	5	10	22	15			
Weather Condition		O	O	S	O	O	O	S	S	S	O			
High Marsh														
BBW														
T3-2	C	13.8	21.0	31.5	IN	IN	IN	IN	IN	IN	-	22.1 ± 8.91	-	22.1 ± 8.91
C1	SP	26.7	27.6	30.9	17.3	14.3	IN	13.7	14.8	25.0	14.8	25.0 ± 6.08	15.0 ± 1.57	20.6 ± 6.88
BB2-5	HM	25.1	27.3	28.7	19.9	20.2	18.4	21.4	20.7	20.4	28.6	26.0 ± 3.50	20.1 ± 1.14	23.1 ± 3.95
BBM														
BBM1H2	HM	-	-	-	-	19.3	19.7	20.8	19.2	17.0	DS	17.0 ± 0.00	19.7 ± 0.71	19.2 ± 1.36
BBM1H1	HM	-	-	-	-	18.2	17.1	20.0	19.0	18.4	DS	18.4 ± 0.00	18.6 ± 1.26	18.5 ± 1.10
BBE														
BBE1H2	HM	20.5	13.3	20.2	14.5	11.6	10.7	9.49	7.53	7.07	8.54	13.9 ± 6.28	10.8 ± 2.59	12.3 ± 4.82
BBE1H1	HM	7.84	19.1	22.2	7.31	8.90	6.48	12.4	8.52	5.98	3.90	11.8 ± 8.26	8.72 ± 2.27	10.3 ± 5.94
BBE2H2	HM	-	-	-	8.18	9.09	14.1	-	-	-	-	-	10.5 ± 3.19	10.5 ± 3.19
BBE2H1	HM	-	-	-	10.2	15.0	9.71	-	-	-	-	-	11.6 ± 2.89	11.6 ± 2.89
BBE3H2	HM	-	-	-	-	-	10.4	-	-	-	-	-	10.4 ± 0.00	10.4 ± 0.00
BBE3H1	HM	-	-	-	-	-	9.31	-	-	-	-	-	9.31 ± 0.00	9.31 ± 0.00
Average ± SD		18.8 ± 7.91	21.7 ± 6.00	26.7 ± 5.20	12.9 ± 5.13	14.6 ± 4.44	12.9 ± 4.60	16.3 ± 5.07	15.0 ± 5.74	15.7 ± 7.57	14.0 ± 10.8	19.2 ± 5.43	13.5 ± 4.48	14.6 ± 5.16

Location ID	Marsh Zonation	Jun	Jul	Aug	Nov	Dec	Jan	Feb	Mar	Apr	May	Avg. Summer Salinity (ppt)	Avg. Winter Salinity (ppt)	Avg. Annual Salinity (ppt)
Low Marsh														
BBW														
BB1-1	LM	-	-	29.3	IN	IN	IN	11.9	13.7	30.5	22.5	27.5 ± 4.31	12.8 ± 1.28	21.6 ± 8.63
BB2-4	LM	26.3	28.0	28.8	20.8	19.9	18.9	19.9	22.0	22.4	24.3	26.0 ± 2.65	20.3 ± 1.16	23.1 ± 3.54
BBM														
BBM1M	LM	28.0	25.6	28.1	26.6	17.8	17.6	19.2	18.2	20.8	25.1	25.5 ± 2.96	19.9 ± 3.82	22.7 ± 4.38
BBM1L	LM	21.4	21.9	30.2	15.3	16.9	17.8	18.9	16.3	20.7	19.5	22.7 ± 4.29	17.0 ± 1.38	19.9 ± 4.25
BBE														
BBE1M	LM	20.7	22.2	24.3	16.7	16.7	20.4	18.3	IN	17.1	20.7	21.0 ± 2.62	18.0 ± 1.77	19.7 ± 2.66
BBE1L	LM	-	-	26.3	IN	15.1	13.1	11.5	IN	24.1	16.1	22.2 ± 5.38	13.2 ± 1.84	17.7 ± 6.09
BBE2M	LM	-	-	-	11.9	9.12	7.79	-	-	-	-	-	9.61 ± 2.10	9.61 ± 2.10
BBE2L	LM	-	-	-	10.7	17.5	20.5	-	-	-	-	-	16.3 ± 5.04	16.3 ± 5.04
BBE3M	LM	-	-	-	-	-	12.1	-	-	-	-	-	12.1 ± 0.00	12.1 ± 0.00
BBE3L	LM	-	-	-	-	-	15.4	-	-	-	-	-	15.4 ± 0.00	15.4 ± 0.00
MB														
MB1L	LM	15.6	17.4	10.4	15.4	IN	8.16	-	13.1	12.1	12.7	13.6 ± 2.83	12.2 ± 3.69	13.1 ± 3.00
Average ± SD		22.4 ± 4.92	23.0 ± 4.03	25.4 ± 6.88	16.8 ± 5.45	16.2 ± 3.42	15.2 ± 4.72	16.6 ± 3.88	16.7 ± 3.65	21.1 ± 5.74	20.1 ± 4.48	22.6 ± 4.60	15.2 ± 3.47	17.4 ± 4.50

*HM = High Marsh, LM = Low Marsh, SP = Salt Panne, C= Channel, DS = Dry Soil (locations where porewater was not collected at 25 cm depth since the soil was too dry, indicating a depth of groundwater table below 25 cm from the soil surface), IN = Inundated (location where porewater was not collected due to site inaccessibility due to tidal or marsh inundation), O = Overcast, S = Sunny.

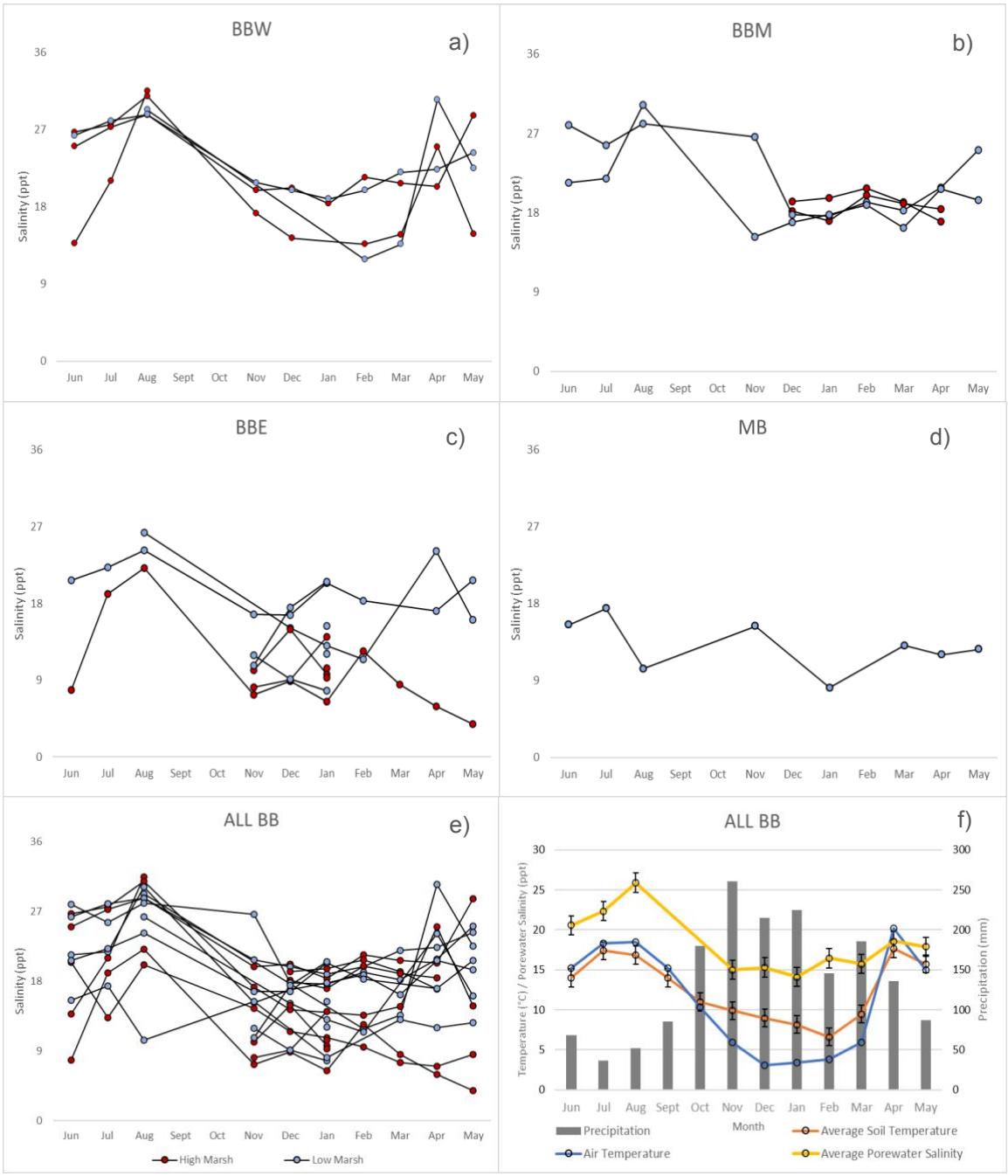

Figure 2.12 Porewater salinities collected at a) BBW (n=5) b) BBM (n=4) c) BBE (n = 12) d) MB (n=1) e) all Boundary Bay (n=22) relative to f) average porewater salinity (± SD) (ppt) – yellow line, air temperature (°C) – blue line, soil temperature (± SD) (°C) – orange line, and precipitation (mm) – grey bars. Red markers represent high marsh salinities and blue markers represent low marsh salinities.

Porewater salinities and soil temperatures were collected biweekly from June - August 2020 and monthly from November 2020 – May 2021. No salinities were recorded for September and October 2020 due to technical errors with the YSI device. Monthly average temperature and precipitation data was retrieved from Environment and Climate Change Canada climate reports for 2020 and 2021, collected at Delta Ladner South weather station (ECCC 2021).

2.5. Discussion

2.5.1. Carbon Stocks and Storage

Significantly higher C stocks are buried in the western portion of Boundary Bay (BBM, BBW) compared to the east (BBE, MB), in part due to high C stocks in both the high and low marsh zones in BBM (Figure 9a). Compared to eastern sites such as BBE and MB, western Boundary Bay sites, especially BBM, has a more mature and diverse plant canopy that enables in-situ and ex-situ organic matter brought in by tides to be stored more easily in the soil. This above-ground accumulation leads to thicker organic matter layers at the top of the sediment cores, resulting in higher C stocks compared to other sites. Unlike all other parts of Boundary Bay, no significant difference was observed between high (108.0 ± 11.1 Mg C ha^{-1}) and low marsh (115 ± 4.3 Mg C ha^{-1}) C stocks at BBM. The high C stocks observed in BBM low marsh could be attributed to the somewhat bay-like shape of this location (Figure 1), which facilitates the accumulation of higher-than-normal amounts of seagrass and other organic matter (Dashtgard 2011). It is also worth noting that a limited number of cores (n=4 for 84 ha) were collected in BBM compared to BBW (n=22 covering 80 ha). Additional cores along multiple transects within BBM might reveal a higher variability in C stocks, as is seen in other parts of the Boundary Bay marsh.

Lower C stocks in the eastern (BBE, MB) compared with the western (BBW, BBM) portions of Boundary Bay could be attributed to differences in sedimentation behavior associated coastal geography, sediment sources, and circulation dynamics. (Swinbanks and Murray 1981). Our study sites extend across the 19 km length of Boundary Bay, and each area of the marsh has variable geographical placement, tidal inundation, vegetation, sedimentation levels and carbon accumulation. The western portion of the marsh is expanding due to the accumulation of sediment breaking off the Pleistocene cliffs at Point Roberts (Swinbanks and Murray 1981). The abundance of nooks and sheltered “bay-like” areas in mid and western marsh areas may facilitate the accumulation of sediments and organic debris. Simultaneously, eastern portions are receding due to the river and water current and wind dynamics in the Bay (Dashtgard 2011; Swinbanks and Murray 1981). These differences lead to the observed variability in C stocks across the marsh.

Mud Bay consistently had %C, SCD and C stock values that were lower than the other parts of the marsh, likely due to its thin organic layer (< 6 cm) and relatively young marsh age. According to the 1930 satellite photo from NRCan (Figure 8), all cores at Mud Bay were extracted on new marsh area formed after 1930 (< 91 years old), likely on areas cleared and filled in during the construction of Highway-99 adjacent to Mud Bay in 1942 (Figure 8a) and dike renovations in 1948. The overall reduction in marsh area in Mud Bay in the past 91 years (1930 - 2021) could likely be attributed to disturbance through highway construction. To minimize its impacts, extracting and analyzing sediment cores from marsh areas that lie immediately east or west of the current coring site (likely > 91 years old) would be useful to derive a more accurate estimate of C stocks at MB (Figure 8b).

Western Boundary Bay (BBW and BBM) holds nearly 90% of the total C storage at Boundary Bay marsh. I estimated the total C storage for BBW (80 ha) using three different approaches, where the simplified (6,100 ± 1,300 Mg C) and kriging volumetric (6,400 ± 1,300 Mg C) based estimates were 27-33% higher than the traditional estimate (4,800 ± 2,800 Mg C), respectively. Similarly, Gailis et al. (2021) estimated the C stocks for a smaller bounded area of 32.5 ha in BBW at 2,120 ± 1,145 MgC (traditional), 3,186 ± 2,269 MgC (simplified), and 3,192 ± 1,862 Mg C (kriging). When estimates by Gailis et al. (2021) are extrapolated to the total BBW marsh area in this study (80ha), the extrapolated traditional C stock estimate of 5215 ± 2817 Mg C is comparable to our traditional estimate. However, the extrapolated simplified volumetric estimate (7838 ± 5582 Mg C) is 28% higher and the extrapolated kriging estimate (7852 ± 4581 Mg C) is 23% higher than our estimates. The higher C stocks yielded through extrapolation may be an overestimation of BBW C stocks.

Of the three methods utilized to calculate C storage, the simplified volumetric method may yield the most accurate C storage estimates. All methods assume that average core C stocks and SCDs remain constant throughout the marsh area. Given these assumptions, the traditional method is likely an underestimation of C storage since it does not factor in marsh depth, and therefore, volume, in its calculation of C storage. On the other hand, the kriging volumetric method may be an overestimation of C storage. The accuracy of the kriging interpolation is limited if the number of sampled sites is small relative to the study area (Zimmerman et al. 1999). Methods such as land-use regression and Bayesian approaches are recommended over kriging interpolation

for spatial prediction with relatively small number of sample points (Le & Zidek 2006). Furthermore, the depth of the marsh for the kriging method is derived using the depth of refusal (DoR) readings throughout the marsh. However, DoR is often an overestimation of marsh depth compared to the DoP readings from in-lab sediment core length measurements. As such, the simplified volumetric method, which utilizes DoP, is likely a more accurate estimation of marsh depth compared to DoR. However, this method may also lead to slight overestimations of C storage due to limited cores used to derive DoPs. Based on these considerations, the rest of this paper will present only the simplified volumetric C storage estimates.

The Boundary Bay compressed C stocks of 40.7 ± 36.4 Mg C ha^{-1} for low marsh and 69.7 ± 35.7 Mg C ha^{-1} for high marsh are 3-6 times lower than the estimated global carbon stock of 250 Mg C ha^{-1} (Chmura et al. 2003; Pendleton et al. 2012). However, these global carbon estimates are calculated down to 1 m depth from the soil surface (Chmura et al. 2003; Duarte et al. 2013) whereas the uncompressed depth of peat base averaged only 24 ± 17 cm at Boundary Bay. Our uncompressed SCD value for all parts of Boundary Bay (0.025 ± 0.007 g C cm^{-3}) is 35% lower to the global estimate of 0.039 ± 0.003 g cm^{-3} (Chmura et al. 2003). However, when extrapolated down to 1 m (250 Mg C ha^{-1}), Boundary Bay C stocks are comparable to global averages.

In the Pacific Northwest (PNW) Kauffman et al. (2019) quantified average total ecosystem carbon stocks of 417 ± 70 Mg C ha-^{1} and 551 ± 47 Mg C ha^{-1} for low and high marsh, down to a depth of 3 m. Of this estimate, >98% of the stock was stored in the soil profile, and the top 1 m of soil only accounted for 48-53% of the total C stock. Therefore, global estimates down to 1 m of soil may greatly underestimate C stocks (Kauffman et al. 2019). Down to a depth of 1 m, Kauffman et al. estimated C stocks of 191 ± 17 Mg C ha^{-1} and 262 ± 35 Mg C ha^{-1} for low and high marsh, respectively. Boundary Bay low (180 ± 70 Mg C ha^{-1}) and high marsh (310 ± 70 Mg C ha^{-1}) C stocks extrapolated down to 1 m are comparable to these PNW estimates. PNW C stocks down to 30 cm (88 ± 10 Mg C ha^{-1}) are comparable to our C stocks in BBM (111 ± 8 Mg C ha^{-1}), estimated to the base of peat layer (38 cm). This similarity could be attributed to the thicker peat layers at BBM, and study sites documented in Kauffman et al. (2019).

Depths of organic soil layers in PNW marshes ranging from Northern California to the US-Canada border average 260 ± 23 cm, while peat layers at the Boundary Bay

salt marsh are one order of magnitude shallower at 24 ± 17 cm. Our shallow depths may simply indicate a younger marsh (Shepperd 1981), in which the depths of refusal range from 33 to 124 years old (Gailis et al. 2021). The young marsh age can be attributed to the recent formation of the Fraser River Delta from fluvial sediment over the past 5000 years. Prior to the formation of the bay-like structure bound by Point Roberts to the west, the exposed Boundary Bay region was subject to stronger wind-generated ocean currents compared to present day, which may have inhibited marsh growth (Dashtgard 2011). Similarly, the eastern portion of the bay has been subject to erosion in throughout the past 4000 years and lacks sufficient sediment input to support vertical accretion (Shepperd 1981). Sedimentological studies also suggest that the current marsh is underlain by a sandy gravel beach-ridge complex (Engels and Roberts 2005; Dashtgard 2011). Therefore, extrapolating salt marsh carbon stocks to a fixed depth can substantially overestimate regional carbon stocks, especially for marshes with depths of marsh initiation shallower than the reference horizon of 1 meter (Gailis et al. 2021).

This study's assumption that core refusal in sand represents the Pleistocene surface, and therefore beginning of the Holocene marsh record, raises some uncertainty. Although the basal sand observed at Boundary Bay is likely Pleistocene, it is important to note that other sources of sand such as tsunami events and fluvial deposition through Fraser River floods could have influenced the sand composition of marsh (Pilarczyk et al. 2021; Dashtgard 2011). In general, the Pleistocene surface is much deeper in coastal Lower Mainland stratigraphy and is characterised by either a blue grey glaciomarine clay or glacially derived till (Bednarski 2015), distinguishable from event deposits such as tsunamis, storms, rivers, and anthropogenic change (e.g., highway construction). With this information in mind, it is likely that the sand layer at the bottom of cores extracted in this study may not be the beginning of the marsh record.

2.5.2. Carbon Accumulation Rates and Marsh Processes

Boundary Bay marsh exhibits strong variability in CARs ranging from 24 ± 13 to 288 ± 130 g C $m^{-2}yr^{-1}$ with no significant differences between its western and eastern portions. Average CARs in BBE (37 ± 27 g C m^{-2} yr^{-1}) are significantly lower than regional averages, while overall Boundary Bay marsh CAR average (103 ± 37 g C $m^{-2}yr^{-1}$) is comparable to regional averages on the Pacific coast of North America. Peck et al. (2020) reported an average CAR of 77 ± 35 g C $m^{-2}yr^{-1}$ for high marsh areas within

seven estuaries in Oregon, USA. CARs measured in Clayoquot Sound, BC, averaged 115 ± 34.2 g C m^{-2} yr^{-1} (Chastain et al. 2021). However, CAR values from the Pacific Northwest region are substantially lower than global estimates of 244.7 ± 26.1 g C m^{-2} yr^{-1} (Ouyang and Lee 2014).

Several lines of evidence suggest that the eastern portion of the marsh is eroding, likely in response to a combination of hydrodynamic activities, vegetation, low sediment discharge, and anthropogenic disturbances. I observe extremely low unsupported ^{210}Pb activity in low marsh core BBE1L, which is consistent with the strong variability within the marsh and evidence suggesting that low marsh in eastern Boundary Bay is degrading. Comparisons with aerial photographs show that BBE1L coring site was once part of the upper low marsh in 1930 (Figure 8a), whereas it lies outside the boundary of green vegetation layer of the satellite imagery in the present day (Figure 8b). In fact, Swinbanks and Murray (1981) hypothesized that this decrease in marsh area has been a long process over 4000 years.

This lack of stability or growth in the eastern marsh has several potential contributing factors. Vegetation at BBE1L was dominated by *Salicornia spp*., whose lower productivity and shallow root systems could be producing and trapping less C (Chastain et al. 2021; Kelleway et al. 2017; Gailis et al. 2021). This, combined with hydrodynamic activities such as storms, winds, erosion could lead to soil loss at marsh edge. Furthermore, sediment discharge from the neighbouring Serpentine and Nicomekl rivers is relatively low (Swinbanks and Murray 1981, Dashtgard 2011), which has been shown to contribute to low CARs (Peck et al. 2020). Anthropogenic disturbance due to Highway 99 construction adjacent to the marsh in 1942 likely further contributed to the observed decrease in marsh area.

No cores were dated from MB study site due to financial constraints. In 2019, preliminary analyses based on surface elevation tables and marker horizons placed at MB by Ducks Unlimited Canada and Smart Shores Inc suggest some evidence to support the accretion of sediments and increasing mean elevation during a three-to-six-month sampling interval over a period of one year (Christensen and Vadeboncoeur 2019). The use of marker bed horizons as a means of measuring accumulation rates is relatively inexpensive and simple. However, there are several drawbacks, including the potential disturbance of the layer by bioturbation, hydrological activities (tides) and

smearing of markers when coring. Furthermore, this method only indicates resolution of the order of ± 1 mm and limited in temporal resolution for detection of seasonal or yearly variations in accumulations (Thomas and Ridd 2004). Therefore, further monitoring over longer time periods is necessary to draw conclusions on current sediment dynamics at the leading edge of eastern Boundary Bay after highway construction.

One limitation of using the ^{210}Pb dating method to understand CARs in this study is that ^{210}Pb chronologies can be complex in coastal sediments due to constant tidal action and reworking of the sediments at the land-water interface (Arias-Oritiz et al. 2018). In addition, ^{210}Pb Chronologies in Cascadia salt marshes ranging from northern California to southern BC have been subject to high bioturbation and land-level change because of earthquakes (Arnaud et al. 2002). Although the ^{210}Pb dating technique has been used previously in BC saltmarshes including Boundary Bay (Gailis et al. 2021) and Clayoquot Sound (Chastain et al. 2021; Postlethwaite et al. 2018), sediment reworking is evident in profiles obtained at Boundary Bay. Therefore, it is likely that the Boundary Bay marsh is older than the average basal age of 78 years obtained through ^{210}Pb dating.

2.5.3. Porewater Salinity, Greenhouse Gas Emissions, and Blue Carbon

Year-round porewater salinity data is a novel contribution to previous blue carbon research conducted at Boundary Bay. In July 2019, Gailis et al. (2021) collected one-time porewater salinities at nine locations at BBW, where high marsh salinities averaged 17.4 ± 11.7 (mesohaline) and low marsh averaged 25.8 ± 0.21 (polyhaline). Porewater salinities >18 ppt have been suggested as one of the factors that contribute to lower methane (CH_4) emissions (Poffenbarger et al. 2011; Janousek et al. 2021). Reduced emissions from polyhaline (> 18 ppt) marshes result from the presence of high sulfate concentrations in the soils, where CH_4 production is inhibited by sulfate-reducing bacteria that outcompete methanogens (DeLaune et al. 1983; Bartlett et al. 1987; Kroeger et al. 2017; Wang et al. 1996).

A seasonal cycle of salinity measurements enabled us to further investigate the poly-mesohaline balance of the BBW marsh. During the summer months, BBW monthly averages were >18 ppt 100% of the time. Higher summer salinities could be attributed to higher soil sulfate concentrations in the summer months when soil contains less

moisture. Importantly, high marsh sites in BBM dried out completely in the summer month of August 2020 and May 2021. This seasonal drying likely indicates that the water table is not close to the surface of the marsh, and previous research suggests that CH_4 emissions remain very low under these conditions due to lower methanogen activity in drier soil (Janousek et al. 2021).

In the winter months, high precipitation led to lower porewater salinities. Between November 2020 and March 2021, BBW salinity average fell below 18 ppt 60% of the time in high marsh and 40% of the time in low marsh, which might suggest a possible environment for higher methane emissions. However, low soil and air temperatures in winter do not provide ideal environmental conditions for high CH_4 emissions (Janousek et al. 2021). A seasonal cycle of salinity measurements therefore provides insights to potential GHG emissions in the absence of constant GHG monitoring.

High and low marsh areas in eastern Boundary Bay are mesohaline year-round, with annual averages: 10.74 ± 1.07 in BBE high marsh, 15.12 ± 3.69 in BBE low marsh, and 13.091 ± 3.00 at MB. Mesohaline ecosystems have the potential to offset the carbon being stored in the marsh through emission of greenhouse gases such as CH_4 and nitrous oxide (N_2O) through anaerobic decomposition of organic matter (Poffenbarger et al. 2011; Wollenberg et al. 2018). Specifically, this study found that high marsh sites BBE1H2 and BBE1H1 measured groundwater table within 25 cm of the surface, and salinities below 18 ppt 80% of the time. These two sites could be prioritized for further year-round monitoring of CH_4 emissions at eastern Boundary Bay, especially during the warm summer months due to their high likelihood of methane emissions based on environmental indicators such as high groundwater table, low salinity, and warm air/soil temperature (Janousek et al. 2021).

Differences in year-round salinity between western and eastern portions in Boundary can in part be linked to vegetation assemblages and geographical placement of the sites within the Bay. Vegetation serves as a preliminary guide to the salinity of a marsh (Porter 1982; Weinmann et al. 1984). Salt-tolerant species such as *Salicornia virginica, Atriplex patula, Triglochin maritima* dominated 80% of BBW and BBM salinity sampling locations. In BBE and MB, plant species with moderate salt tolerance such as *Deschampsia caespitosa, Agrostis stolonifera,* and *Suaeda maritima* dominated 62% of the marsh area (Weinmmann et al. 1984). Additionally, I observed consistently low year-

round porewater salinity at MB (13.62 ± 2.83 summer average salinity, 12.21 ± 3.69 winter average salinity). Low salinity could be attributed to the site's proximity to freshwater input from Serpentine and Nicomekl Rivers to the east of Mud Bay (Kellerhals and Murray 1969; Swinbanks et al. 1981).

Diurnal variability in porewater salinities may produce another level of variability in potential greenhouse gas emissions from the marsh. To characterize this variability, daily or weekly field measurements may be needed. Chmura et al. (2016) recorded porewater salinities during low tide over four consecutive days and found that readings fluctuated daily between 23 ± 7 and 20 ± 3 at two tidal marshes in New Brunswick, Canada. Similarly, I collected porewater during three consecutive weeks in one high marsh and three low marsh areas in BBW and BBM. I found that readings fluctuated between 27.1 - 30.6 in high marsh and 27.9 - 32.9 in low marsh during low tide. These recorded salinity values are likely high enough to result in minimal emissions of CH_4 at these two sites. However, this level of variability could make a difference at sites with lower salinities, such as BBE and MB. Placing salinity loggers at 25 - 30 cm depth along mesohaline marsh locations in BBE and MB would therefore be useful to observe diurnal variability in porewater salinity.

2.5.4. Sea Level Rise and Boundary Bay Living Dike Project

Salt marshes can be threatened by sea level rise if they do not have the space to migrate inland or accretion rates that exceed projected sea level rise (SLR) – known as coastal squeeze (Mcleod et al. 2011; Chmura 2013; Schuerch et al. 2018). If a marsh is drowned and permanently lost, then the carbon stored in the marsh will be released into the atmosphere, contributing to greenhouse gas emissions (Duarte et al. 2013; Sheehan et al. 2019). Assessing whether a salt marsh will persist into the future is essential to verifying if the site is appropriate for a greenhouse gas offset credits or programs (Chmura 2013; Macreadie et al. 2019). A regional study conducted across western Canada estimates the relative rate of SLR around Vancouver at 0.6 ± 0.1 mm yr^{-1} (Mazzotti et al. 2008), which is slower than the global mean rate at 3.7 mm yr^{-1} (IPCC 2021). This lower rate of SLR might mean that salt marshes in Vancouver area may face minimal loss in area given the availability of accommodation space for inland migration and sufficient sediment load for vertical accretion to continue marsh growth.

Nature-based adaptation solutions that maximize inland migration of tidal wetlands may help safeguard wetland persistence with SLR. Inland displacement of coastal flood defences such as dikes, and the designation of nature reserve buffers in upland areas surrounding coastal wetlands are existing solutions (Schuerch et al. 2018). The shoreline management plans in England and Wales (Nicholls et al. 2013) and the coastal master plan in Louisiana (Peyronnin et al. 2013) are examples of implemented nature-based adaptation solutions of coastal wetlands to SLR.

Low marsh areas in eastern Boundary Bay (BBE, MB) made up 62% of its total marsh area, but only 36% of its total carbon storage. Although substantial, low marsh C storage in eastern Boundary Bay remain significantly lower compared high marsh, in par with findings in western Boundary Bay (Gailis et al. 2021). The planned location for a living dike by Cities of Surrey and Delta, West Coast Environmental Law, and the Semiahmoo First Nation in eastern Boundary Bay overlaps with the eastern BBE and MB study sites. The living dike aims to raise marsh elevation to offset the projected loss of marsh area due to inundation by SLR. This pilot project plans to deposit sediment in the low marsh areas over three decades (Readshaw, Wilson, and Robinson 2018). Buildup of carbon may be time-dependent to develop a mature plant canopy that can trap and store more in-situ and ex-situ carbon, as observed in BBM low marsh areas. Lower C storage capability of low marsh compared to high marsh areas suggested by Gailis et al. (2021) and verified in this study suggest that sediment amendment in Boundary Bay needs to be geared toward high marsh rather than low marsh areas to maximize the co-benefit of the living dike. To increase the marsh's ability to vertically accrete, the living dike project will need to ensure that the rates of sediment deposition and marsh development is greater than the local rate of SLR.

2.5.5. Climate Change Mitigation and Wetland Management

Salt marshes provide valuable ecosystem services such as habitat for estuarine wildlife, protection from coastal flooding, and carbon sequestration (Peck et al. 2020; Chmura 2013, Duarte et al. 2013; McLeod et al. 2011). The carbon sequestration and co-benefits of conservation are important due to their potential inclusion in regional, national, and global climate change adaptation and mitigation strategies (Kauffman et al. 2019). Greenhouse gas emissions from wetland conversion to agricultural land have been reported to be as high as 1,067 - 3,003 Mg CO_2e ha-1, and land-use change sector

is one of the top five sources of current GHG emissions (Kauffman et al. 2019). Since European settlement in the US Pacific, ~85% of vegetated tidal wetlands have been lost to human land use conversion (McLeod et al. 2011; Brophy et al. 2019). Due to relatively high C stocks, the blue carbon ecosystems have been recognized in regional and global climate change mitigation strategies (Kauffman et al. 2019; Donato et al. 2011; Duarte et al. 2013; McLeod et al. 2011). Therefore, blue carbon stock data are essential for using blue carbon ecosystems in climate change mitigation policy.

In Boundary Bay, I have demonstrated that C stocks and accumulation rates are comparable to regional and global estimates when extrapolated down to 1 m depth of soil (Gailis et al. 2021). This quantification of C stocks presents a new opportunity for the valuation of blue carbon at the Boundary Bay salt marsh through provincial and federal carbon offset initiatives and carbon finance markets (Kauffman et al. 2019; Emmer et al. 2015). In 2021, the government of British Columbia dedicated $27 million to 70 watershed and wetland initiatives through Stronger BC: BC's Economic Recovery Plan (Government of British Columbia 2021). This Healthy Watershed initiative focuses on urban, rural, and indigenous communities highly impacted by COVID-19 pandemic to strengthen natural carbon sinks through restoration and natural flood management. The Government of British Columbia also introduced a voluntary carbon market that includes wetland restoration, which allows individuals and corporations to offset their greenhouse gas emissions outside of legally mandated reductions (Sheehan et al. 2019). In addition, British Columbia has legislated greenhouse gas reduction targets of 40% below 2007 by 2030, 60% by 2040, and 80% by 2050 (Climate Change 2007) and introduced a carbon tax in 2008 that applies to the purchase and use of fossil fuels (Government of British Columbia, n.d.).

The economic benefits of incorporating salt marsh carbon sequestration into an offset/credit system are significant and raise the political profile for blue carbon initiatives and policy (Ullman, Bilbao-Bastida, and Grimsditch 2013). Currently, salt marshes are not included in any carbon offset programs or regulated carbon markets in British Columbia and Canada. Our study takes initial work at Boundary Bay by Gailis et al. (2021) one step further, but on-going monitoring of blue carbon sequestration and storage potential would be required for its incorporation in provincial carbon markets and offset initiatives (Gailis et al. 2021; Emmer et al. 2015; IPCC 2000).

2.5.6. Next Steps

This study quantified marsh type, area, volume, C stocks, marsh C storage, and CARs for BBM, BBE, and MB, with novel year-round porewater salinities presented for all sites at Boundary Bay marsh. I built upon published research (Gailis et al. 2021) in western Boundary Bay to develop an improved understanding of marsh processes and blue carbon storage across all parts of Boundary Bay. Several additional areas of research could further serve as next steps to form a complete carbon budget of the Boundary Bay salt marsh ecosystem. These steps include (1) using gas flux chambers to develop a complete greenhouse gas budget of the marsh, (2) installing sulfate, salinity, pH, and temperature loggers for year-round measurements, (3) understanding how local SLR affects inland migration of low marsh zone at Boundary Bay.

Developing an understanding of the greenhouse gas fluxes is an important next step to form a more complete picture of the blue carbon budget at Boundary Bay. Current estimates of C stocks and CARs at Boundary Bay assume that there is no net flux of carbon out of the marsh (Gailis et al. 2021), which can result in an overestimation of the overall carbon sequestration. To form a more accurate estimate, the balance between marsh greenhouse gas emissions and soil carbon sequestration potential needs to be examined (Poffenbarger et al. 2011; Janousek et al. 2021). Wetland ecosystems can act as greenhouse gas sinks through the uptake of carbon dioxide through photosynthesis and carbon storage in above and below ground plant biomass. However, wetlands can double as a greenhouse gas source through the release of methane (CH_4) and nitrous oxide (N_2O) produced during anaerobic decomposition of organic matter (Poffenbarger et al. 2011; Janousek et al. 2021; Roughan et al. 2018). Mesohaline areas in BBE and MB could be prioritized for gas flux chamber installations. Monitoring of CH_4 emissions would be required to estimate net carbon sequestration at eastern Boundary Bay BBE and MB, especially during the warm summer months (Janousek et al. 2021). Accounting for greenhouse gas fluxes at mesohaline areas of the Boundary Bay marsh will establish an understanding of the portion of soil carbon sequestration offset by greenhouse gas emissions. Therefore, installing flux chambers will lead to a more comprehensive understanding of the overall blue carbon potential of the marsh.

Another important measurement that should be collected at Boundary Bay is year-round porewater sulfate concentrations at all coring locations. Sulfate concentration is a more accurate correlate of porewater methane than salinity (Poffenbarger et al. 2011). It is generally understood that presence of high sulfate concentrations in marsh soils emit CH_4 at relatively low rates (Poffenbarger et al. 2011; Keller et al. 2009; DeLaune et al. 1983; Bartlett et al. 1987), since sulfate-reducing bacteria outcompetes methanogens for energy sources. However, salinity may not be a good predictor of sulfate concentrations in wetlands that are frequently inundated, which can lead to high porewater methane concentrations despite high salinity (Poffenbarger et al. 2011). At Boundary Bay, several sites in the western portion of the marsh were inaccessible during the winter months due to permanent inundation associated with high precipitation and tides. Therefore, sulfate concentrations would be a more accurate indicator of methane emissions at the western portion of the Boundary Bay marsh, especially during the winter months. In-situ salinity, temperature, sulfate concentrations, and pH loggers, and depth of groundwater table measurements will allow for more consistent year-round porewater data that contribute to a deeper understanding of the greenhouse gas fluxes of the marsh (Janousek et al. 2021).

Lastly, the resilience of the Boundary Bay marsh to long-term SLR and changes to its ability to sequester carbon need to be examined. A recent study based in the PNW region finds that tidal inundation and increased porewater salinity due to SLR will likely decrease ecosystem C stocks in the absence of upslope wetland migration buffer zones (Kauffman et al. 2019). Increased storm surges and high tides will result in inundation of low elevation marshes, resulting in landward expansion of low marshes into sites formerly occupied by high marshes, decreasing the total ecosystem C stocks. Given relatively low average C stocks in low marsh areas, upland migration of low marsh could potentially decrease the net C stock at Boundary Bay. Further research that utilizes Topographic Lidar to produce digital elevation models with vertical resolution relevant to marshes and would help determine the permanency of Boundary Bay marsh relative to local SLR (Gailis et al. 2021; Chmura et al. 2013).

This study, while focused on blue carbon, has also provided a range of valuable baseline information about the processes operating in Boundary Bay. Assessing the living dike project will require ongoing monitoring of these sedimentary processes and incorporating carbon measurements as a logical extension of any proposed and ongoing

monitoring. To understand the physical processes that determine elevation change and the potential for SLR in estuary habitats, precise measurements of sediment elevation and vertical accretion over long time scales will be required in these areas. The rod surface elevation table (rSET) provides accurate and precise measurements of sediment elevation of intertidal areas, that could be utilized going forward (Christensen and Vadeboncoeur 2019).

Chapter 3. Blue Carbon in British Columbia

3.1. Abstract

Blue carbon ecosystems such as tidal salt marshes provide co-benefits through carbon (C) storage and sequestration and have been suggested as natural climate solutions (NCS). In addition to quantification of C storage and accumulation rates, the development of sustainable NCS for tidal salt marshes requires more robust estimations of their areal distribution. In this regional case study, I compare three different areal estimates made for three tidal salt marshes in southern coastal British Columbia (BC): Boundary Bay (BB), Cypress River Flats (CRF), and Grice Bay – Kennedy River (GBK). I use one regional: Commission for Environmental Cooperation 2021 (CEC dataset) and one global**:** United Nations Environment Programme World Conservation Monitoring Centre 2021 (UNEP dataset) salt marsh distribution dataset, coupled with one areal dataset produced in this study: the Basnayake dataset. Our results indicate that C storage and annual carbon accumulation (ACA) estimates made using the UNEP dataset are two times larger and the CEC dataset estimates are five times larger than our estimates. Our results show that existing salt marsh distribution datasets largely overestimate marsh distribution, leading to overestimations in blue carbon storage and accumulation. Such miscalculations have far-reaching policy implications including overestimating the carbon mitigation potential of wetland related NCS. Therefore, it is crucial that salt marsh distribution is mapped accurately to avoid discrepancy between datasets and for it to be valuable for climate change mitigation policy.

Keywords: blue carbon; salt marsh; British Columbia; climate change mitigation; marsh distribution; GIS dataset

3.2. Introduction

Over the past 15 years, coastal ecosystems have been recognized as substantial contributors to carbon (C) storage and sequestration (Duarte et al. 2005). Ever since the coining of the term “blue carbon” (Nellemann et al. 2009), blue carbon storage has been suggested as a potential tool for climate mitigation (Mcleod et al. 2011). The long-term accumulation of C stocks in blue carbon ecosystems is used as an argument for the

conservation of tidal salt marshes (Pendleton et al. 2012). Furthermore, in the recent years, restoration of tidal salt marshes has also received increased attention as a natural method for blue carbon ecosystems to compensate for anthropogenic global C emissions (Janousek et al. 2021; Irving et al. 2011) due to their role as a net carbon sink.

For the purposes of this study, natural climate solutions (NCS) are defined as natural interventions that sequester carbon, while their contributions to ecosystem services are considered co-benefits (Drever et al. 2021; ECCC 2021). Ecosystem services provided by tidal salt marshes make them potentially important contributors to NCS (Temmerman et al. 2013; Macreadie et al. 2021; Drever et al. 2021). Avoided conversion of wetlands is one NCS pathway of accounting for avoided CO_2 equivalent (CO_2e) emissions of above and belowground biomass and soil carbon due to the prevention of anthropogenic disturbances (Drever et al. 2021). Previous studies estimate that full implementation of all cost-effective NCS, including avoided conversion and restoration of natural wetlands, provide up to one-third of the global mitigation needed in 2030 to keep warming below 2°C (Griscom et al. 2017). In the United States, NCS projects could mitigate up to 21% of net annual emissions (Fargione et al. 2018). A recent study finds that in Canada, coastal blue carbon ecosystems have the potential to mitigate 1.7 Tg CO_2e/yr in 2030 (Drever et al. 2021), mitigating ~0.3% of Canada's projected net annual emissions in 2030 under Canada's strengthened climate plan (503 Mt CO_2e) (ECCC 2021). It is important to note that many Canadian provinces have "no net loss" policies for wetlands that is enforced through the 1991 Federal Policy on Wetland Conservation that mean avoided conversion may not meet an additionality constraint in such instances (Government of Canada 1991).

NCS projects rely on accurate ecosystem carbon budgets to produce deployable solutions that can contribute to emission reductions. For example, estimates of carbon sequestration in tidal salt marshes rely heavily on areal estimates from GIS databases to understand their carbon dynamics, including C storage and accumulation. Duarte et al. (2013) noted a 20-fold uncertainty in global estimates of salt marsh area, ranging from 2,200,000 to 40,000,000 ha, associated with ambiguous classification systems for wetland types and areas (Duarte et al. 2013; Chastain et al. 2021). Therefore, estimating the potential for sustainable NCS in tidal salt marshes requires more robust estimations of their areal distribution, C storage, and C accumulation rate potential. The best way to

acquire this information is to examine each salt marsh individually and incorporate site-specific field and aerial photographic data. Obviously, gathering site-specific data for every marsh is not practical for a global dataset, which necessitates the incorporation of several assumptions that can influence the accuracy of these global datasets.

The goal of this study is to examine how much these simplifying assumptions can affect the areal estimates and therefore also blue carbon storage and accumulation. Here, I investigate how the use of different spatial datasets of salt marsh extent might impact regional estimates of blue carbon storage and accumulation rates within the province of British Columbia, Canada. I examine salt marsh distributions in three important areas of southern BC, specifically, Boundary Bay (BB), Cypress River Flats (CRF), and Grice Bay – Kennedy River (GBK). In these three salt marshes, I map high and low marsh zones delineated by eye using differences in vegetation color, further verified by site visits and vegetation surveys. I then compare our marsh areal estimates for the three marshes with one regional salt marsh distribution dataset: CEC 2021 (Commission for Environmental Cooperation 2021), and one global dataset: UNEP-WCMC 2021 (Mcowen et al. 2017). Using C stock (Mg C) and carbon accumulation rate (CAR, g C m^{-2} yr^{-1}) data from three recent regional studies (Gailis et al. 2021; Chastain et al. 2021; Chapter 2), I compare how areal extents from these three datasets affect our estimates of C storage (Mg C) and annual carbon accumulation (ACA, Mg C yr^{-1}) for each of the three salt marshes study areas. More accurate mapping efforts could facilitate a more precise integration of blue carbon ecosystems into regional and global coastal planning of NCS.

3.3. Methods

3.3.1. Study Area

Recent estimates suggest that British Columbia (BC) holds an estimated 74,029 ha of intertidal salt marshes (Mcowen et al. 2017). The coastline of BC is generally characterized by mountains, narrow continental shelf, and rocky, steep-sloped shorelines. The coast is generally dissected into fjords and archipelagos, and subject to recent glacial erosion and isostatic uplift – conditions which do not generally favour coastal marsh development (Porter 1982). Therefore, BC marshes tend to be young (~30-50 years at its base), small in areal extent, and restricted to isolated bays,

estuaries, and river deltas (Chastain et al. 2021). In this study, I conduct three case studies within two regions in BC: (a) Boundary Bay (BB) near Metro Vancouver, BC, and (b) Clayoquot Sound (CS) on the Pacific Coast of Vancouver Island (Figure 1).

BB is a shallow, sheltered bay situated on the Canada-United States border and is the largest salt marsh in southwestern British Columbia, spanning more than 200 ha at its leading edge and 0.5 km at its widest point. To its north, the entire length of the marsh is bounded by a 26 km man-made dike built in 1895 and renovated in 1948 following the Fraser Valley Flood (Shepperd 1981). As a provincial Wildlife Management Area (WMA), it provides critical habitat for many aquatic and wildlife species, and an urban blue carbon ecosystem. Sedimentation rates at BB are low (0.42 mm yr^{-1}) with relatively clear, saline (24-29 ppt) waters (Swinbanks and Murray 1981). The tides in the Bay are a mixed semidiurnal type, with two high and two low tides every day (Shepperd 1981). The mean tidal range is 2.7 m, with a maximum spring tide of 4.1 m and minimum neap tide of 1.5 m (Swinbanks and Murray 1981). The area experiences a west coast maritime climate with mild, wet winter and warm, dry summers (Shepperd 1981), with an average rainfall of 976.5 mm yr^{-1} and snowfall of 31.6 mm yr^{-1}. Average annual temperature is 9.6°C, with the highest recorded in July and August at 16.9°C and lowest in January at 2.8°C (Government of Canada 2021).

I examine the two largest marshes in CS: Cypress River Flats (CRF) and Grice-Bay Kennedy River (GBK). CS is a complex system of inlets situated in the west coast of Vancouver Island. These marshes include small, pocket marshes encompassing enclosed, semi-circular areas of coastline as well as larger, estuarine marshes (Chastain et al. 2021). CS falls within the UNESCO Clayoquot Sound Biosphere Reserve, which protects 366,000 hectares of the west coast of Vancouver Island. The region is part of the temperate rainforest biome with high annual rainfall (3270 mm yr^{-1}), average annual temperature of 9.5°C. The mean tidal range in Tofino is 2.14 m, with surface water salinity ranging from 24 in GBK to 29 at CRF (Chastain et al. 2021; Postlethwaite et al. 2018).

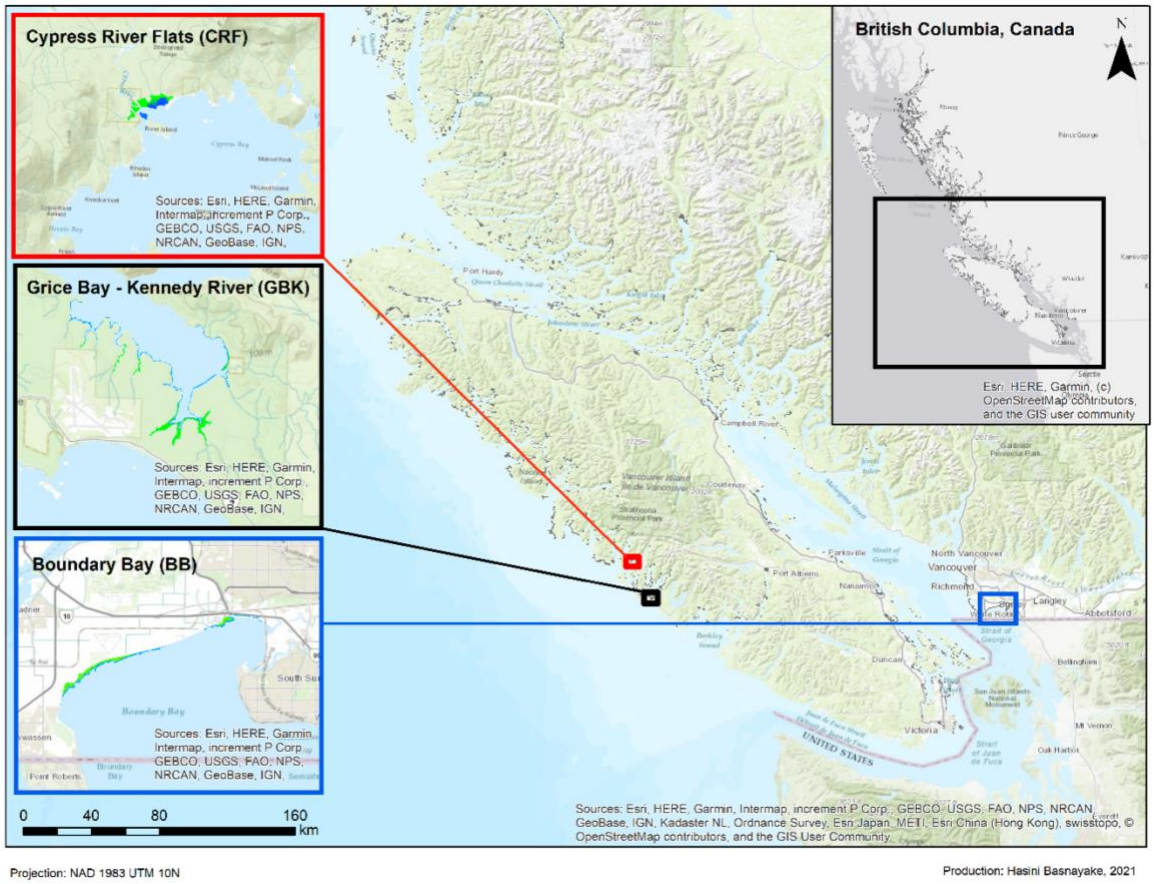

Figure 3.1 Map of three salt marsh case study locations sites within British Columbia. In Clayoquot Sound region, Cypress River Flats (CRF) is shown in the red map insert, and Grice Bay-Kennedy River (GBK) is shown in black. Boundary Bay (BB) is shown in the blue map insert. High (green) and low (blue) marsh areas shown within the map inserts were delineated using satellite imagery on Google Earth Pro 2021. British Columbia salt marsh extent polygons shown in the main map frame were downloaded from the UNEP-WCMC dataset version 7.1 (Mcowen et al. 2017). Base map source: ArcGIS 2021. Projection: NAD 1983 UTM 10N.

3.3.2. Salt Marsh Distribution Datasets

I compare salt marsh areal extents for BB, CRF, and GBK using three datasets: Basnayake et al. 2021 (hereafter “the Basnayake dataset”), The UN Environment Programme World Conservation Monitoring Centre (UNEP-WCMC) 2021, and Commission for Environmental Cooperation (CEC) 2021.

In the Basnayake dataset, I map high and low marsh zones using Google Earth Pro 2021 tools on a Google satellite base map compiled from images taken on June 12, 2019. High and low marsh zones were delineated by eye using differences in vegetation

color on Google Satellite base map imagery. Halophyte-dominated low marsh plant assemblages were a lighter shade of green compared to the darker green of the high marsh plant assemblages (Chastain et al. 2021; Gailis et al. 2021). This delineation was further verified by site visits and vegetation surveys using a 50 x 50 cm quadrat at 194 sampling points (40 sediment coring sites and 154 vegetation sampling points) in BB (Chapter 2; Gailis et al. 2021), and 14 sediment coring sites in CRF and GBK (Chastain et al. 2021). In BB and CS, previous research determined that designations determined using vegetation surveys aligned perfectly with the visual delineations made using satellite color (Chastain et al. 2021; Gailis et al. 2021).

The UNEP-WCMC global saltmarsh occurrence polygon dataset version 6.1 (hereafter, the “UNEP dataset”) was published in March 2021. The dataset was developed to provide a baseline inventory of the extent of global distribution of salt marshes. This composite dataset was sourced from peer-reviewed articles, reports, and databases created by non-governmental and governmental organisations, universities, research institutes, and independent researchers globally (Mcowen et al. 2017). For British Columbia, the British Columbia Marine Conservation Analysis (BCMCA) holds ownership of the salt marsh distribution data for BC published in November 2009. The marsh areas were mapped using aerial low tide oblique field surveys between 1995 and 2002 under BC Physical and Biophysical ShoreZone Mapping System. This dataset is represented using vector line features using two salt marsh vegetation biobands. The *Salicornia* bioband used its species *Salicornia virginica* to represent assemblages of marsh grasses, dune grass, sedges, and other salt-tolerant herbaceous plants. In more recent surveys, an additional dune grass bioband was mapped along certain areas of the BC coast (BCMCA 2009). The BCMCA source data contain vector line features, measuring salt marsh extent using bioband length only (km). However, the UNEP dataset has converted the vector lines to polygons using a buffer of fixed diameter around each saltmarsh bioband. The creation of a polygon using this method yields a marsh area for each polygon in hectares.

The North American Blue Carbon dataset (hereafter, the “CEC dataset”) was published by the CEC in May 2021 and shows the distribution of salt marshes in North America. Data were compiled from approximately 50 source datasets, including international (UNEP), national, and provincial sources, along with information from individual investigators. BC salt marsh polygons were retrieved from a ShoreZone

polygon dataset published by the BC Ministry of Forests, Lands, Natural Resource Operations and Rural Development (FLNRORD) in 2018. ShoreZone mapping procedures utilize salt marsh extent information from air photos, aerial video/slide imagery and ground field survey data (Howes et al. 1995). To create this dataset, raw data of BC marshes were downloaded from the BC Geographic Warehouse Custom Download (BC FLNRORD 2018), and all polygons with species information including "marsh grasses and sedges" and "*Salicornia virginica*" were exported to a final BC saltmarshes layer. In areas where ShoreZone polygon data were absent, such as GBK, the CEC dataset utilizes salt marsh polygons from the UNEP dataset (Mcowen et al. 2017). This 2021 release is an updated layer from the CEC 2015 Blue Carbon Map, which utilized BC ShoreZone data published in 2014 (CEC 2021).

3.3.3. Carbon Stock and Accumulation Rates Data

I used existing information from published regional studies to estimate C storage (Mg C) and annual carbon accumulation (ACA, Mg C yr^{-1}) for each of the three case study salt marshes in BC (Table A4, Appendix A). To estimate C storage (Mg C) for BB, CRF, and GBK, I gathered published average core C stock (Mg C ha^{-1}) data for high and low marsh in studies where calculations are made down to the base of peat layer (Table A4). The average core C stocks were then multiplied by marsh area (ha) from each of the three datasets to derive the C storage for each marsh:

$$C\ storage\ (Mg\ C) = Average\ core\ C\ stock\ \left(\frac{Mg\ C}{ha}\right) \times Marsh\ area\ (ha) \quad (1)$$

Next, to estimate annual C accumulation (ACA, Mg C yr^{-1}) for BB, CRF, and GBK, I gathered average C accumulation rate (CAR, Mg C ha^{-1} yr^{-1}) data from regional studies where separate values for high and low marsh areas are available (Table A4). The average CARs were then multiplied by marsh area (ha) from each of the three datasets to derive the ACA for each marsh:

$$ACA\ \left(\frac{Mg\ C}{yr}\right) = Average\ CAR\ \left(\frac{Mg\ C}{ha \cdot yr}\right) \times Marsh\ area\ (ha) \quad (2)$$

Distinction between high and low marsh areas was only available in the Basnayake et al. 2021 area dataset. Thus, the high and low marsh core C stock and accumulation values were averaged to derive an all-marsh C stock and CAR value. To test for how averaging high and low marsh zones rather than separating them affects the

overall estimate of C storage and ACA, I calculate both all-marsh and separated high-low marsh estimates of C storage and ACA for all three marshes using the Basnayake dataset. I then test for any statistically significant differences between the all-marsh and separated high-low marsh values for each marsh using a t-test in R studio 2015.

3.4. Results

3.4.1. Areal Extents

At Boundary Bay (BB), I estimate a total marsh area of 222 ha, with high and low marsh each accounting for 50% of that area (Figure 2a). The UNEP dataset estimates a higher total area of 331 ha. This dataset extends further down on the eastward side of BB, where I verified through field visits that there is no salt marsh currently present. Additionally, the bioband buffer is placed around the man-made dike, cutting into adjacent farmland north of the dike and only covering a small portion of the existing high marsh area. The UNEP dataset does not include any low marsh area (Figure 2b). The CEC dataset estimates a total area of 1207 ha, an order of magnitude higher than the other two estimates. The CEC dataset includes large areas of non-vegetated sandbars and mudflat areas in its estimation of salt marsh area (Figure 2c).

At Cypress River Flats (CRF), I estimate a total marsh area of 24.8 ha, with 16.1 ha in high marsh and 8.73 ha in low marsh (Figure 3a). The UNEP dataset estimates a higher total area at 56.8 ha. This bioband polygon extends along the shoreline at CRF, feeding into the adjacent terrestrial forest boundary and into the high marsh area, while low marsh areas are largely excluded (Figure 3b). The CEC 2021 dataset reports the highest area for CRF at 84.4 ha. This polygon includes existing high and low marsh areas, as well as non-vegetated sandbars and mudflats (Figure 3c).

At Grice Bay – Kennedy River (GBK) marsh, I estimate a total marsh area of 55.4 ha, where high marsh area accounts for 32.6 ha and low marsh area occupies 22.8 ha (Figure 4a). The UNEP and CEC datasets report the same area for GBK at 244 ha (Figure 4b, 4c), which is 4-5 times higher than our estimate. The CEC and UNEP datasets cover the full areal extent of the GBK marsh but cut into the adjacent terrestrial forest boundary and into the mudflat areas past the low marsh, leading to a very high areal estimate.

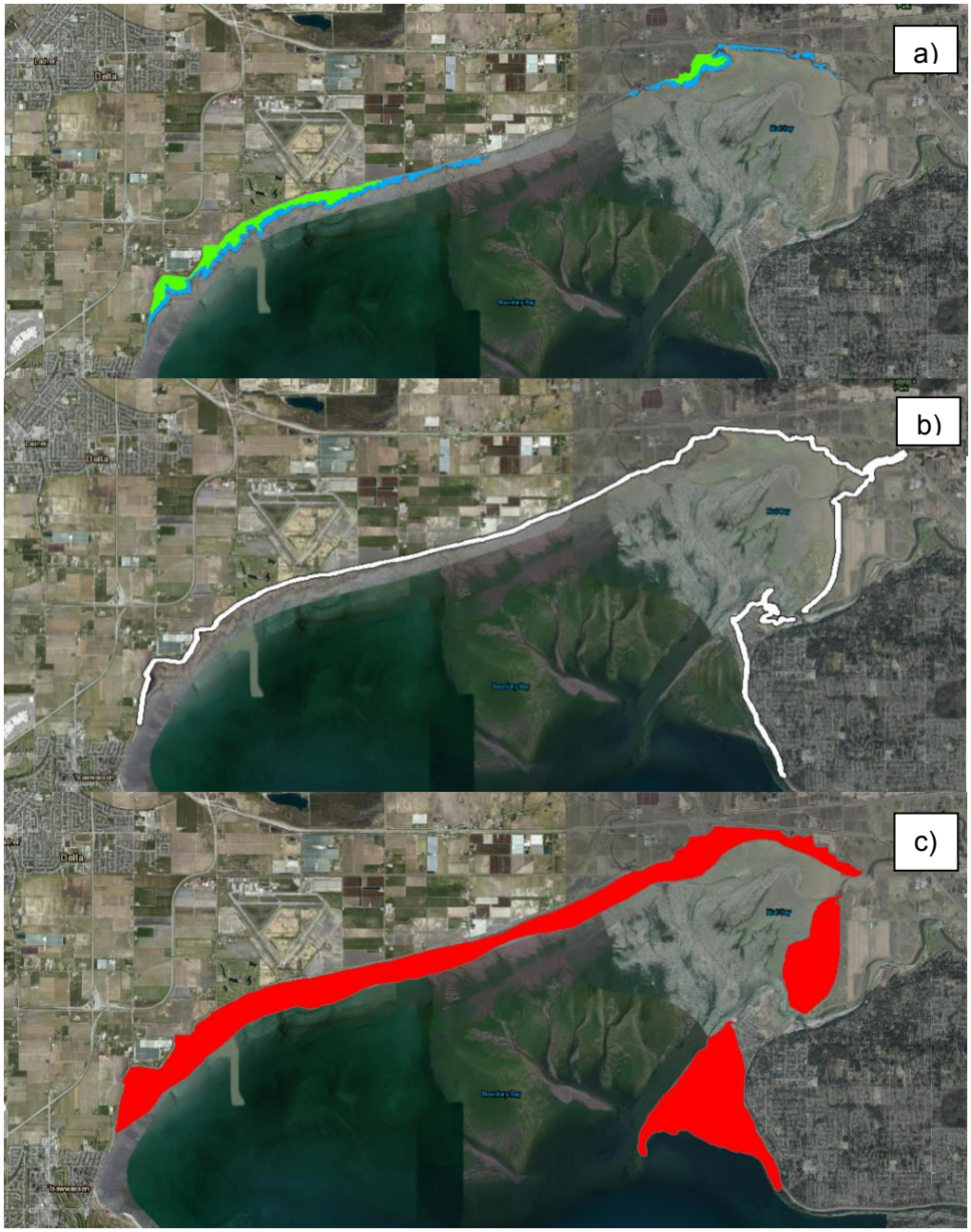

Figure 3.2 Comparison of marsh areal extent at Boundary Bay (BB) salt marsh, Delta/Surrey, British Columbia as mapped in three datasets.

a) Basnayake dataset (222 ha), where high marsh areas (111 ha) are in green and low marsh areas (111 ha) in blue b) UNEP dataset (Mcowen et al. 2017) (331 ha), where all marsh areas are represented in white, c) CEC dataset (1207 ha), where all marsh areas are represented in red. No distinction between high and low marsh areas was made in datasets b and c. Map projection: NAD 1983 UTM Zone 10 N. Base map source: Satellite Imagery, ArcGIS 2021.

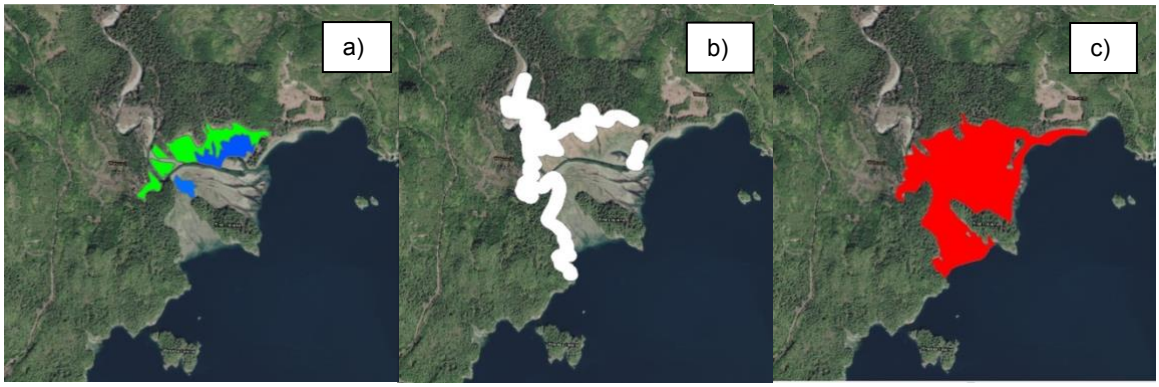

Figure 3.3 Comparison of marsh areal extent at Cypress River Flats (CRF) salt marsh, Clayoquot Sound, British Columbia as mapped in three datasets.

a) Basnayake dataset (24.8 ha), where high marsh areas (16.1 ha) are in green and low marsh areas (8.73 ha) in blue b) UNEP dataset (Mcowen et al. 2017) (56.8 ha), where all marsh areas are represented in white, c) CEC dataset (84.4 ha), where all marsh areas are represented in red. No distinction between high and low marsh areas was made in datasets b and c. Map projection: NAD 1983 UTM Zone 10 N. Base map source: ArcGIS 2021.

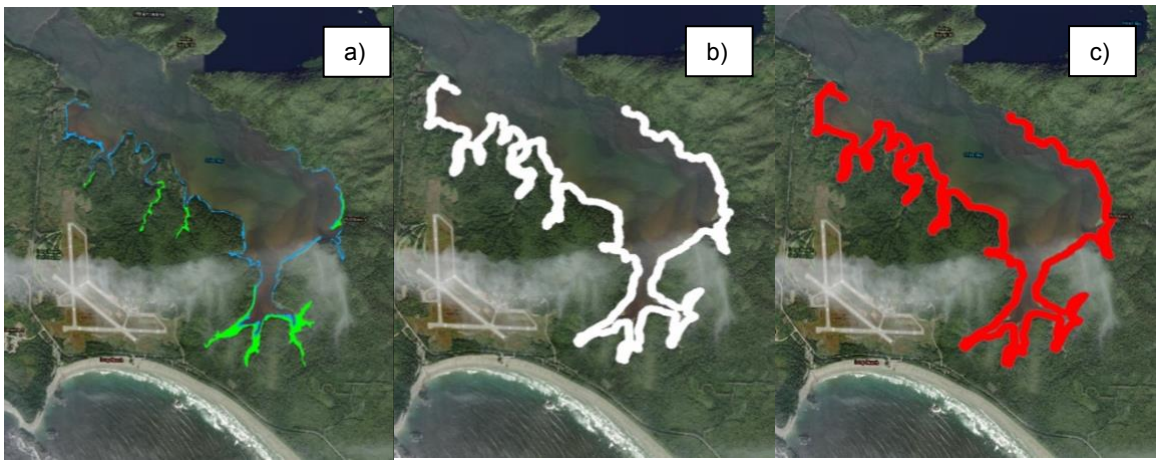

Figure 3.4 Comparison of several small salt marsh areal extents at Grice Bay – Kennedy River (GBK) salt marsh, Clayoquot Sound, British Columbia as mapped in three datasets.

a) Basnayake dataset (55.4 ha), where high marsh areas (32.6 ha) are in green and low marsh areas (22.8 ha) in blue. (Note: high marsh may be overestimated due to limitations in distinguishing fringe beach grass from salt marsh vegetation from satellite imagery in this area). b) UNEP dataset (Mcowen et al. 2017) (244 ha), where all marsh areas are represented in white, c) CEC dataset (244 ha), where all marsh areas are represented in red. No distinction between high and low marsh areas was made in datasets b and c. Map projection: NAD 1983 UTM Zone 10 N. Base map source: ArcGIS 2021.

3.4.2. Marsh Carbon Storage

Using the marsh area from Basnayake dataset, I estimate a total marsh C storage of 12,200 ± 2,010 Mg C at BB, with 63% of the carbon stored in the high marsh

(7,700 ± 929 Mg C) and 37% in the low marsh (4,530 ± 1,080 Mg C) (Table 1). BB marsh area from the UNEP dataset leads to a total marsh C storage estimate of 18,900 ± 2,240 Mg C, which is 1.5 times higher than the Basnayake dataset. The CEC dataset C storage estimate for BB is 68,800 ± 8,170 Mg C, 5.6 times higher than estimates from the Basnayake dataset (Figure 5a).

At CRF, I estimate a total marsh C storage of 2,880 ± 327 Mg C, with 73% in the high marsh (2,100 ± 257 Mg C) and 27% in the low marsh (777 ± 69.8 Mg C) using the Basnayake dataset (Table 1). UNEP dataset marsh area leads to a C storage estimate of 6,240 ± 710 Mg C, and the CEC dataset estimates the highest C storage of 9,280 ± 1,060 Mg C (Figure 5b). The UNEP dataset C storage value for CRF is twice larger, while the CEC dataset C storage is three times larger than the Basnayake dataset value.

GBK marsh reports the lowest C storage among all sites at 2,620 ± 196 Mg C, with 63% in the high marsh (1,660 ± 196 Mg C) and 37% in the low marsh (957 ± 0 Mg C) (Basnayake et al. 2021) (Table 1). Both UNEP and CEC datasets report the same marsh area for GBK, leading to the same C storage estimate of 11,900 ± 1,150 Mg C (Figure 5c), which is 4.5 times higher than Basnayake dataset C storage estimates for this marsh.

Table 3.1 Comparison of areal extents, C storage ± SE (Mg C) and ACA ± SE (Mg C yr^{-1}) estimates for high and low marsh areas in three case study salt marsh sites in British Columbia: Boundary Bay (BB), Cypress River Flats (CRF), and Grice Bay-Kennedy River (GBK).

Dataset	Marsh Area (ha)				Marsh C Storage ± SE (Mg C)			Annual Marsh C Accumulation (ACA) ± SE (Mg C yr^{-1})	
	Total	HM	LM	Marsh Total*	HM	LM	Marsh Total*	HM	LM
Boundary Bay (BB)									
Basnayake et al. 2021	222	111	111	12,600 ± 1,500*	7,700 ± 929	4,530 ± 1080	229 ± 27.5*	147 ± 22.9	74 ± 14.4
UNEP-WCMC 2021	331	-	-	18,900 ± 2,240	-	-	342 ± 41.1	-	-
CEC 2021	1,210	-	-	68,800 ± 8,170	-	-	1,250 ± 150	-	-
Cypress River Flats (CRF)									
Basnayake et al. 2021	24.8	16.1	8.73	2,720 ± 310*	2,100 ± 257	777 ± 69.8	51.3 ± 6.30*	56.5 ± 5.94	5.41 ± 1.22
UNEP-WCMC 2021	56.8	-	-	6,240 ± 710	-	-	118 ± 14.5	-	-
CEC 2021	84.4	-	-	9,280 ± 1,060	-	-	175 ± 21.5	-	-
Grice Bay – Kennedy River (GBK)									
Basnayake et al. 2021	55.4	32.6	22.8	2,700 ± 260*	1,660 ± 196	957 ± 0.00	120 ± 7.80*	126 ± 5.87	10.7 ± 2.28
UNEP-WCMC 2021	244	-	-	11,900 ± 1,150	-	-	527 ± 34.1	-	-
CEC 2021	244	-	-	11,900 ± 1,150	-	-	527 ± 34.1	-	-

*HM = High Marsh, LM = Low Marsh, Marsh Total = values calculated using all-marsh average C stocks and CARs, rather than separated high-low marsh averages (refer to results section 3.4.4 for comparison of all-marsh with high-low marsh separated value totals for Basnayake dataset).

3.4.3. Annual Carbon Accumulation

Using the marsh area from Basnayake dataset, I estimate a total ACA of 221 ± 37.3 Mg C yr^{-1} at BB, with 67% of the accumulation the high marsh (147 ± 22.9 Mg C yr^{-1}) and 33% in the low marsh (74 ± 14.4 Mg C yr^{-1}) (Table 1). BB marsh area from the UNEP and CEC datasets lead to total ACA estimates of 342 ± 41.1 Mg C yr^{-1} and 1,250 ± 150 Mg C yr^{-1}, respectively. The UNEP dataset-based estimate is 1.5 times larger, while the CEC dataset-based estimate is an order of magnitude (5.7 times) higher than the Basnayake dataset (Figure 5d).

At CRF, I estimate a total ACA of 61.9 ± 7.16 Mg C yr^{-1}, with majority (91%) of the accumulation the high marsh (56.5 ± 5.94 Mg C yr^{-1}) and very low (9%) accumulation in the low marsh (5.41 ± 1.22 Mg C yr^{-1}) (Table 1). CRF marsh area from the UNEP and CEC datasets lead to total ACA estimates of 118 ± 14.5 Mg C yr^{-1} and 175 ± 21.5 Mg C yr^{-1}, respectively (Figure 5e), twice and three times larger than Basnayake dataset estimates, respectively.

At GBK, I estimate a total ACA of 137 ± 8.15 Mg C yr^{-1}, with majority (92%) of the accumulation the high marsh (126 ± 5.87 Mg C yr^{-1}) and 8% in the low marsh (10.7 ± 2.28 Mg C yr^{-1}) (Table 1). GBK marsh area from the UNEP and CEC datasets lead to higher total ACA estimate of 527 ± 34.1 Mg C yr^{-1} (Figure 5f), which is four times larger than the Basnayake dataset estimate.

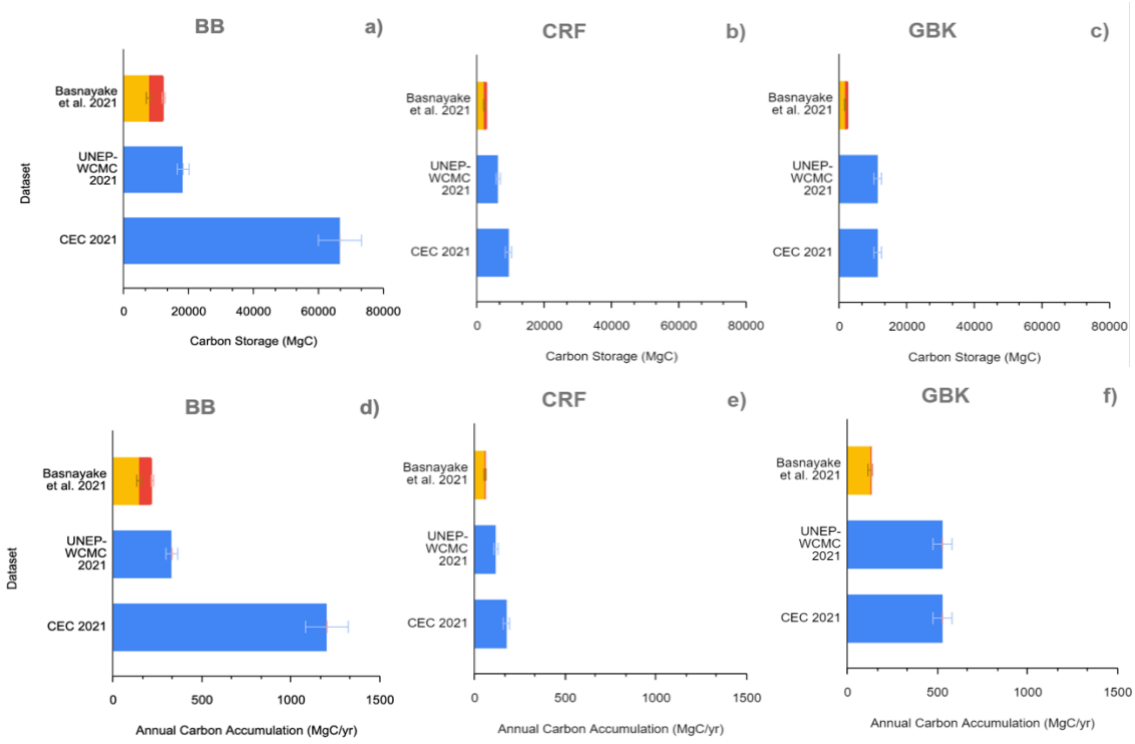

Figure 3.5 Comparison of C Storage ± SE (Mg C) (top panels) and ACA ± SE (Mg C yr^{-1}) (bottom panels) using three datasets for salt marsh areal extent.

Basnayake, UNEP and CEC datasets, at: a, d) Boundary Bay (BB), where high marsh values are represented in yellow, and low marsh values in red, b, e) Cypress River Flats (CRF) and c, f) Grice Bay-Kennedy River (GBK) salt marshes, where all marsh values are represented in blue. C storage and ACA values are calculated down to the peat layer for all sites.

3.4.4. Effect of Separating High and Low Marsh Areas

For the Basnayake dataset, I calculated C storage and ACA using whole marsh averages of C stocks and CARs to examine how it compares with calculating high and low marsh values separately and them adding together as described in sections 3.4.2 and 3.4.3.

At BB, C storage calculated using the whole marsh average value for C stocks (57.0 ± 6.77 Mg C ha^{-1}) was 12,600 ± 1,500 Mg C, which is 400 Mg C higher than the high and low marsh summation value. ACA calculated using the whole marsh CAR average value (103 ± 12.4 g C m^{-2} yr^{-1}) was 229 ± 27.5 Mg C yr^{-1}, which is 9 Mg C yr^{-1} higher than high and low marsh summation value.

At CRF, C storage calculated using the whole marsh average value for C stocks (110 ± 12.5 Mg C ha^{-1}) was 2,720 ± 310 Mg C, which is 160 Mg C lower than the high and low marsh summation value. ACA calculated using the whole marsh CAR average value (207 ± 26.0 g C m^{-2} yr^{-1}) was 51.3 ± 6.30 Mg C yr^{-1}, which is 10.6 Mg C yr^{-1} lower than high and low marsh summation value.

At GBK, C storage calculated using the whole marsh average value for C stocks (48.7 ± 4.70 Mg C ha^{-1}) was 2,700 ± 260 Mg C, which is 80 Mg C higher than the high and low marsh summation value. ACA calculated using the whole marsh CAR average value (217 ± 14.0 g C m^{-2} yr^{-1}) was 120 ± 7.80 Mg C yr^{-1}, which is 17 Mg C yr^{-1} lower than high and low marsh summation value.

Based on these calculations, the difference between C storage and ACA values obtained through separate high and low marsh calculations versus using a whole marsh average is not statistically significant for all three marshes ($p>0.05$).

3.5. Discussion

Our results show that regional and global salt marsh distribution datasets report areas for select BC marshes can be as much as two to five times larger than their actual magnitude. A key factor that impacts the accuracy of a spatial dataset is the methodology through which salt marsh distribution is mapped. In the case of three to five-fold overestimations of marsh area in the CEC dataset, I observe difficulty excluding

sandbars and mudflats from tidal marsh areal estimations, which has led to high uncertainty in marsh area, especially in CS. This dataset includes any bare land, including mudflats and sandbars. A study conducted in the Cowichan estuary, BC reported a soil organic C stock of 16.9 ± 4.36 Mg C ha^{-1} in the lower mudflats, which is 3 times lower than low salt marsh C stock average ± SE at our three case study sites (57 ± 5.19 Mg C ha^{-1}) (Douglas 2021). Previous studies found the lowest C stocks at sandy, exposed sites in the Baltic Sea (Rohr et al. 2016) and in Clayoquot Sound (Postlethwaite et al. 2018). Therefore, including mudflats and sandbar areas in salt marsh distribution leads to inaccurate estimates of salt marsh C storage. I observe two to four-fold overestimations in salt marsh area in the UNEP dataset. This dataset uses a buffer method around BCMCA salt marsh biobands lines to derive marsh area. Therefore, this dataset lacks precision in both its geographical placement of the marshes, as well as the method used to derive marsh area.

Recent studies such as Drever et al. 2021 and Macreadie et al. 2021 rely on regional-to-global datasets of salt marsh areas to examine C storage potential of salt marsh ecosystems, to act as NCS for climate change mitigation. Therefore, accuracy in areal estimates is important to avoid overestimating the ability of salt marshes to sequester and store blue carbon. Such miscalculations have far-reaching policy implications including overestimating the carbon mitigation potential of wetland related NCS such as avoided conversion and restoration.

NCS can help reach emission reduction goals to achieve Canada's goals under the Paris Agreement (ECCC 2019; Drever et al. 2021). At present, Canada is committed to NCS to build resilience and help Canada meet its 2030 and 2050 climate change objectives through the Nature Smart Climate Solutions Fund (NSCSF) (ECCC 2021). NSCSF aims to reduce 2 - 4 Mt CO_2e of GHG emissions per year by supporting projects that conserve, restore, and enhance wetlands to store and capture carbon.

A recent study in Canada estimated that blue carbon ecosystems have the potential to mitigate 1.7 Tg CO_2e/year in 2030 (Drever et al. 2021). At present, avoided loss and restoration of salt marsh habitats provide a relatively small contribution to mitigation at a national scale. However, this study identifies their high potential to deliver NCS on a per-hectare basis. Drever et al. (2021) identify that dykelands provide the most extensive opportunities for restoration of coastal marshes in Canada. Dykelands

are salt marshes that were dyked and drained to create agricultural land, such as the Boundary Bay salt marsh. Dykelands are widespread in coastal BC and Atlantic Canada, such as in the Bay of Fundy, New Brunswick, and St. Lawrence Estuary in Nova Scotia. However, BC dykelands were not included in this calculation due to the absence of reliable areal estimates and records (Drever et al. 2021). This current work emphasizes the importance of exercising caution when generalizing from global datasets – future estimates should rely on careful, local estimations to avoid 2-5-fold overestimations.

Studies estimate that full implementation of all cost-effective NCS, including avoided conversion and restoration of natural lands can provide up to one-third of the global mitigation needed in 2030 to keep warming below 2°C (Griscom et al. 2017; Drever et al. 2021). Globally, blue carbon ecosystems are calculated to store >30,000 Tg C across ~185 million ha, with their conservation potentially avoiding emissions of 304 (141–466) Tg CO_2e/yr (Macreadie et al. 2021). To arrive at this calculation of potentially avoided emissions, Macreadie et al. (2021) use the UNEP salt marsh dataset (Mcowen et al. 2017) for their estimate of global areal extent of salt marshes. This case study suggests that UNEP dataset salt marsh areal estimates could be up to two times higher than actual marsh area. If we assume that the UNEP dataset relied on regional studies that employed the same assumptions as used in BC, then the above-mentioned C storage, area, and avoided emissions estimates need to be cut by half to derive reliable estimates.

At the UN Climate Change Conference (COP26) held in 2021, 45 governments around the globe pledged to ramp up efforts to shift towards NCS (UNCCC 2021). At this event, Canada announced 1 billion Canadian dollars in international support for nature-based solutions, a fifth of its climate finance. It supports an international target to protect 30 per cent of lands, oceans, and coral reefs by 2030 (UN 2021). Internationally, the Glasgow Leaders' Declaration on Forests and Land Use was adopted at COP26 and endorsed by 141 countries to end and reverse deforestation by 2030 using NCS (Nasi 2022). At present, NCS efforts disproportionately focus on forest ecosystems; efforts were made at COP26 to advance NCS implementation beyond forests into marshes and marine ecosystems (Austin et al. 2021). Accurate quantification of global marsh area and C sequestration are therefore necessary for the advancement of NCS in blue carbon ecosystems.

Chapter 4. Conclusion

In chapter 2 of this study, I quantified marsh type, area, volume, carbon (C) stocks, marsh C storage, and carbon accumulation rates (CARs) for mid Boundary Bay (BBM), eastern Boundary Bay (BBE), and Mud Bay (MB), with novel year-round porewater salinities presented for all sites at Boundary Bay (BB) marsh. I built upon published research (Gailis et al. 2021) in western Boundary Bay (BBW) to develop an improved understanding of marsh processes and blue carbon storage across all parts of the marsh. My synthesis not only provides information about carbon fluxes, but also contribute supporting information about the sedimentary dynamics in the marsh. This study suggests that the eastern portion of the marsh (BBE, MB) has decreased by ~35% since 1930, which might be partially attributed to the construction of Highway 99 and dike renovations between early 1940's and 1960's. The planned expansion of low marsh area in BBE and MB through sediment deposition during living dike construction has implications for long-term increase in its low-marsh C stocks over the next three decades.

Year-round porewater salinity data indicate that high and low marsh areas in eastern BB are mesohaline year-round, which suggest its potential to offset the carbon being stored in the marsh through emission of greenhouse gases (GHGs). I recommend introducing GHG flux measurements in mesohaline marsh areas with groundwater levels within 25 cm of the soil surface in the summer months, and on-going monitoring of sea level rise (SLR) and sedimentation rates at the leading edge of the marsh to ensure continued carbon sequestration. Implementation of the above-mentioned steps will produce a more comprehensive carbon budget of BB salt marsh. I expect this robust profile of carbon sequestration will facilitate incorporating BB into provincial wetland management and/or carbon offset initiatives in British Columbia (BC).

Chapter 3 presents a simple case study of three salt marshes in BC and calls for a re-evaluation of current salt marsh distribution mapping efforts for them to be valuable for climate change mitigation policy. In this study, I mapped high and low marsh areas for three tidal salt marshes in BC with the goal of reducing uncertainty around salt marsh areal extent in existing datasets. I compared our areal estimates with one regional (CEC 2021) and one global (UNEP-WCMC 2021) salt marsh distribution dataset that has been

used to estimate the global potential of natural climate solutions (NCS) in salt marsh habitats (Mcowen et al. 2017; Drever et al. 2021; Macreadie et al. 2021). I used these areal estimates, coupled with C stocks and CARs data from recent regional studies to quantify C storage and annual carbon accumulation (ACA) for each of the three marshes. These existing salt marsh distribution datasets largely overestimate marsh distribution in BB and Clayoquot Sound and can lead to overestimations in blue carbon storage and accumulation. Specifically, our results indicate that at all three case study sites, using areal estimates from the UNEP and CEC datasets resulted in C storage and ACA values were two times and five times larger than our ground-truthed estimates, respectively. Moving forward, I recognize the need for more detailed salt marsh distribution mapping efforts to avoid large discrepancies between datasets and to provide accurate C storage and accumulation estimates towards the development of effective NCS and climate change mitigation policy.

References

Adams, C. A., J. E. Andrews, and T. Jickells. 2012. "Nitrous oxide and methane fluxes vs. carbon, nitrogen and phosphorous burial in new intertidal and saltmarsh sediments." Science of The Total Environment 434:240-51. doi: https://doi.org/10.1016/j.scitotenv.2011.11.058.

Amante, Christopher J. 2018. "Estimating Coastal Digital Elevation Model Uncertainty." Journal of Coastal Research 34 (6):1382-97. doi: 10.2112/jcoastres-d-17-00211.1.

Anderson, R.F., S.L. Schiff and R.H. Hesslein. 1987. Determining sediment accumulation and mixing rates using Pb-210, Cs-137, and other tracers: Problems due to postdepositional mobility or coring artifacts. Canadian Journal of Fisheries and Aquatic Sciences. 44(S1), 231-250.

Appleby, P. G., and F. Oldfield. 1978. “The Calculation of Lead- 210 Dates Assuming a Constant Rate of Supply of Unsupported 210Pb to the Sediment.” *Catena* 5 (1): 1–8. doi:10.1016/S0341-8162(78)80002-2.

Appleby, P. G. 2001. Chapter 9 Chronostratigraphic techniques in recent sediments. In W. M. Last, & J. P. Smol (Eds.), Tracking environmental change using lake sediments. Volume 1: Basin analysis, coring, and chronological techniques (pp. 171–203). Kluwer Academic Publishers Appleby, P. G. (2001). Chapter 9 Chronostratigraphic techniques in recent sediments. In W. M. Last, & J. P. Smol (Eds.), Tracking environmental change using lake sediments. Volume 1: Basin analysis, coring, and chronological techniques (pp. 171–203). Kluwer Academic Publishers.

Arias-Ortiz, A., P. Masque, J. Garcia-Orellana, O. Serrano, I. Mazarrasa, N. Marba, C. E. Lovelock, P. S. Lavery, and C. M. Duarte. 2018. "Reviews and syntheses: Pb-210-derived sediment and carbon accumulation rates in vegetated coastal ecosystems - setting the record straight." Biogeosciences 15 (22):6791-818. doi: 10.5194/bg-15-6791-2018.

Arnaud, Fabien & Lignier, Vincent & Revel, M. & Desmet, Marc & Beck, Christian & Pourchet, M. & Charlet, Francois & Alain, Trentesaux & Tribovillard, Nicolas. 2002. Flood and earthquake disturbance of 210Pb geochronology (Lake Anterne, NW Alps). Terra Nova. 14. 225 - 232. 10.1046/j.1365-3121.2002.00413.x.

Austin W, Cohen F, Coomes D, Hanley N, Lewis S, Luque-Lora R, Marchant R, Naylor L, Queiros AM, Savaresi A, Seddon N, Smith A, Smith P & Wheeler C. 2021. COP26 Universities Network Briefing: Nature based solutions for climate change, people and biodiversity. University of Stirling. https://www.stir.ac.uk/research/public-policy-hub/policy-briefings/

Barbier, E.B., Hacker, S.D., Kennedy, C., Koch, E.W., Stier, A.C. and Silliman, B.R. 2011. The value of estuarine and coastal ecosystem services. Ecological Monographs, 81: 169-193. https://doi.org/10.1890/10-1510.1

Bartlett, Karen B., David S. Bartlett, Robert C. Harriss, and Daniel I. Sebacher. 1987. "Methane emissions along a salt marsh salinity gradient." Biogeochemistry 4 (3):183-202. doi: 10.1007/BF02187365.

Bednarski, J.M. 2015. Surficial Geology and Pleistocene stratigraphy from Deep Bay to Nanoose Harbour, Vancouver Island, British Columbia; Geological Survey of Canada, Open File 7681, 1 .zip file. doi:10.4095/295609

Bridgham, S.D., Megonigal, J.P., Keller, J.K. et al. 2006. The carbon balance of North American wetlands. Wetlands 26, 889–916. https://doi.org/10.1672/0277-5212(2006)26[889:TCBONA]2.0.CO;2

British Columbia Marine Conservation Analysis (BCMCA), a Tides Canada Initiatives Project. 2009. Dataset: BCMCA_ECO_VascPlants_salicornia_bioband_data. Retrieved from https://bcmca.ca/datafeatures/eco_vascplants_saltmarshbioband/

British Columbia Ministry of Forests, Lands, Natural Resource Operations and Rural Development (BC FLNRORD). 2018. British Columbia Shorezone Observed Habitat Polygons – GeoBC, Victoria, BC, Canada. Retrieved from https://catalogue.data.gov.bc.ca/dataset/shorezone-observed-habitat-polygons/resource/995afa79-05d4-4c68-8d30-a81e0bf2b67d#edc-pow

Brophy, L.S, van de Wetering, S, Ewald, M.J., Brown, L. A, Janousek, C.N. 2014. Ni-les'tun tidal wetland restoration effectiveness monitoring: Year 2 post-restoration (2013). Institute for Applied Ecology, Corvallis, OR

Callaway, J.C., E.L. Borgnis, R.E. Turner, and C.S. Milan. 2012. "Carbon sequestration and sediment accretion in San Francisco Bay tidal wetlands." Estuaries and Coasts 35:1163–81.

Chastain, S., K. E. Kohfeld, M.G. Pellatt, Olid, C., and Gailis, M. 2021. Quantification of Blue Carbon in Salt Marshes of the Pacific Coast of Canada. Submitted to Biogeosciences. https://doi.org/10.5194/bg-2021-157.

Chmura, Gail, A. Coffey, and R. Crago. 2001. "Variation in surface sediment deposition on salt marshes in the Bay of Fundy." Journal of Coastal Research 17:221-7.

Chmura, Gail L. 2013. "What do we need to assess the sustainability of the tidal salt marsh carbon sink?" Ocean & Coastal Management 83:25-31. doi: https://doi.org/10.1016/j.ocecoaman.2011.09.006.

Chmura, Gail L., Shimon C. Anisfeld, Donald R. Cahoon, and James C. Lynch. 2003. "Global carbon sequestration in tidal, saline wetland soils." Global Biogeochem. Cycles 17 (4,1111): doi:10.1029/2002GB001917.

Chmura, Gail L., Lisa Kellman, Lee van Ardenne, and Glenn R. Guntenspergen. 2016. "Greenhouse Gas Fluxes from Salt Marshes Exposed to Chronic Nutrient Enrichment." PLOS One 11 (2): e0149937. doi: 10.1371/journal.pone.0149937.

Christensen, M, and Vadeboncoeur, N. 2019. Mud Bay Monitoring Report. Ducks Unlimited Canada and Smart Shores Inc.

Church, J.A., P.U. Clark, A. Cazenave, J.M. Gregory, S. Jevrejeva, A. Levermann, M.A. Merrifield, G.A. Milne, R.S. Nerem, P.D. Nunn, A.J. Payne, W.T. Pfeffer, D. Stammer and A.S. Unnikrishnan. 2013: Sea Level Change. In: Climate Change 2013: The Physical Science Basis. Contribution of Working Group I to the Fifth Assessment Report of the Intergovernmental Panel on Climate Change [Stocker, T.F., D. Qin, G.-K. Plattner, M. Tignor, S.K. Allen, J. Boschung, A. Nauels, Y. Xia, V. Bex and P.M. Midgley (eds.)]. Cambridge University Press, Cambridge, United Kingdom and New York, NY, USA.

City of Surrey. 2021. “Mud Bay Foreshore Enhancements”. *Accessed* January 10. https://www.surrey. ca/mud-bay-foreshore-enhancements

Climate Change Accountability Act, Statutes of British Columbia 2007, c 42, s 2.

Commission for Environmental Cooperation (CEC). 2021. North American Blue Carbon, 2021. CEC_North_America_Saltmarshes_Py.shp. Retrieved from http://www.cec.org/north-american-environmental-atlas/north-american-blue-carbon-2021/

Connor, Richard F., Gail L. Chmura, and C. Beth Beecher. 2001. "Carbon accumulation in Bay of Fundy salt marshes: Implications for restoration of reclaimed marshes." Global Biogeochemical Cycles 15 (4):943-54. doi: 10.1029/2000gb001346.

Crooks, S., J. Rybczyk, K. O’Connell, D.L. Devier, K. Poppe, and S. Emmett-Mattox. 2014. " Coastal Blue Carbon Opportunity Assessment for the Snohomish Estuary: The Climate Benefits of Estuary Restoration." In, 19-43. Bellingham, WA, USA: Environmental Science Associates.

Dashtgard, S. E. 2011. “Linking invertebrate burrow distributions (neoichnology) to physicochemical stresses on a sandy tidal flat: implications for the rock record.” Sedimentology (58), 1303-1325. doi: 10.1111/j.1365-3091.2010.01210.x.

Dashtgard, S.E.& La Croix, A.D. 2015. Chapter 3: Sedimentological trends across the tidal-fluvial transition, Fraser River, Canada: A review and some broader implications. Developments in Sedimentology (68), 111-126. http://dx.doi.org/10.1016/B978-0-444-63529-7.00005-5

DeLaune, Ronald D., Chris J. Smith, and William H. Patrick. 1983. "Methane release from Gulf coast wetlands." Tellus B: Chemical and Physical Meteorology 35 (1):8-15. doi: 10.3402/tellusb.v35i1.14581.

Donato, D., Kauffman, J., Murdiyarso, D. et al. 2011. Mangroves among the most carbon-rich forests in the tropics. Nature Geosci 4, 293–297. https://doi.org/10.1038/ngeo1123

Douglas, T. 2021. Blue carbon storage in the Cowichan Estuary, British Columbia. Master's Thesis. University of Victoria, Victoria, British Columbia.

Drake, K., H. Halifax, S. C. Adamowicz, and C. Craft. 2015. "Carbon Sequestration in Tidal Salt Marshes of the Northeast United States." Environ Manage 56 (4):998-1008. doi: 10.1007/s00267-015-0568-z.

Drexler, J., Woo, I., Fuller, C., and Nakai, G. 2019. Carbon accumulation and vertical accretion in a restored vs. historic salt marsh in southern Puget Sound, Washington, USA. Restoration Ecology. 27. 10.1111/rec.12941.

Drever CR, Cook-Patton SC, Akhter F, Badiou PH, Chmura GL, et al. 2021. Natural climate solutions for Canada. Sci Adv. (23). doi: 10.1126/sciadv.abd6034

Duarte, Carlos M., Iñigo J. Losada, Iris E. Hendriks, Inés Mazarrasa, and Núria Marbà. 2013. "The role of coastal plant communities for climate change mitigation and adaptation." Nature Climate Change 3 (11):961-8. doi: 10.1038/nclimate1970.

Durham, R.W. and S.R. Joshi. 1980. The Pb-210 and Cs-137 profiles in sediment cores from Lakes Matagami and Quevillon, northwest Quebec, Canada. CAN. J. Earth Sci. 17, 1746-1750.

Eakins, J. D. and R. T. Morrison. 1978. A new procedure for the determination of lead-210 in lake and marine sediments. International Journal of Applied Radiation and Isotopes. 29, 531-536.

Elsey-Quirk, Tracy, Denise Seliskar, Christopher Sommerfield, and John Gallagher. 2011. "Salt Marsh Carbon Pool Distribution in a Mid-Atlantic Lagoon, USA: Sea Level Rise Implications." Wetlands 31:87-99. doi: 10.1007/s13157-010-0139-2.

Emmer, I.M., B.A. Needelman, S. Emmett-Mattox, S. Crooks, J.P. Megonigal, D. Myers, M.P.J. Oreska, K.J. McGlathery, and D. Verified Carbon Standard Shoch, Washington, D.C. 2015 "VCS Methodology VM0033: Methodology for tidal wetland and seagrass restoration." In, 115.

Engels, S., and M. C. Roberts. 2005. "The Architecture of Prograding Sandy-Gravel Beach Ridges Formed during the Last Holocene Highstand: Southwestern British Columbia, Canada." Journal of Sedimentary Research 75 (6): 1052–1064. doi:10.2110/jsr.2005.081.

Environment and Climate Change Canada (ECCC). 2019. Canada's 4th Biennial Report to the United Nations Framework Convention on Climate Change (UNFCCC), p. 184.

Environment and Climate Change Canada (ECCC). 2021. Nature Smart Climate Solutions Fund (NSCSF). Retrieved from https://www.canada.ca/en/environment-climate-change/services/environmental-funding/programs/nature-smart-climate-solutions-fund.html

Environment and Climate Change Canada (ECCC). 2021. Canadian Environmental Sustainability Indicators: Progress towards Canada's greenhouse gas emissions reduction target. Retrieved from www.canada.ca/en/environment-climate-change/services/environmental-indicators/progress- towards-canada-greenhouse-gas-emissions-reduction-target.html.

Environmental Measurements Laboratory, US Department of Energy - HASL-300 Method Ga-01-R Gamma Emitters in the Environment by Energy, HASL EML Procedures Manual, 28th Edition, Februray 1997.

Fargione, J. E., Bassett, S., Boucher, T., Bridgham, S. D., Conant, R. T., Cook-Patton, S. C., Ellis, P. W., Falcucci, A., Fourqurean, J. W., Gopalakrishna, T. 2018. Natural climate solutions for the United States. Sci. Adv. 4, eaat1869.

Gailis, M., Kohfeld, K. E., Pellatt, M. G., and Carlson, D. 2021. Quantifying blue carbon for the largest salt marsh in southern British Columbia: implications for regional coastal management. Coastal Engineering Journal. DOI: 10.1080/21664250.2021.1894815

Government of British Columbia. 2020. “Clean BC: 2020 Climate Change Accountability Report”. British Columbia Ministry of Environment. Retrieved from https://www2.gov.bc.ca/assets/gov/environment/climate-change/action/cleanbc/2020_climate_change_accountability_report.pdf

Government of British Columbia. 2020. "Boundary Bay wildlife management area." British Columbia Ministry of Environment. Retrieved from https://www2.gov.bc.ca/gov/content/environment/plants-animals-ecosystems/wildlife/wildlife-habitats/conservation-lands/wma/wmas-list/boundary-bay.

Government of British Columbia. n.d. British Columbia Ministry of Environment. Consultation Backgrounder – Carbon Pricing. Retrieved from https://www2.gov.bc.ca/assets/gov/environment/climate-change/action/legislation/carbon-pricing-bg.pdf.

Government of British Columbia. 2021. “Watershed, wetland projects create jobs, protect environment”. British Columbia Ministry of Environment, Accessed May 26, 2021. https://news.gov.bc.ca/releases/2021ENV0020-000463

Government of Canada. 1991. The Federal Policy on Wetland Conservation. Published by Authority of the Minister of Environment, Minister of Supply and Services Canada. Environment Canada. Retrieved from http://publications.gc.ca/collections/Collection/CW66-116-1991E.pdf.

Government of Canada. 2021. Canadian Climate Normals:1971-2000 Station Data: Delta Ladner South. Retrieved from https://climate.weather.gc.ca/climate_normals/results_e.html

Griscom, B. W., Adams, J., Ellis, P. W., Houghton, R. A., Lomax, G., Miteva, D. A., Schlesinger, W. H., Shoch, D., Siikamäki, J. V., and Smith, P. 2017. Natural climate solutions. Proc. Natl. Acad. Sci. U.S.A. 114, 11645–11650.

Heiri, O., Lotter, A., and Lemcke, G. 2001. Loss on Ignition as a Method for Estimating Organic and Carbonate Content in Sediments: Reproducibility and Comparability of Results. Journal of Paleolimnology. 25. 10.1023/A:1008119611481.

Howard, J., S. Hoyt, K. Isensee, E. Pidgeon, and M. Telszewski. 2014. "Coastal Blue Carbon: Methods for assessing carbon stocks and emissions factors in mangroves, tidal salt marshes, and seagrass meadows." In, 184. Arlington, Virginia, USA. Conservation International, Intergovernmental Oceanographic Commission of UNESCO, International Union for Conservation of Nature.

Howes, D., J.R. Harper, and E.H. Owens. 1995. British Columbia Physical Shorezone Mapping System, Ver. 1.0. Province of British Columbia, Ministry of Environment, Lands and parks, Environmental Emergency Services for the Coastal Task Force, Resources Inventory Committee, Victoria, BC, 79pp. Retrieved from https://www2.gov.bc.ca/assets/gov/data/geographic/topography/bc_shorezonemappingsystem.pdf

Huntingford, C., Atkin, O.K., Martinez-de la Torre, A. et al. 2017. Implications of improved representations of plant respiration in a changing climate. Nat Commun 8, 1602. https://doi.org/10.1038/s41467-017-01774-z

Infrastructure Canada. 2020. "Infrastructure Canada projects since 2002 – British Columbia: Coastal Flood protection for the cities of Surrey and Delta, and the Semiahmoo First Nation." Accessed September 1. https://www.infrastructure.gc.ca/investments-2002-investissements/projects-list-liste-de-projets-eng.html?pt=bc&cat=Disaster%20Mitigation.

IPCC, Intergovernmental Panel on Climate Change. 2000. "Land use, land-use change, and forestry." In, edited by R.T. Watson, I.R. Noble, B. Bolin, N.H. Ravindranath, Verardo D.J. and D.J. Dokken, 375. Cambridge, United Kingdom.

IPCC, Intergovernmental Panel on Climate Change. 2021. Summary for Policymakers. In: Climate Change 2021: The Physical Science Basis. Contribution of Working Group I to the Sixth Assessment Report of the Intergovernmental Panel on Climate Change [Masson-Delmotte, V., P. Zhai, A. Pirani, S.L.Connors, C. P an, S. Berger, N. Caud, Y. Chen, L. Goldfarb, M.I. Gomis, M. Huang, K. Leitzell, E. Lonnoy, J.B.R. Matthews, T.K. Maycock, T. Waterfield, O. Yelek i, R. Yu, and B. Zhou (eds.)]. In Press.

Irving, Andrew & Connell, Sean & Russell, Bayden. 2011. Restoring Coastal Plants to Improve Global Carbon Storage: Reaping What We Sow. PloS one. 6. e18311. 10.1371/journal.pone.0018311.

Janousek C., Bailey, S., van de Wetering, S., Brophy, L., Bridgham, S., Schultz, M., Tice-Lewis, M. 2021. Early post-restoration recovery of tidal wetland structure and function at the Southern Flow Corridor project, Tillamook Bay, Oregon. Oregon State University, Tillamook Estuaries Partnership, Confederated Tribes of Siletz Indians, Institute for Applied Ecology, and University of Oregon.

Kauffman, JB, Giovanonni, L, Kelly, J, et al. 2020. Total ecosystem carbon stocks at the marine-terrestrial interface: Blue carbon of the Pacific Northwest Coast, United States. Glob Change Biol. 26: 5679– 5692. https://doi.org/10.1111/gcb.15248

Kellerhalls, P., and J. W. Murray. 1969. “Tidal Flats at Boundary Bay, Fraser River Delta, British Columbia.” Bulletin of Canadian Petroleum Geology 17 (1): 67–97.

Kelleway, J. J., N. Saintilan, P. I. Macreadie, J. A. Baldock, and P. J. Ralph. 2017. "Sediment and carbon deposition vary among vegetation assemblages in a coastal salt marsh." Biogeosciences 14 (16):3763-79. doi: 10.5194/bg-14-3763-2017.

Kiehl, K., Esselink, P. and Bakker, J.P. 1997. Nutrient limitation and plant species composition in temperate salt marshes. Oecologia, 111, 325-330.

Kroeger, K. D., Crooks, S., Moseman-Valtierra, S., and Tang, J. 2017. "Restoring tides to reduce methane emissions in impounded wetlands: A new and potent Blue Carbon climate change intervention." Nature 7 (11914):1-12. doi: DOI:10.1038/s41598-017-12138-4.

Le, D.N. & Zidek, J.V. 2006. Statistical analysis of environmental space-time processes. New York: Springer. Ch. 7: “Spatial Prediction: Classical Approaches”

MacKenzie, A. B., S. M. L. Hardie, J. G. Farmer, L. J. Eades, and I. D. Pulford. 2011. "Analytical and sampling constraints in 210Pb dating." Science of The Total Environment 409 (7):1298-304. doi: https://doi.org/10.1016/j.scitotenv.2010.11.040.

Macreadie, P. I., A. Anton, J. A. Raven, N. Beaumont, R. M. Connolly, D. A. Friess, J. J. Kelleway, et al. 2019. "The future of Blue Carbon science." Nature Communications 10. doi: 10.1038/s41467-019-11693-w.

Macreadie, P.I., Costa, M.D.P., Atwood, T.B. et al. 2021. Blue carbon as a natural climate solution. Nature Review Earth Environment. https://doi.org/10.1038/s43017-021-00224-1

Mahaney, W. M., Smemo, K. A., and Gross, K. L. 2008. "Impacts of C4 grass introductions on soil carbon and nitrogen cycling in C3-dominated successional systems." Oecologia 157 (2):295-305. doi: 10.1007/s00442-008-1063-5.

Marcoe, K. and Pilson, S. 2017. Habitat change in the lower Columbia River estuary, 1870–2009. Journal of Coastal Conservation. 21. 1-21. 10.1007/s11852-017-0523-7.

Mathieu, G.G., P.E. Biscaye, R.A. Lupton and D.E. Hammond. System for measurement of 222Rn at low levels in natural waters. 1988. Health Physics. 55, 989 – 992.

Mathieu, G.G. Appendix I - Rn222-Ra226 Technique of Analyses. 1977. Transport and transfer rates in the waters of the continental shelf. Contract EY 76-S-02-2185.

Mazzotti, S., Jones, C., and Thomson, R. E. 2008. Relative and absolute sea level rise in western Canada and northwestern United States from a combined tide gauge-GPS analysis, J. Geophys. Res., 113, C11019, doi:10.1029/2008JC004835.

Mcleod, E., Chmura, G. L., Bouillon, S., Salm, R., BjoÈrk, M., Duarte, C. M., Lovelock, C. E., Schlesinger, W. H., and Silliman, B. R. 2011. "A blueprint for blue carbon: toward an improved understanding of the role of vegetated coastal habitats in sequestering CO_2." Frontiers in Ecology and the Environment 9 (10):552-60.

Mcowen C, Weatherdon LV, Bochove J, Sullivan E, Blyth S, Zockler C, Stanwell-Smith D, Kingston N, Martin CS, Spalding M, Fletcher S. 2017. A global map of saltmarshes (v6.1). Biodiversity Data Journal 5: e11764. Paper DOI: https://doi.org/10.3897/BDJ.5.e11764; Data DOI: https://doi.org/10.34892/07vk-ws51

Moomaw, W. R., Chmura, G. L., Davies, G. T., Finlayson, C. M., Middleton, B. A., Natali, S. M., Perry, J. E., Roulet, N. and Sutton-Grier, A. E. 2018. "Wetlands in a Changing Climate: Science, Policy and Management." Wetlands 38 (2):183-205. doi: 10.1007/s13157-018-1023-8.

Morton, R. A., and William A. White. 1997. "Characteristics of and corrections for core shortening in unconsolidated sediments." Journal of Coastal Research 13 (3):761-9.

Nasi, R. 2022. The Glasgow leaders' declaration on forests and land use: Significance toward "Net Zero". Glob Change Biol. https://doi.org/10.1111/gcb.16039

Nellemann, C., Corcoran, E., Duarte, C.M., Valdés, L., De Young, C., Fonseca, L., Grimsditch, G. 2009. Blue Carbon. A Rapid Response Assessment. United Nations Environment Programme, GRID-Arendal, Birkeland, Norway, p. 80.

Nicholls, R. J., Townend, I. H., Bradbury, A. P., Ramsbottom, D. & Day, S. A. 2013. Planning for long-term coastal change: experiences from England and Wales. Ocean Eng. 71, 3–16.

O'Keefe Suttles, J.A., Eagle, M.J., Mann, A.G., Moseman-Valtierra, S., Pratt, S.E., Kroeger, K.D., 2021. Collection, analysis, and age-dating of sediment cores from salt marshes, Rhode Island, 2016: U.S. Geological Survey data release, https://doi.org/10.5066/P94HIDVU.

Ouyang, X., and S. Y. Lee. 2014. "Updated estimates of carbon accumulation rates in coastal marsh sediments." Biogeosciences 11 (18):5057-71. doi: 10.5194/bg-11-5057-2014.

Peck, E. K., Wheatcroft, R. A., & Brophy, L. S. 2020. Controls on sediment accretion and blue carbon burial in tidal saline wetlands: Insights from the Oregon coast, USA. Journal of Geophysical Research: Biogeosciences, 125, e2019JG005464. https://doi.org/10.1029/2019JG005464

Pendleton, L., DC Donato, BC Murray, S Crooks, WA Jenkins, S Sifleet, Christopher Craft, et al. 2012. "Estimating global blue carbon emissions from conversion and degradation of vegetated coastal ecosystems." PLOS One 7 (9):e43542. doi: doi:10.1371/journal.pone.0043542.

Pendleton, Linwood H., Ariana E. Sutton-Grier, David R. Gordon, Brian C. Murray, Britta E. Victor, Roger B. Griffis, Jen A. V. Lechuga, and Chandra Giri. 2013. "Considering “Coastal Carbon” in Existing U.S. Federal Statutes and Policies." Coastal Management 41 (5):439-56. doi: 10.1080/08920753.2013.822294.

Pennings, S.C., and Bertness, M.D. 2001. "Salt marsh communities." In Marine Community Ecology edited by M. E. Hay, 289-316 Sunderland: Sinauer Associates.

Pennington, W., R.S. Cambray and E.M. Fisher. 1973. Observations on lake sediments using fallout Cs-137 as a tracer. Reprint from Nature. 242(5396), 324-326. March 30, 1973

Peyronnin, N. et al. 2013. Louisiana’s 2012 coastal master plan: overview of a science-based and publicly informed decision-making process. J. Coast. Res. 67, 1–15.

Pilarczyk, J.E., Sawai, Y., Namegaya, Y. et al. 2021. A further source of Tokyo earthquakes and Pacific Ocean tsunamis. Nat. Geosci. 14, 796–800. doi.org/10.1038/s41561-021-00812-2

Poffenbarger, Hanna J., Brian A. Needelman, and J. Patrick Megonigal. 2011. "Salinity Influence on Methane Emissions from Tidal Marshes." Wetlands 31 (5):831-42. doi: 10.1007/s13157-011-0197-0.

Porter, Glendon Leslie. 1982. "Vegetation-environment relationships in the tidal marshes of the Fraser River Delta, British Columbia.", The University of British Columbia.

Postlethwaite, Victoria, Aimee McGowen, Karen Kohfeld, C. Robinson, and Marlow Pellatt. 2018. "Low blue carbon storage in eelgrass (Zostera marina) meadows on the Pacific Coast of Canada." PLOS One 13. doi: 10.1371/journal.pone.0198348.

Readshaw, J., J. Wilson, and C. Robinson. 2018. Design Basis for the Living Dike Concept, 35. Vancouver, BC: West Coast Environmental Law. https://wcel.org/sites/default/files/ publications/2019-livingdikeconceptbrief-final.pdf

Ritchie, J.C. and J. R. McHenry. 1990. Application of radioactive fallout cesium-137 for measuring soil erosion and sediment accumulation rates and patterns: a review. J. Environ. Qual. 19, 215-233.

Rohr ME, BostroÈm C, Canal-VergeÂs P, Holmer M. 2016. Blue carbon stock in Baltic Sea eelgrass (Zostera marina) meadows. Biogeosciences. 13:6139-6153.

Rosentreter, J., Maher, D., Erler, D., Murray, R., and Eyre, B. 2018. Methane emissions partially offset “blue carbon” burial in mangroves. Science Advances, 4(6). DOI: 10.1126/sciadv.aao4985

Roughan, B. L., Kellman, L., Smith, E., and Chmura, G. L. 2018. Nitrous oxide emissions could reduce the blue carbon valu8e of marshes on eutrophic estuaries. Environ. Res. Lett. 13 044034. DOI:10.1088/1748-9326/aab63c.

Rozema, J., & Blom, B. 1977. Effects of Salinity and Inundation on the Growth of Agrostis Stolonifera and Juncus Gerardii. Journal of Ecology, 65(1), 213-222. doi:10.2307/2259075

Schuerch, M., Spencer, T., Temmerman, S. et al. 2018. “Future response of global coastal wetlands to sea-level rise”. Nature 561**,** 231–234. https://doi.org/10.1038/s41586-018-0476-5

Sheehan, Lindsey, Edward Sherwood, Ryan Moyer, Kara Radabaugh, and Stefanie Simpson. 2019. "Blue Carbon: an Additional Driver for Restoring and Preserving Ecological Services of Coastal Wetlands in Tampa Bay (Florida, USA)." Wetlands. doi: 10.1007/s13157-019-01137-y.

Shepperd, Jane Elizabeth. 1981. "Development of a salt marsh on the Fraser River delta at Boundary Bay, British Columbia,." The University of British Columbia,.

Snidvongs, A., G.M. McMurtry and S.V. Smith. 1992. Pb-210 and Cs-137 in sediments and soils of Tomales Bay Watershed, Northen California. Department of Oceanography, Univ. of Hawaii at Manoa Hololulu, HI 96822, U.S.A. Aug 1992.

Stagg, Camille L., Ken W. Krauss, Donald R. Cahoon, Nicole Cormier, William H. Conner, and Christopher M. Swarzenski. 2016. "Processes Contributing to Resilience of Coastal Wetlands to Sea-Level Rise." Ecosystems 19 (8):1445-59. doi: 10.1007/s10021-016-0015-x.

Sutton-Grier, Ariana E., and Amber Moore. 2016. "Leveraging Carbon Services of Coastal Ecosystems for Habitat Protection and Restoration,." Coastal Management:DOI: 10.1080/08920753.2016.1160206.

Sutton-Grier, Ariana E., Kateryna Wowk, and Holly Bamford. 2015. "Future of our coasts: The potential for natural and hybrid infrastructure to enhance the resilience of our coastal communities, economies and ecosystems." Environmental Science & Policy 51:137-48. doi: https://doi.org/10.1016/j.envsci.2015.04.006.

Swinbanks, David D., and James W. Murray. 1981. "Biosedimentological zonation of Boundary Bay tidal flats, Fraser River Delta, British Columbia." Sedimentology 28 (2):201-37. doi: 10.1111/j.1365-3091.1981.tb01677.x.

Temmerman, S., T. J. Bouma, G. Govers, Z. B. Wang, M. B. De Vries, and P. M. J. Herman. 2005. "Impact of vegetation on flow routing and sedimentation patterns: Three-dimensional modeling for a tidal marsh." Journal of Geophysical Research: Earth Surface 110 (F4). doi: 10.1029/2005jf000301.

Temmerman, Stijn, Patrick Meire, Tjeerd J. Bouma, Peter M. J. Herman, Tom Ysebaert, and Huib J. De Vriend. 2013. "Ecosystem-based coastal defence in the face of global change." Nature 504 (7478):79-83. doi: 10.1038/nature12859.

Thomas, Severine and Ridd, Peter. 2004. “Review of methods to measure short time scale sediment accumulation”. Marine Geology. 207 (1-40): 95-114. https://doi.org/10.1016/j.margeo.2004.03.011

Ullman, Roger, Vasco Bilbao-Bastida, and Gabriel Grimsditch. 2013. "Including Blue Carbon in climate market mechanisms." Ocean & Coastal Management 83:15-8. doi: https://doi.org/10.1016/j.ocecoaman.2012.02.009.

United Nations (UN). 2021. COP26 Day 7: Sticking points and nature-based solutions. Retrieved from https://www.un.org/en/climatechange/cop26-day-7-sticking-points-and-nature-based-solutions

United Nations Climate Change Conference (UNCCC). 2021. COP26: The Glasgow Climate Pact. Retrieved from https://ukcop26.org/wp-content/uploads/2021/11/COP26-Presidency-Outcomes-The-Climate-Pact.pdf

van Ardenne, L. B., Hughes, J. F., & Chmura, G. L. 2021. “Tidal marsh sediment and carbon accretion on a geomorphologically dynamic coastline”. Journal of Geophysical Research: Biogeosciences, 126, e2021JG006507. https://doi.org/10.1029/2021JG006507

Villa, Jorge A., and Blanca Bernal. 2018. "Carbon sequestration in wetlands, from science to practice: An overview of the biogeochemical process, measurement methods, and policy framework." Ecological Engineering 114:115-28. doi: https://doi.org/10.1016/j.ecoleng.2017.06.037.

Wang, Z., D. Zeng, and W. H. Patrick, Jr. 1996. "Methane emissions from natural wetlands." Environ Monit Assess 42 (1-2):143-61. doi: 10.1007/bf00394047.

Weinmmann F., Boule, M., Brunner, K., Malek, J. and Yoshino, V. 1984. Wetland plants of the Pacific northwest. U.S. Army Corps of Engineers, Seattle District pp.85.

Wollenberg JT, Biswas A, Chmura GL. 2018. Greenhouse gas flux with reflooding of a drained salt marsh soil. PeerJ 6:e5659 http://doi.org/10.7717/peerj.5659

Zhou, Junli, Ying Wu, Jing Zhang, Qinshu Kang, and Zhengtao Liu. 2006. "Carbon and nitrogen composition and stable isotope as potential indicators of source and fate of organic matter in the salt marsh of the Changjiang Estuary, China." Chemosphere 65 (2):310-7. doi: 10.1016/j.chemosphere.2006.02.026.

Zimmerman, D., Pavlik, C., Ruggles, A., & Armstrong, M. P. 1999. An experimental comparison of ordinary and universal kriging and inverse distance weighting. Mathematical Geology, 31(4), 375-390.

Appendix A. Supplemental Tables and Data

Table A.1. Species composition and marsh zonation of coring sites in Boundary Bay, Delta/Surrey, BC.

Site	Core ID	Common Name	Species	Percent Cover (%)	Marsh Zonation
Mid Boundary Bay	BBM1H2	Pickleweed	Salicornia virginica	40	High Marsh
		Creeping bentgrass	Agrostis stolonifera	60	
	BBM1H1	Pickleweed	Salicornia virginica	30	High Marsh
		Creeping bentgrass	Agrostis stolonifera	70	
	BBM1M	Creeping bentgrass	Agrostis stolonifera	100	Low Marsh
	BBM1L	Spear saltbush	Atriplex patula	100	Low Marsh
Eastern Boundary Bay	BBE1H2	Tufted hairgrass	Deschampsia caespitosa	100	High Marsh
	BBE1H1	Spear saltbush	Atriplex patula	100	High Marsh
	BBE1M	Pickleweed	Salicornia virginica	50	Low Marsh
		Seaside Arrowgrass	Triglochin maritima	50	
	BBE1L	Pickleweed	Salicornia virginica	100	Low Marsh
	BBE2H2	Creeping bentgrass	Agrostis stolonifera	100	High Marsh
	BBE2H1	Creeping bentgrass	Agrostis stolonifera	75	High Marsh
		Seaside Arrowgrass	Triglochin maritima	25	
	BBE2M	Creeping bentgrass	Agrostis stolonifera	50	Low Marsh
		Tufted hairgrass	Deschampsia caespitosa	25	
		Annual Sea-blite	Suaeda maritima	25	
	BBE2L	Pickleweed	Salicornia virginica	100	Low Marsh
	BBE3H2	Creeping bentgrass	Agrostis stolonifera	100	High Marsh
	BBE3H1	Tufted hairgrass	Deschampsia caespitosa	70	High Marsh
		Creeping bentgrass	Agrostis stolonifera	30	
	BBE3M	Annual Sea-blite	Suaeda maritima	100	Low Marsh
	BBE3L	Pickleweed	Salicornia virginica	100	Low Marsh
Mud Bay	MB1M	Creeping bentgrass	Agrostis stolonifera	100	Low Marsh
	MB1L	Creeping bentgrass	Agrostis stolonifera	100	Low Marsh

Table A.2. Coordinates, species composition, and depth (cm) of 128 additional sampling sites in eastern Boundary Bay study site (BBE), Delta, B.C.

Location ID	Latitude	Longitude	Depth (cm)
1-1	49.090079	-122.892263	95
1-2	49.090023	-122.891673	91
1-3	49.089884	-122.891067	29
1-4	49.089603	-122.890147	87
1-5	49.089378	-122.889675	73
1-6	49.089062	-122.889385	70
1-7	49.088777	-122.889249	63
2-1	49.089886	-122.892139	98
2-2	49.089671	-122.891713	82
2-3	49.089408	-122.891252	69
2-4	49.089155	-122.890817	82
2-5	49.08892	-122.890447	48
2-6	49.088639	-122.890082	58
2-7	49.088249	-122.889615	25
3-1	49.089789	-122.8925	91
3-2	49.089502	-122.892257	47
3-3	49.089158	-122.891951	75
3-4	49.088775	-122.891516	35
3-5	49.088522	-122.89128	67
3-6	49.08822	-122.891012	55
3-7	49.087907	-122.890685	48
4-1	49.089592	-122.893212	83
4-2	49.089366	-122.893107	82
4-3	49.089091	-122.892945	81
4-4	49.088764	-122.892766	71
4-5	49.088504	-122.892648	65
4-6	49.0881	-122.89245	69
4-7	49.087594	-122.892241	52
5-1	49.0892	-122.893971	89
5-2	49.088981	-122.893888	85
5-3	49.088812	-122.893813	71
5-4	49.088587	-122.893695	67
5-5	49.088263	-122.89358	68
5-6	49.087947	-122.893463	53
5-7	49.087557	-122.893345	44
6-1	49.089078	-122.894525	80

Location ID	Latitude	Longitude	Depth (cm)
6-2	49.088891	-122.894494	65
6-3	49.088652	-122.894434	67
6-4	49.088399	-122.894375	68
6-5	49.088086	-122.894321	58
6-6	49.087794	-122.894283	25
6-7	49.087415	-122.894235	40
7-1	49.08914	-122.895227	79
7-2	49.08869	-122.895094	74
7-3	49.088486	-122.895046	75
7-4	49.088162	-122.894975	68
7-5	49.087914	-122.894902	65
7-6	49.087582	-122.894824	59
7-7	49.086902	-122.894688	33
8-1	49.089231	-122.895994	88
8-2	49.088988	-122.895951	76
8-3	49.088763	-122.895908	76
8-4	49.088538	-122.89587	80
8-5	49.088325	-122.895856	85
8-6	49.088093	-122.895816	73
8-7	49.087766	-122.8958	68
9-1	49.08936	-122.897121	32
9-2	49.089142	-122.897062	65
9-3	49.088938	-122.896962	91
9-4	49.088751	-122.896858	85
9-5	49.088457	-122.896751	81
9-6	49.088039	-122.896611	80
9-7	49.08766	-122.896445	75
10-1	49.089155	-122.898311	95
10-2	49.088915	-122.898055	65
10-3	49.088655	-122.897755	89
10-4	49.088402	-122.897519	95
10-5	49.088226	-122.897294	84
10-6	49.087973	-122.89709	85
10-7	49.087796	-122.896959	80
11-1	49.088595	-122.899232	10
11-2	49.088314	-122.898831	20
11-3	49.088068	-122.898483	25
11-4	49.087878	-122.898247	11

Location ID	Latitude	Longitude	Depth (cm)
11-5	49.087653	-122.898011	40
11-6	49.087414	-122.897711	21
11-7	49.087182	-122.897325	15
12-1	49.088154	-122.899604	20
12-2	49.087881	-122.899298	16
12-3	49.087718	-122.899017	10
12-4	49.087416	-122.898676	40
12-5	49.087121	-122.898325	20
12-6	49.086819	-122.897923	38
12-7	49.086492	-122.897475	15
13-1	49.087851	-122.899853	12
13-2	49.087503	-122.899572	10
13-3	49.087215	-122.899293	7
13-4	49.086906	-122.899046	7
13-5	49.086534	-122.898767	15
13-6	49.086204	-122.898445	40
13-7	49.085775	-122.897984	40
14-1	49.087078	-122.899569	12
14-2	49.086807	-122.899439	12
14-3	49.086645	-122.899345	10
14-4	49.086483	-122.89927	15
14-5	49.086293	-122.899179	20
14-6	49.086117	-122.899109	13
14-7	49.085755	-122.898894	5
15-1	49.086466	-122.89986	22
15-2	49.08622	-122.899698	13
15-3	49.085924	-122.899593	27
15-4	49.085601	-122.899429	30
15-5	49.085279	-122.899266	28
15-6	49.085062	-122.899158	70
15-7	49.084225	-122.89882	35
16-1	49.085992	-122.900145	16
16-2	49.085777	-122.900033	27
16-3	49.085615	-122.899931	40
16-4	49.085477	-122.899869	35
16-5	49.085273	-122.899797	60
16-6	49.085069	-122.899743	30
16-7	49.084936	-122.899716	35

Location ID	Latitude	Longitude	Depth (cm)
17-1	49.085719	-122.900885	33
17-2	49.085587	-122.900827	35
17-3	49.085429	-122.90079	35
17-4	49.08526	-122.900747	15
17-5	49.08507	-122.900715	38
17-6	49.084922	-122.900651	35
17-7	49.084637	-122.90056	32
18-1	49.085473	-122.901611	20
18-2	49.085304	-122.901557	22
18-3	49.085093	-122.901498	20
18-4	49.084917	-122.901434	35
18-5	49.084703	-122.90137	35
18-6	49.084471	-122.901295	47
18-7	49.084102	-122.901177	40
19-1	49.085391	-122.902481	40
19-2	49.085261	-122.902476	60
19-3	49.085113	-122.902455	27
19-4	49.084983	-122.902428	46
19-5	49.084846	-122.902428	35
19-6	49.084695	-122.902401	40
19-7	49.084479	-122.902383	40
20-1	49.08525	-122.90346	35
20-2	49.085053	-122.903397	50
20-3	49.084909	-122.903342	25
20-4	49.084746	-122.903275	32
20-5	49.084537	-122.903222	25
20-6	49.08438	-122.903169	30
20-7	49.084131	-122.903083	52

Table A.3. Downcore distribution of ^{210}Pb and ^{226}Ra in the four cores chosen for geochronological dating. Cores BBE1H1 and BBE3H1 are high marsh cores, and cores BBE1L and BBE3M are low marsh cores.

Core BBE1H1					
Depth (cm)	**Supported 210Pb (Bq/g)**	**210Pb total activity (Bq/g)**	**± (Bq/g)**	**Unsupported 210Pbexs (Bq/g)**	**Sediment Type**
1	0.008	0.138	0.005	0.130	Peat
3	0.008	0.126	0.005	0.118	Peat
5	0.008	0.093	0.004	0.085	Peat
7	0.009	0.026	0.002	0.017	Peat
9	0.009	0.015	0.002	0.006	Peat
13	0.009	0.012	0.001	0.003	Peat
17	0.009	0.013	0.002	0.004	Peat
21	0.007	0.010	0.001	0.003	Peat
29	0.007	0.013	0.001	0.006	Peat
33	0.007	0.007	0.001	0.000	Peat/Silt
38	0.009	0.009	0.001	0.000	Peat/Silt
5 (226Ra)		0.008	0.001		-
17 (226Ra)		0.009	0.001		-
Core BBE1L					
Depth (cm)	**Supported 210Pb (Bq/g)**	**210Pb total activity (Bq/g)**	**± (Bq/g)**	**Unsupported 210Pbexs (Bq/g)**	**Sediment Type**
1	0.003	0.013	0.002	0.009	Sand
5	0.003	0.009	0.001	0.006	Sand
9	0.003	0.011	0.001	0.007	Sand
13	0.003	0.008	0.001	0.005	Sand
17	0.003	0.010	0.001	0.007	Sand
21	0.003	0.008	0.001	0.005	Sand
27	0.003	0.008	0.001	0.005	Sand
27 (226Ra)		0.003	0.000		-

Core BBE3H1					
Depth (cm)	**Supported 210Pb (Bq/g)**	**210Pb total activity (Bq/g)**	**± (Bq/g)**	**Unsupported 210Pbexs (Bq/g)**	**Sediment Type**
1	0.006	0.240	0.009	0.234	Peat
2	0.006	0.206	0.006	0.200	Peat
3	0.006	0.123	0.005	0.117	Peat
4	0.006	0.085	0.004	0.079	Peat
5	0.006	0.079	0.004	0.073	Peat
6	0.006	0.068	0.003	0.062	Peat
7	0.006	0.053	0.003	0.047	Peat
8	0.006	0.037	0.003	0.031	Peat
9	0.009	0.020	0.002	0.012	Peat
10	0.009	0.015	0.002	0.006	Peat/Silt
13	0.007	0.008	0.001	0.002	Sand
16	0.007	0.007	0.001	0.000	Sand
27	0.010	0.010	0.001	0.000	Sand
5 (226Ra)		0.006	0.001		-
9 (226 Ra)		0.009	0.001		-
16 (226Ra)		0.007	0.001		-
Core BBE3M					
Depth (cm)	**Supported 210Pb (Bq/g)**	**210Pb total activity (Bq/g)**	**± (Bq/g)**	**Unsupported 210Pbexs (Bq/g)**	**Sediment Type**
1	0.008	0.120	0.004	0.111	Peat
3	0.008	0.138	0.005	0.129	Peat
5	0.008	0.101	0.004	0.093	Peat
7	0.008	0.063	0.003	0.055	Peat
9	0.008	0.034	0.003	0.025	Peat/Clay
11	0.007	0.020	0.002	0.013	Peat/Clay
13	0.007	0.016	0.001	0.009	Peat/Silt
17	0.007	0.008	0.001	0.001	Sand
19	0.007	0.008	0.001	0.001	Sand
23	0.007	0.008	0.001	0.001	Sand
27	0.009	0.011	0.001	0.002	Sand
31	0.009	0.016	0.002	0.006	Sand
37	0.009	0.019	0.002	0.010	Sand
5 (226Ra)		0.008	0.001		-
19 (226Ra)		0.007	0.001		-
37 (226Ra)		0.009	0.001		-

Table A.4. Average Core C Stocks ± SE (Mg C ha^{-1}) and CARs ± SE (Mg C ha^{-1} yr^{-1}) for high and low marsh areas at the three case study marshes in British Columbia: Boundary Bay (BB), Cypress River Flats (CRF), and Grice Bay – Kennedy River (GBK). All values down to peat base.

Average Core Carbon Stock	Carbon Accumulation Rate	References	Data Availability, Screening and Use

(± SE) (Mg C ha^{-1})				(± SE) (Mg C ha^{-1} yr^{-1})					
HM	**n**	**LM**	**n**	**HM**	**n**	**LM**	**n**		
Boundary Bay (BB)									
70 ± 8.4	18	41 ± 9.7	14	1.3 ± 0.21	5	0.66 ± 0.13	4	Chapter 2 Gailis et al. 2021	All BB compressed C stocks (± SE) down to peat layer obtained from Table 2, Chapter 2. Published CARs (± SE) for western BB obtained directly from Table 3 (Gailis et al. 2021) and combined with CARs (± SE) for eastern BB from Table 5, Chapter 2 to derive CARs for all BB. High and low marsh CARs for all BB are averaged separately and shown in this table.
Cypress River Flats (CRF)									
130 ± 16	3	89 ± 8.0	3	3.5 ± 0.37	1	0.62 ± 0.14	1	Chastain et al. 2021	C stock to peat base (± SE) from Table A1. CARs to peat base (± SE) from Table 2.
Grice Bay – Kennedy River (GBK)									
51 ± 6.0	3	42 ± 0.0	1	3.9 ± 0.18	1	0.47 ± 0.10	1	Chastain et al. 2021	C stock to peat base (± SE) from Table A1. CARs to peat base (± SE) from Table 2.

*HM = High Marsh, LM = Low Marsh, n = number of samples.

Appendix B. Supplemental Figures

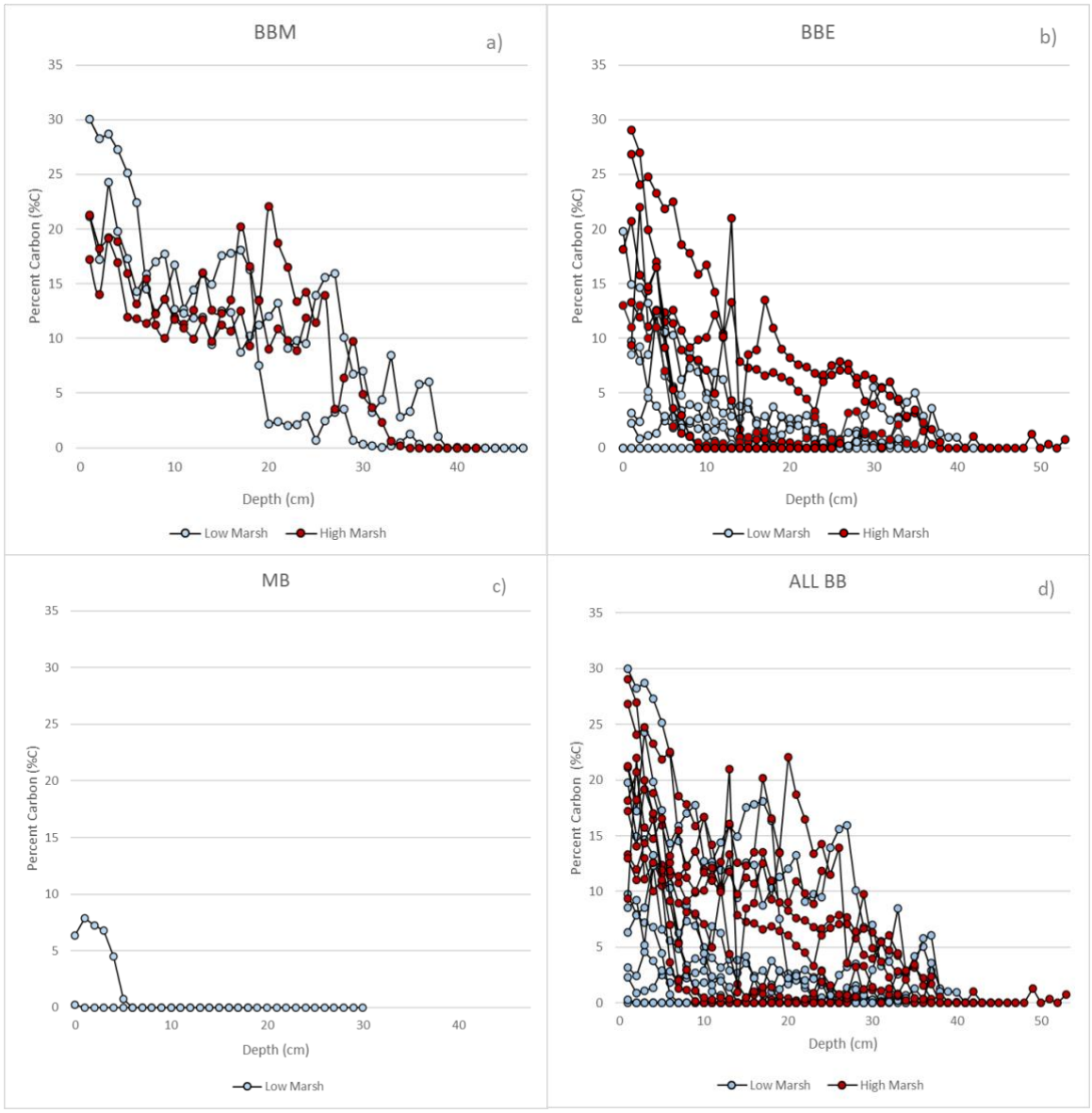

Figure B.1. **Profiles of sediment percent carbon (%C) for the entire length of each core in relationship to depth (cm) in a) BBE b) BBM c) MB and d) all parts of Boundary Bay (BBW, BBM, BBE and MB). Red markers represent high marsh cores and blue markers represent low marsh cores.**

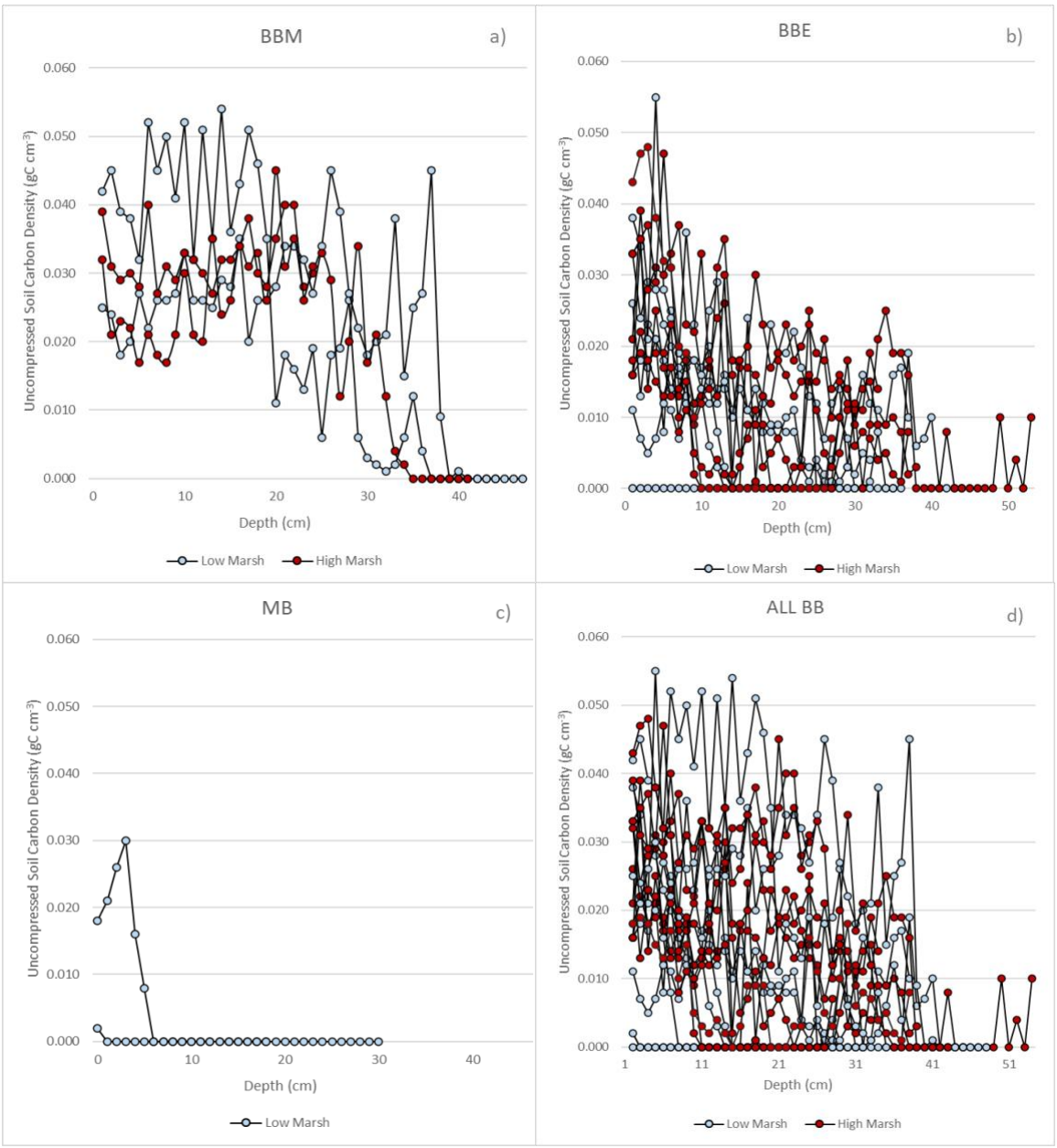

Figure B.2. **Profiles of uncompressed soil carbon densities (g C cm^{-3}) for entire length of core in relationship to depth of each core (cm) in a) BBE b) BBM c) MB and d) all parts of Boundary Bay (BBW, BBM, BBE and MB). Red markers represent high marsh cores and blue markers represent low marsh cores.**

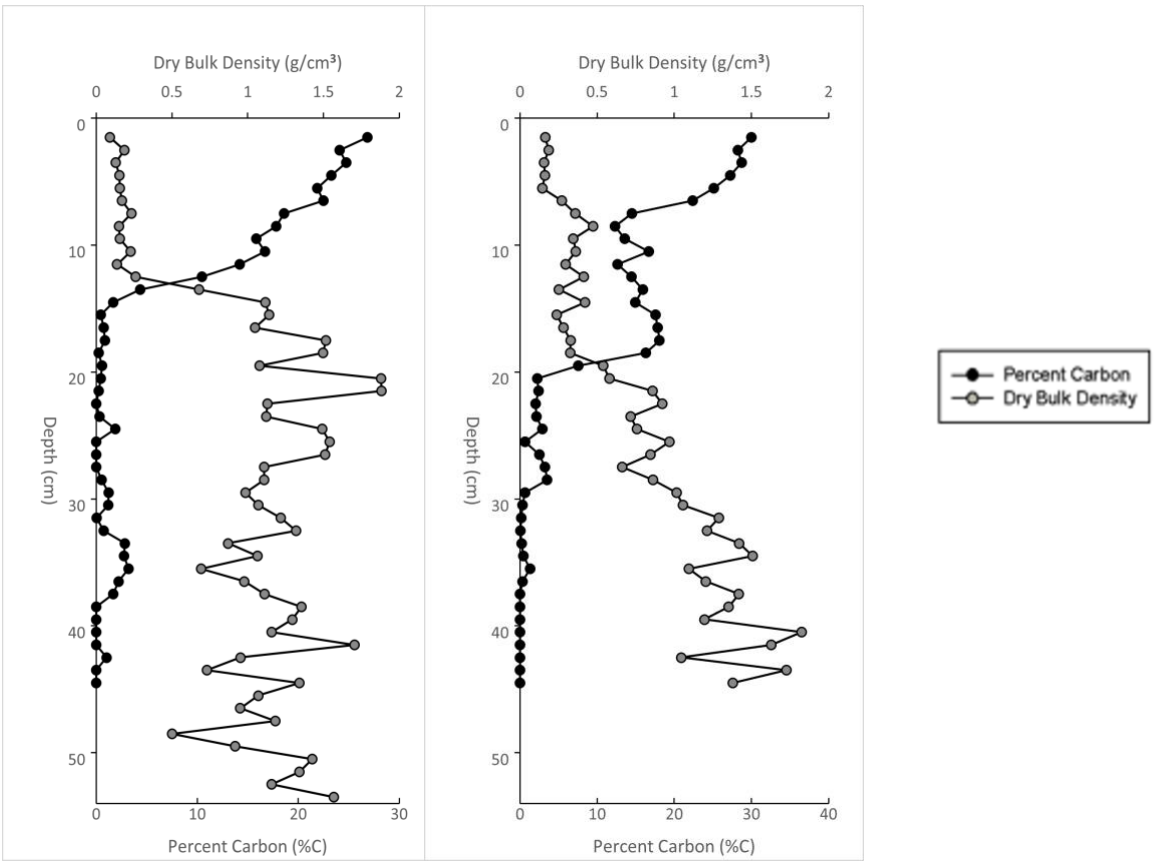

Figure B.3. Profiles of sediment compressed dry bulk density and percent carbon for the entire length of cores selected from high marsh (Core ID BBE1H2) and low marsh (core ID BBM1L). It can be observed that DBD and %C are inversely related, in that high DBD corresponds to low %C and vice versa.

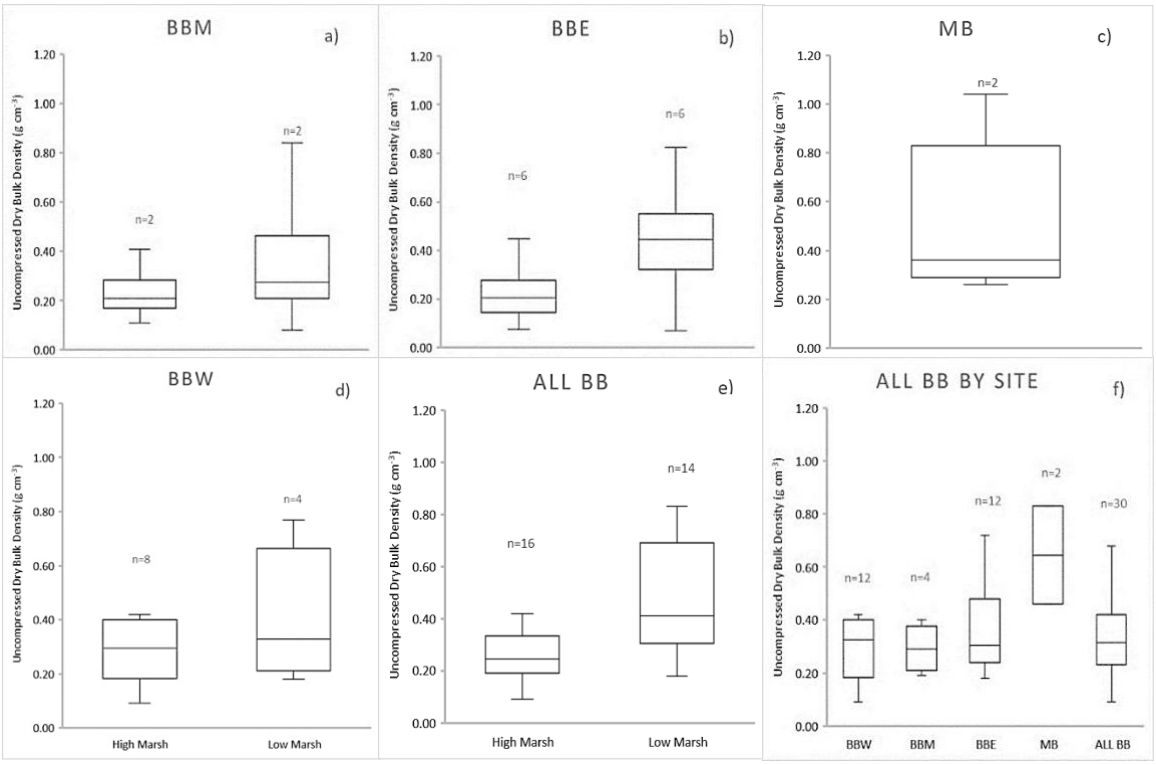

Figure B.4. Average uncompressed dry bulk densities (g cm^{-3}) down to the base of peat layer comparing high marsh cores to low marsh cores.

a) BBM (t-value = 1.471, p-value = 0.380, p>0.05), b) BBE (t-value = 2.773, p-value = 0.0197, p<0.05). c) MB and d) BBW (t-value=0.793, p-value=0.486, p>0.05). e) all parts of Boundary Bay (t-value = 3.216, p-value =0.007, p<0.05).f) Comparison of DBD for all parts of Boundary Bay by site, where ALL BB is a compilation of all cores in Boundary Bay. The middle line is the median and the top and bottom of the box are quantiles (Q1 and Q3), and the error bar is the largest and smallest value.

Appendix C. Supplemental Maps

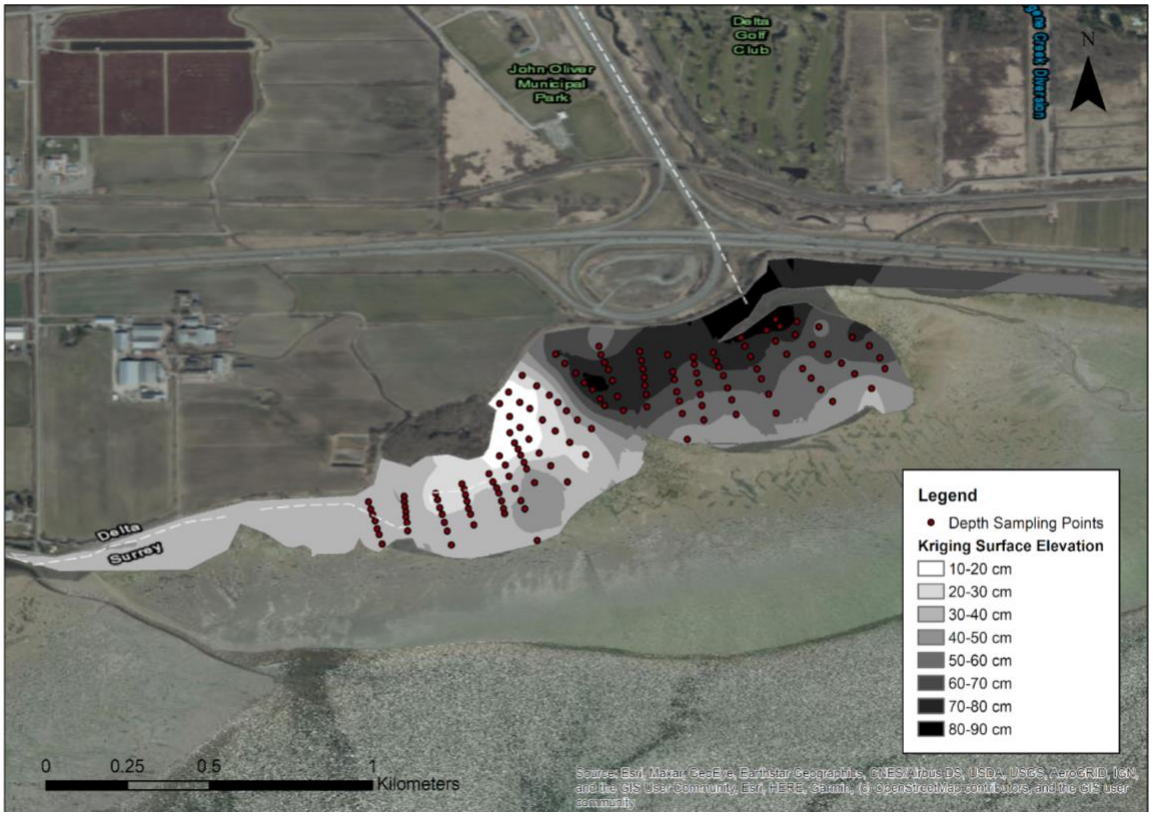

Figure C.1. **The kriging spatial analysis completed in ArcMap 10.3 to estimate the marsh volume for eastern Boundary Bay based on the bounded area of 52 ha (522,500 m^2). The red dots represent the 140 depth sampling points. The kriging analysis yielded an average depth profile of 51.84 ± 18.42 cm. Base Map Source: ArcGIS 2021.**

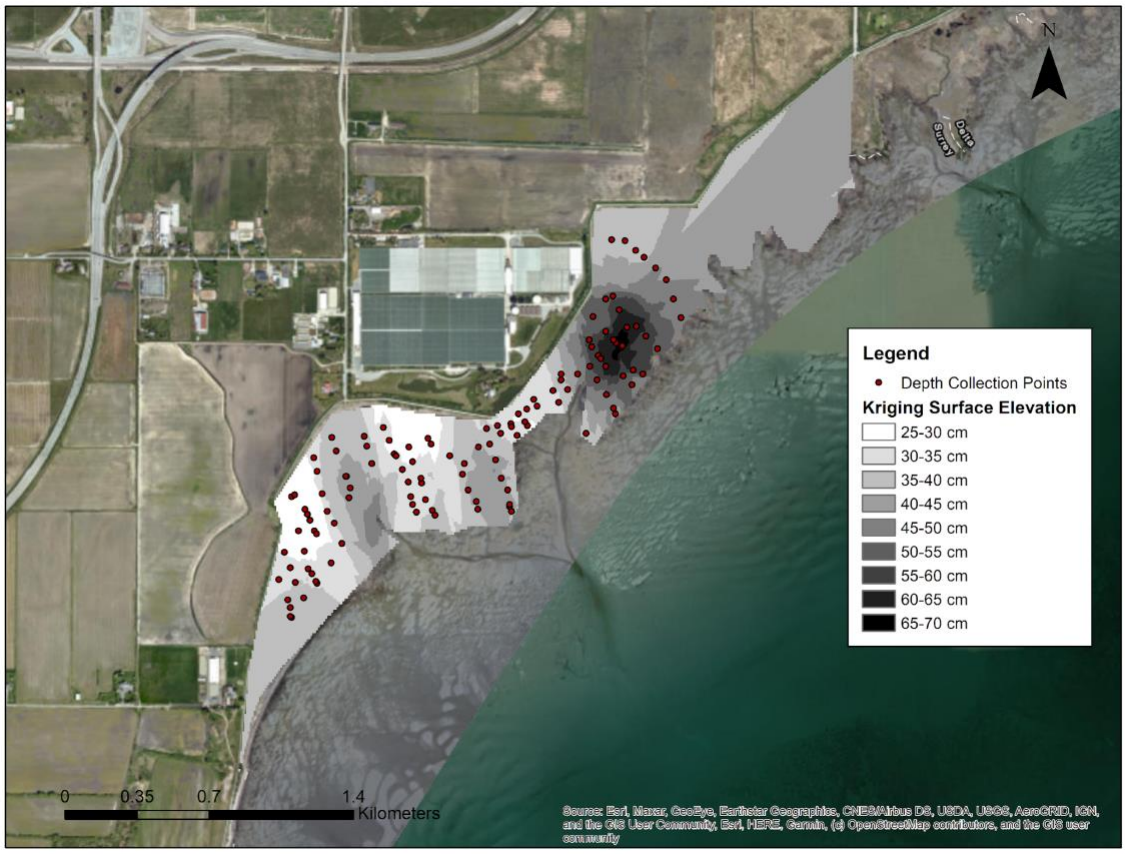

Figure C.2. **The kriging spatial analysis completed in ArcMap 10.3 to estimate the marsh volume for western Boundary Bay based on a bounded area of 80 ha (796,300 m^2). The red dots represent 139 depth sampling points collected by Gailis et al. (2021). The kriging analysis yielded an average depth profile of 40.73 ± 7.85 cm. Base Map Source: ArcGIS 2021.**